

## Accepted Article

**Title:** Electrophilic Activation of Silicon-Hydrogen Bonds in Catalytic Hydrosilations

**Authors:** Mark C. Lipke, Allegra L. Liberman-Martin, and T. Don Tilley

This manuscript has been accepted after peer review and appears as an Accepted Article online prior to editing, proofing, and formal publication of the final Version of Record (VoR). This work is currently citable by using the Digital Object Identifier (DOI) given below. The VoR will be published online in Early View as soon as possible and may be different to this Accepted Article as a result of editing. Readers should obtain the VoR from the journal website shown below when it is published to ensure accuracy of information. The authors are responsible for the content of this Accepted Article.

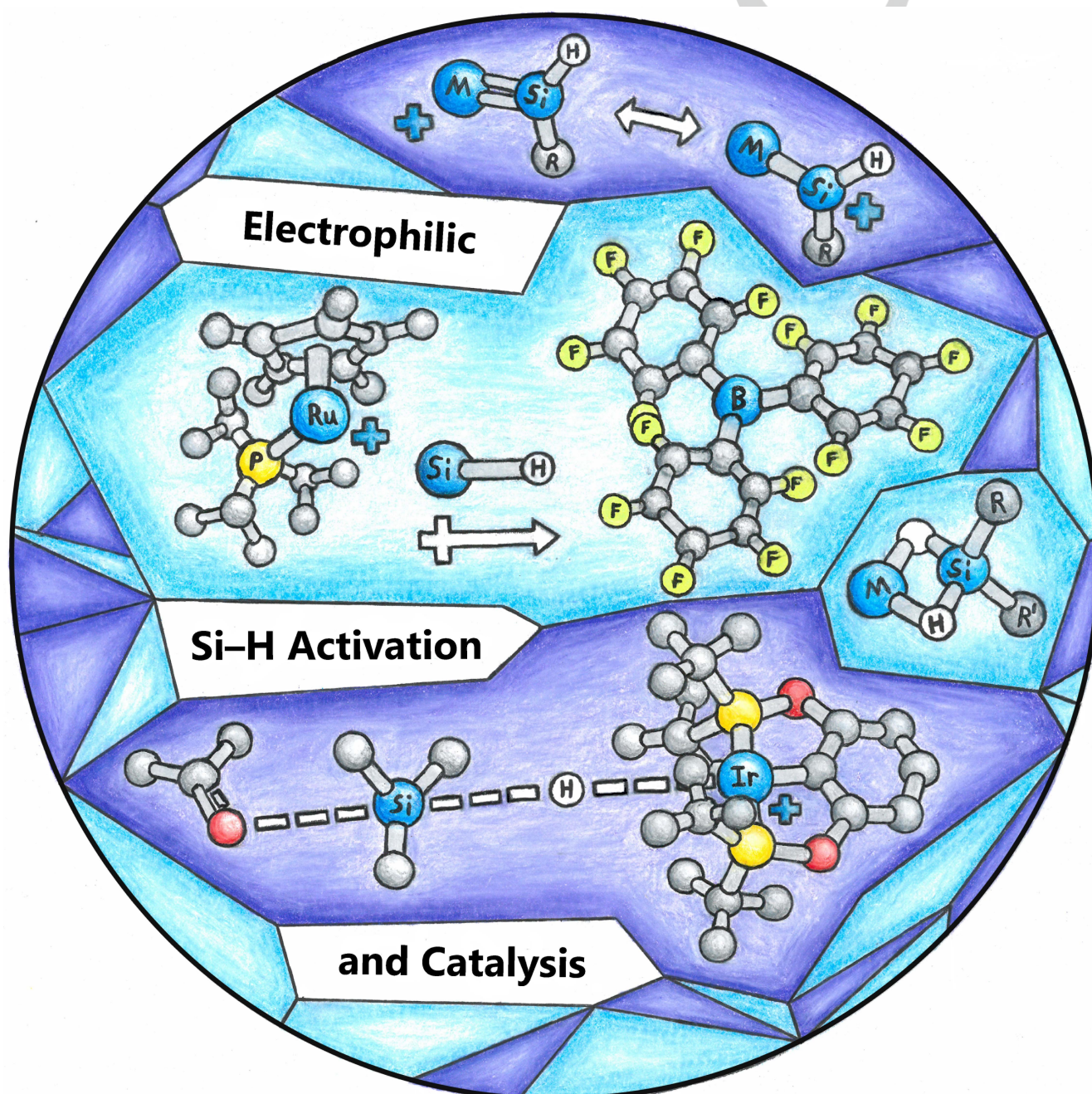
**To be cited as:** *Angew. Chem. Int. Ed.* 10.1002/anie.201605198  
*Angew. Chem.* 10.1002/ange.201605198

**Link to VoR:** <http://dx.doi.org/10.1002/anie.201605198>  
<http://dx.doi.org/10.1002/ange.201605198>

# Electrophilic Activation of Silicon–Hydrogen Bonds in Catalytic Hydrosilations

Mark C. Lipke, Allegra L. Liberman-Martin, and T. Don Tilley\*

Dedicated to the memory of Robert Corriu for his pioneering work on the mechanisms and reactions of silicon compounds.



Accepted Manuscript

**Abstract:** Hydrosilation reactions represent an important class of chemical transformations and there has been considerable recent interest in expanding the scope of these reactions by developing new catalysts. A major theme to emerge from these investigations is the development of catalysts with electrophilic character that transfer electrophilicity to silicon via Si—H activation. This type of mechanism has been proposed for catalysts ranging from Group 4 transition metals to Group 15 main group species. Additionally, other electrophilic silicon species, such as silylene complexes and  $\eta^3\text{-H}_2\text{SiRR}'$  complexes, have been identified as intermediates in hydrosilation reactions. In this Review, different types of catalysts are compared to highlight the range of hydrosilation mechanisms that feature electrophilic silicon centers, and the importance of these catalysts to the development of new hydrosilation reactions is discussed.

## 1. Introduction

Hydrosilation reactions are a broad class of catalytic transformations in which a Si—H bond is added to an unsaturated functional group.<sup>[1]</sup> Suitable substrates include, but are not limited to: olefins,<sup>[2]</sup> alkynes,<sup>[3]</sup> ketones,<sup>[4]</sup> carboxylate esters,<sup>[5]</sup> amides,<sup>[6]</sup> imines,<sup>[7]</sup> nitriles,<sup>[8]</sup> and pyridines.<sup>[9]</sup> Owing to the variety of viable substrates, these reactions have applications ranging from industrial processes to laboratory scale syntheses. For example, olefin hydrosilation reactions are industrially important for the synthesis of silane reagents and for crosslinking of silicone polymers. Catalytic hydrosilations of other substrates (e.g. carbonyl compounds, nitriles, imines) have been developed as useful laboratory methods for the reduction of various functional groups. These reduction reactions combine exceptional reducing power (comparable to  $\text{LiAlH}_4$ ) with high selectivity (e.g. ester to aldehyde conversion,<sup>[10]</sup> amide to imine conversion,<sup>[11]</sup>  $\text{CO}_2$  reduction,<sup>[12]</sup> etc.) while making use of bench-stable hydridosilanes (e.g.  $\text{Et}_3\text{SiH}$ ,  $\text{Et}_2\text{SiH}_2$ , etc.) as reducing agents.

The power, selectivity, and efficiency of hydrosilation reactions are enabled by the variety of catalysts and catalytic cycles available for these reactions. Thus, there has been longstanding interest in understanding the mechanisms of these transformations and applying this knowledge to catalyst development. This review will examine hydrosilation catalysts for which the generation of an electrophilic silicon center is key to the activation of the unsaturated substrate.<sup>[13-16]</sup> These types of mechanisms were first proposed in the 1990's and a range of distinct mechanisms are now known that share electrophilic silicon as a common feature. Likewise, these types of mechanisms are operative for an incredibly wide range of catalysts based on transition metals or main group Lewis acids.

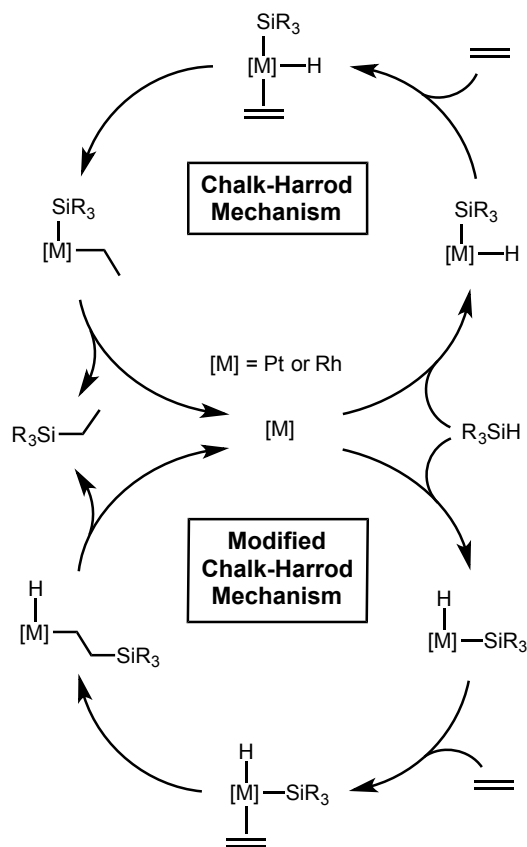
### From the Contents

1. <b>Introduction</b>	2
2. <b>Main Group Lewis Acid Catalysts</b>	4
3. <b>Hydrosilations by Electrophilic Transition Metal H—SiR<sub>3</sub> <math>\sigma</math>-Complexes</b>	9
4. <b>Hydrosilations Involving Electrophilic Silylene Complexes</b>	20
5. <b>Electrophilic Complexes with Multiple M—H—Si 3-center 2-electron Bonds</b>	26
6. <b>Summary and Outlook</b>	31

The mechanisms described in this review differ considerably from those determined in early studies of olefin and ketone hydrosilation reactions using platinum and rhodium catalysts (Scheme 1). An important requirement for these catalysts is their ability to readily engage in oxidative addition, reductive elimination, and migratory insertion processes. These steps are important to the Chalk-Harrod and modified Chalk-Harrod mechanisms for olefin hydrosilation reactions that were first elucidated for platinum catalysts in the 1960's.<sup>[17]</sup> A closely related mechanism for rhodium-catalyzed ketone hydrosilations was proposed by Ojima in 1975.<sup>[18]</sup> These mechanisms allow for efficient catalysis, but the requirement of two-electron oxidative addition/reductive elimination steps has largely limited the range of available catalysts to platinum group metals. These catalysts are expensive and have additional drawbacks such as a tendency to engage in  $\beta$ -hydride eliminations that can lead to the formation of undesired side-products (e.g., those derived from olefin isomerization).<sup>[1]</sup> Thus, there has been considerable interest in developing new catalysts for hydrosilation reactions that do not rely on Chalk-Harrod type mechanisms.

A major advance in the discovery of new hydrosilation mechanisms appeared in the 1990's with the first reports of the strong Lewis acid  $\text{B}(\text{C}_6\text{F}_5)_3$  as a hydrosilation catalyst.<sup>[19]</sup> This simple Lewis acid catalyst cannot engage in the reaction steps necessary for Chalk-Harrod type catalytic cycles, and thus, the ionic hydrosilation mechanism was proposed to explain the catalytic activity of  $\text{B}(\text{C}_6\text{F}_5)_3$  in ketone hydrosilation reactions (Scheme 2, A). In this mechanism, the electrophilic borane activates the Si—H bond of a silane to enhance electrophilic character at silicon. This enables the transfer of  $\text{R}_3\text{Si}^+$  to the nucleophilic oxygen of the ketone substrate to form key ionic

[\*] Dr. M. C. Lipke, Dr. A. L. Liberman-Martin, Prof. T. D. Tilley  
Department of Chemistry, University of California, Berkeley  
Berkeley, CA 94720 (USA). Email: tdtiley@berkeley.edu



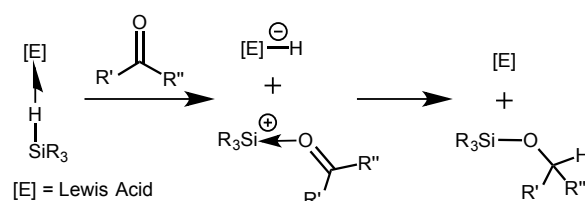
**Scheme 1.** Chalk-Harrod type hydrosilation mechanisms.

intermediates  $[R_2C=O \rightarrow SiR_3]^+$  and  $[HB(C_6F_5)_3]$ . The  $B(C_6F_5)_3$  catalyst has since been applied to the hydrosilation of many substrates including olefins,<sup>[20]</sup> ketones,<sup>[19]</sup> and esters.<sup>[21]</sup> This catalyst is also useful for related transformations such as the reductive cleavage of C—O<sup>[22]</sup> and C—X<sup>[23]</sup> (X = halogen) bonds using hydrosilane reagents. Many other hydrosilation reactions appear to operate *via* polarization of the silane Si—H bond upon coordination to an electrophilic catalyst, with examples featuring main group Lewis acid catalysts (e.g. based on aluminum, phosphorus, and zinc; see Section 2) as well as transition metal catalysts (e.g. utilizing iridium, ruthenium, rhenium, and tungsten; see Sections 3-5).

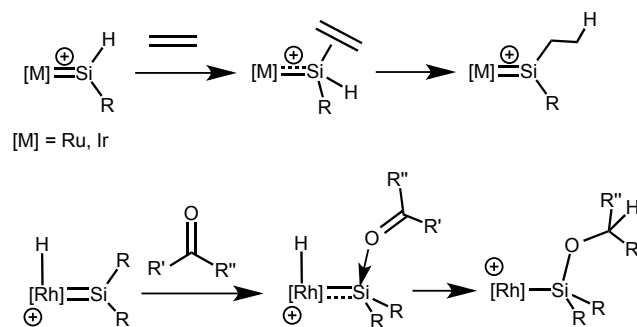
There are other hydrosilation mechanisms that rely on the generation of an electrophilic silicon center, but involve intermediates that are distinct from those invoked in the ionic mechanism (Scheme 2, B and C). For example, a mechanism proposed in 1995 involves the coordination of a ketone substrate to the silicon center of a  $[Rh]-SiR_2H$  ligand to generate an intermediate featuring a 5-coordinate silicon center.<sup>[24]</sup> This particular mechanism has not been experimentally supported, but some of its key features have since been implicated in other electrophilic hydrosilation mechanisms. For example, transition metal silylene complexes bind and activate substrates at the metal-bound silicon center, which has Lewis acidic character (Scheme 2, B).<sup>[15-16]</sup> In these reactions, a metal-silicon bond is

preserved upon binding of the substrate, but the resulting adduct possesses a silicon center that is 4-coordinate rather than 5-coordinate. However, more recently reported hydrosilation mechanisms do invoke the formation of intermediates in which the substrate binds to a 5- or 6-coordinate silicon center (Scheme 2, C).<sup>[25]</sup> In these latter examples, the silicon center engages in multiple M—H—Si interactions that keep it bound to the metal center even upon substrate coordination at silicon. Thus, these examples exhibit significant similarities to the ionic hydrosilation mechanism (i.e. M—H—Si interactions render the Si center electrophilic) and the silylene hydrosilation mechanism (i.e. silicon-substrate adduct remains in the coordination sphere of the catalyst).

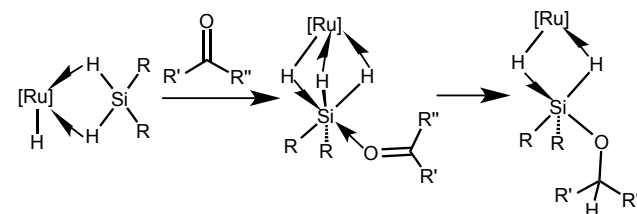
### A Simple Lewis Acid Mechanisms



### B Transition Metal Silylene Complex Mechanisms



### C Hypercoordinate Silicon Mechanisms



**Scheme 2.** Hydrosilation *via* electrophilic silane activation.

This mechanistically-focused Review will compare and contrast the silane activation mechanisms of a variety of hydrosilation catalysts, including main group Lewis acids, silylene complexes, and  $\eta^3$ -silane complexes. We note that in some cases, electrophilic catalysts, including Lewis and

Brønsted acids, can activate ketone or aldehyde substrates rather than the silane reagent,<sup>[26]</sup> however, these catalysts and mechanisms are not discussed in the present Review. Mechanistic comparisons of electrophilic silane activations are enabled by major recent advances that elucidate the structures of key silicon intermediates. For example, borane-silane<sup>[27]</sup> and alane-silane<sup>[28]</sup> adducts have only recently been isolated and characterized, and these studies provide definitive support for intermediates that had long been inferred based on indirect experimental evidence. Similarly, structural data was recently obtained for a cationic ruthenium silylene complex that catalyzes olefin hydrosilation reactions.<sup>[29]</sup> Furthermore, electrophilic hydrosilation mechanisms involving intermediates with multiple M—( $\mu$ -H)—Si interactions are recent additions to the field.<sup>[25,30]</sup>

As described in this Review, a key feature of many of these electrophilic catalysts is the activation of one or more Si—H bonds without significant back donation provided to silicon, thus generating an electrophilic silicon center. A second key feature of these mechanisms is that the unsaturated substrate is activated by direct interaction with the electrophilic silicon center. Other features of these mechanisms vary quite widely and will be examined: the presence or absence of a metal-silicon bond, the coordination number of the electrophilic silicon center, substrate attack before or after full cleavage of the Si—H bond, frontside or backside attack of substrate with respect to the activated Si—H bond, and insertion of the substrate into the activated Si—H bond or into a different Si—H bond on the silicon center.

T. Don Tilley received his B.S. degree from the University of Texas, Austin, in 1977. In 1982, he completed his Ph.D. thesis at UC Berkeley in the group of R. A. Andersen, studying organometallic lanthanide chemistry. In 1982–1983, he participated in an NSF-sponsored exchange program, working with Professors Robert Grubbs and John Bercaw at Caltech, and with Professors Luigi Venanzi and Piero Pino at the ETH in Zürich, Switzerland. He started his independent career at UC San Diego in 1983 and rose to the rank of Professor of Chemistry before moving to his current positions as Professor of Chemistry at UC Berkeley, and Senior Scientist at Lawrence Berkeley National Laboratory. His research interests include synthetic, structural, catalytic, and mechanistic investigations in inorganic and organometallic chemistry.



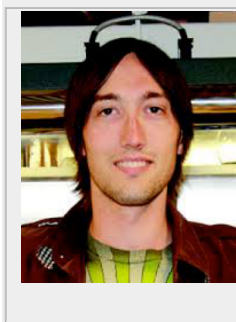
## 2. Main Group Lewis Acid Catalysts

There has been considerable progress in the development of main group compounds that can replicate catalytic transformations associated with transition metal complexes.<sup>[31]</sup> In the field of hydrosilation catalysis, a variety of Lewis acids have been identified that operate by Si—H coordination to the catalyst which renders the silicon center electrophilic, particularly since main group species usually cannot provide back-donation into the Si—H  $\sigma^*$  orbital. This section highlights various main group hydrosilation catalysts that operate by variants of the ionic hydrosilation mechanism shown in Scheme 2a. For the majority of these Lewis acids, intermediate silane adducts are not directly observed but are implied by indirect experimental evidence. Notably however, two examples of adducts of main group Lewis acids (boranes and alanes) with silanes were recently isolated and structurally characterized.<sup>[27,28]</sup> These structures mark an exciting advance in the study of main group-catalyzed hydrosilations by providing the first direct evidence for  $\eta^1$ -silane intermediates in main group chemistry. These advances, described below, offer the opportunity for direct structural comparison of these electrophilic silicon species with those involving transition metals.

### 2.1. Boron catalysts

The first study of hydrosilation catalyzed by  $B(C_6F_5)_3$  (**1**) was reported by Piers in 1996, and described transformation of aromatic aldehyde, ketone, and ester substrates to silyl ether products.<sup>[19]</sup> In the decade following this seminal work, Gevorgyan, Yamamoto, and others extended the substrate scope of  $B(C_6F_5)_3$  catalysis to the reduction of aldehydes, esters, ethers, and alcohols to hydrocarbon products.<sup>[22]</sup>  $B(C_6F_5)_3$  has remained the most prominent main group hydrosilation catalyst for the last twenty years due to its efficient and selective catalysis for a broad range of substrates.

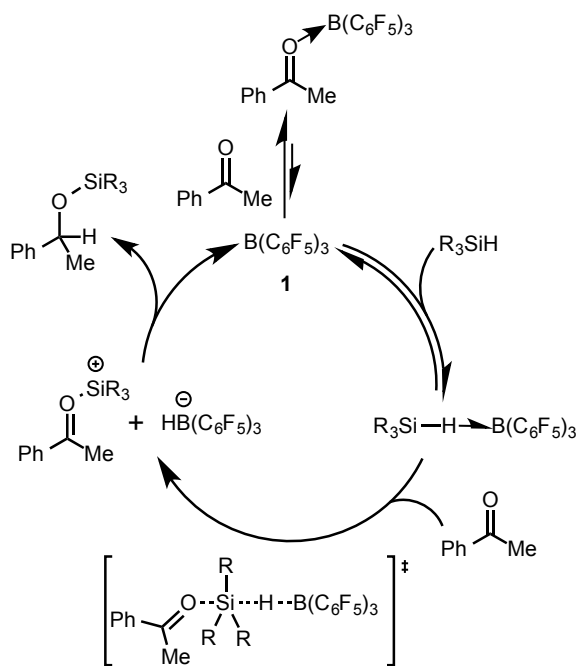
Mark C. Lipke graduated with a B.S. in Chemistry from Case Western Reserve University in 2008. He was awarded an ARCS Fellowship to conduct his PhD research in the group of T. Don Tilley at UC Berkeley. Mark completed his thesis in 2013 on the topic of electrophilic double Si—H activation pathways for silanes. He is currently a post-doctoral scholar in the Stoddart group at Northwestern University. Mark is also a talented artist. He illustrated the title page of this Review.



Allegra L. Liberman-Martin graduated with a B.A. in Chemistry from Scripps College in Claremont, CA in 2010. She earned her Ph.D. in 2015 from UC Berkeley, where she developed strategies to regulate organometallic reactivity using Lewis acid additives with Profs. T. Don Tilley and Robert G. Bergman. She is currently a postdoctoral fellow with Prof. Robert H. Grubbs at Caltech.

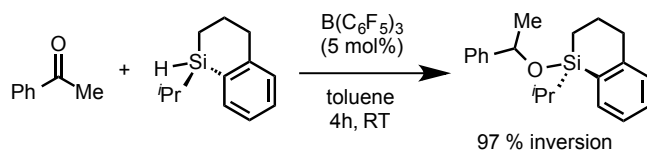


The mechanism of ketone hydrosilylation by  $B(C_6F_5)_3$  is presented in Scheme 3.<sup>[32]</sup> The majority of the catalyst is trapped as an off-cycle ketone adduct, and ketone dissociation followed by silane coordination must occur to generate small quantities of a  $Si-H \cdots B$  intermediate. The  $Si-O$  bond of the silyl ether is formed by coordination of the ketone substrate to the electrophilic silicon center, which breaks the  $Si-H$  bond. Hydride transfer from the borohydride to the silylcarboxonium ion furnishes the silyl ether product.



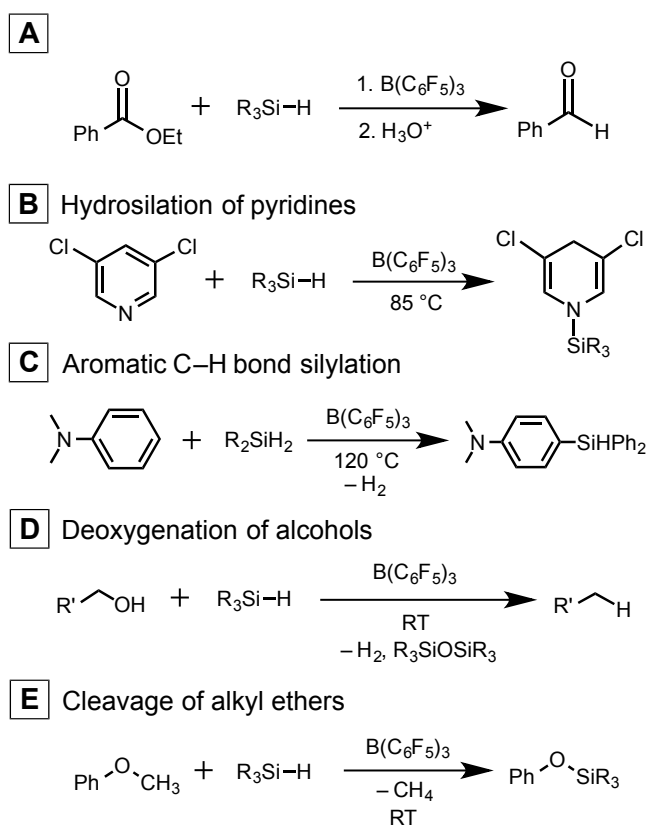
**Scheme 3.** Mechanism of ketone hydrosilylation catalysis by  $B(C_6F_5)_3$ .

Extensive mechanistic studies have been performed that support the mechanism shown in Scheme 3. Kinetics experiments performed by Piers demonstrated that higher concentrations of ketone *decrease* the rate of hydrosilylation catalysis, and that the least basic substrates are reduced most rapidly, arguing against a ketone activation pathway.<sup>[19]</sup> Stereochemical experiments using a chiral silane substrate, performed by Oestreich (Scheme 4), demonstrated an inversion of stereochemistry at silicon during hydrosilylation, consistent with an  $S_N2$ -Si mechanism for the  $Si-O$  bond forming step.<sup>[33]</sup>



**Scheme 4.** Stereochemical experiment to assess the mechanism of  $B(C_6F_5)_3$ -catalyzed hydrosilylation.

A wide range of reactions are catalyzed by  $B(C_6F_5)_3$  via an ionic hydrosilylation mechanism, and particularly challenging transformations are highlighted in Scheme 5.  $B(C_6F_5)_3$  catalyzes the reduction of esters to silyl acetals, which can be cleaved to aldehyde products under acidic conditions (Scheme 5, **A**).<sup>[21]</sup> The 1,4-hydrosilylation of pyridines is also catalyzed by  $B(C_6F_5)_3$  at elevated temperatures (Scheme 5, **B**).<sup>[34]</sup> Additionally, the C-H silylation of electron-rich aromatic compounds is catalyzed by  $B(C_6F_5)_3$  in the absence of a hydrogen acceptor (Scheme 5, **C**).<sup>[35]</sup> Related reactions, such as deoxygenation of alcohols and cleavage of alkyl ethers, are also catalyzed by  $B(C_6F_5)_3$  (Scheme 5, **D** and **E**) and represent convenient methods to cleave the strong C-O bonds of these substrates.<sup>[22]</sup> Although detailed mechanistic studies have not been performed for all of these transformations, the electrophilic silane activation pathway has been proposed to operate in these diverse processes.

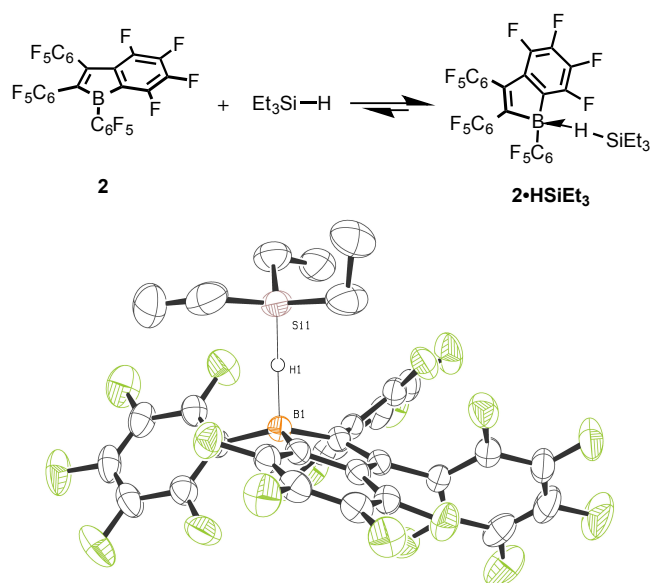


**Scheme 5.** Examples of catalysis by  $B(C_6F_5)_3$  featuring electrophilic silane activation.

There have been extensive attempts to directly observe the  $Et_3Si-H \cdots B(C_6F_5)_3$  intermediate by low-temperature spectroscopic studies; however, this proposed intermediate has remained elusive. Thus, it is notable that an adduct between triethylsilane and 1,2,3-tris(pentafluorophenyl)-4,5,6,7-tetrafluoro-1-boraindene (**2**) was recently characterized in solution and in the solid state (Scheme 6).<sup>[27]</sup> This borane serves

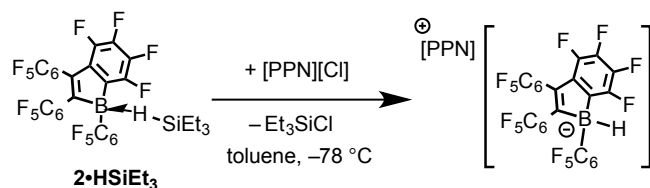
as a model for  $B(C_6F_5)_3$  that is rendered more Lewis acidic due to its anti-aromaticity.

The boraindene–silane adduct **2•HSiEt<sub>3</sub>** has Si–H and B–H distances of 1.51(2) Å and 1.46(2) Å, respectively, which suggest a relatively weak Si–H···B interaction (typical Si–H distances of silanes are ~1.48 Å<sup>[36]</sup> and B–H distances of perfluorohydridoborate anions are 1.14 Å<sup>[37]</sup>). Variable temperature <sup>1</sup>H NMR spectroscopy revealed that adduct formation is favored below room temperature in toluene-*d*<sub>8</sub>. A decrease in the <sup>1</sup>J<sub>Si–H</sub> coupling constant of triethylsilane from 177 Hz at 298 K to 107 Hz at 213 K is consistent with a weakening of the Si–H bond upon interaction with boron (*J*<sub>Si–H</sub> = 180 Hz for free Et<sub>3</sub>SiH). This weakening was also observed by IR spectroscopic comparison of the Si–H stretching frequency for the boraindene adduct (1918 cm<sup>-1</sup>) versus free Et<sub>3</sub>SiH (2103 cm<sup>-1</sup>).



**Scheme 6.** Triethylsilane coordination to a boraindene Lewis acid **2**.

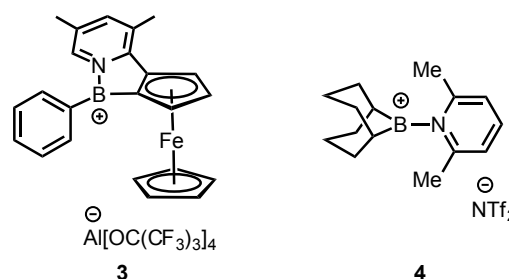
Although hydrosilation studies were not reported for **2**, initial indications are that the coordinated silane is electrophilic. Adduct **2•HSiEt<sub>3</sub>** reacted with bis(triphenylphosphine)iminium chloride, [PPN][Cl], to form a hydridoborate compound by Si–H cleavage and formation of Et<sub>3</sub>Si–Cl (Scheme 7). This result demonstrates that the silicon center of the boraindene-bound



**Scheme 7.** Reaction of **2•HSiEt<sub>3</sub>** with a chloride nucleophile.

silane is sufficiently electrophilic to react with a chloride nucleophile. Further studies are needed to assess whether compound **2** is a viable hydrosilation catalyst that operates *via* a S<sub>N</sub>2-Si mechanism.

The previous examples of boron compounds discussed in this section have utilized extensive ligand fluorination to promote strong Lewis acidity. Another strategy alters the charge of the compound to enhance its Lewis acidity, and these cationic boron complexes, called borenium ions, can display Lewis acidity that is comparable to, or greater than, that of  $B(C_6F_5)_3$ . A planar-chiral ferrocenylborenium catalyst (**3**, Scheme 8) catalyzes ketone hydrosilation in moderate yield (60% for acetophenone) and modest enantiomeric excess (20% *ee*).<sup>[38]</sup> Although a full mechanistic study has not been completed for this catalyst, loss of *H*–Si–CH<sub>2</sub> 3-bond *J*-coupling was observed by <sup>1</sup>H NMR spectroscopy for triethylsilane in the presence of the borenium catalyst **3** at 65 °C, suggesting that a Si–H···B adduct may be formed as a transient intermediate.



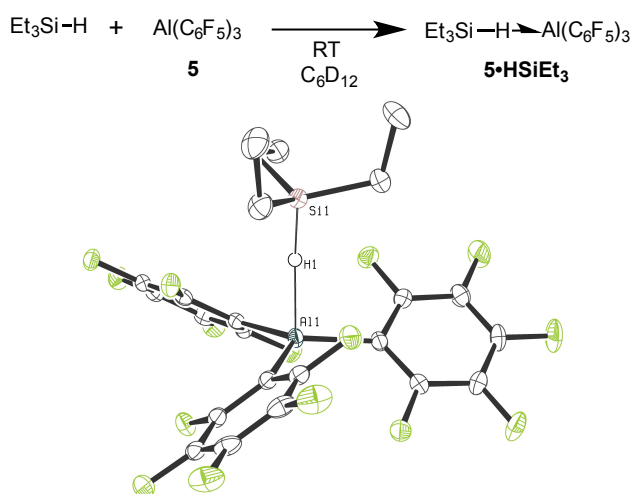
**Scheme 8.** Borenium cation catalysts for ketone hydrosilation.

A second example of a cationic catalyst for ketone hydrosilation features a 9-BBN borenium complex of 2,6-lutidine (**4**, Scheme 8).<sup>[39]</sup> To rule out catalysis by a ketone activation pathway, an independently-synthesized boronate complex was prepared, as this intermediate would be formed upon hydride transfer to a borenium–ketone adduct. Experiments demonstrate that this boronate complex is not catalytically competent, suggesting that the borenium ion catalyst activates the silane substrate instead of the ketone during catalysis.

## 2.2. Aluminum catalysts

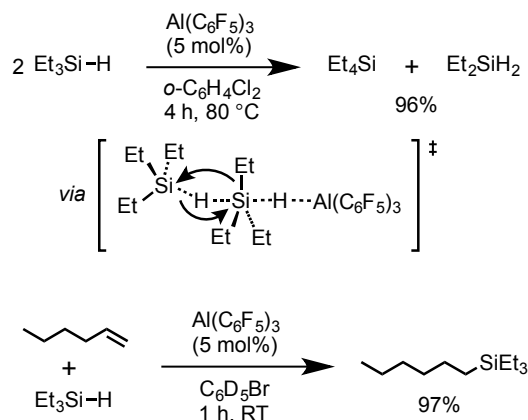
Aluminum compounds are attractive electrophilic catalysts due to their inherently high Lewis acidity. An isolable adduct between triethylsilane and  $Al(C_6F_5)_3$  (**5**), the second-row analogue of the widely-used  $B(C_6F_5)_3$ , has recently been reported.<sup>[28]</sup> The X-ray crystallographic data for Et<sub>3</sub>Si–H···Al( $C_6F_5$ )<sub>3</sub> (**5•HSiEt<sub>3</sub>**) suggest a weak silane–alane interaction, with a Si–H distance of 1.475(16) Å, and an Al–H distance of 1.865(16) Å (Scheme 9). The <sup>1</sup>J<sub>Si–H</sub> coupling constant of the silane–alane adduct in cyclohexane-*d*<sub>12</sub> indicates that the Si–H bond is partially activated by interaction with  $Al(C_6F_5)_3$  (*J*<sub>Si–H</sub> = 180 Hz for free Et<sub>3</sub>SiH versus 104 Hz for Et<sub>3</sub>Si–H···Al( $C_6F_5$ )<sub>3</sub>). Note that structural and spectroscopic data for the Si–H bond in

silane-alane adduct **5**•HSiEt<sub>3</sub> are very similar to those described for the silane-boraindene adduct **2**•HSiEt<sub>3</sub>.<sup>[27]</sup>



**Scheme 9.** Triethylsilane coordination to Al(C<sub>6</sub>F<sub>5</sub>)<sub>3</sub>.

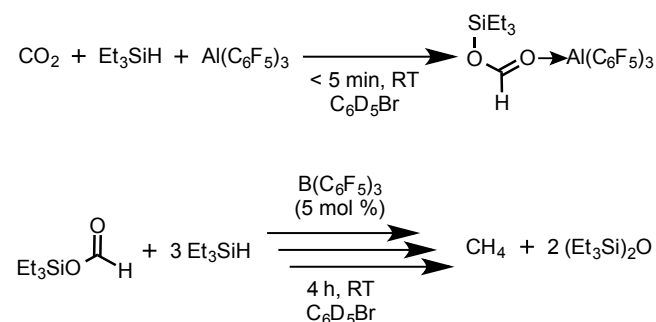
Reactivity studies demonstrate that the silicon center is rendered electrophilic upon Si–H coordination to Al(C<sub>6</sub>F<sub>5</sub>)<sub>3</sub> (Scheme 10). Silane redistribution is catalyzed by Al(C<sub>6</sub>F<sub>5</sub>)<sub>3</sub> to convert tertiary silanes into secondary and quaternary silanes. It is noteworthy that B(C<sub>6</sub>F<sub>5</sub>)<sub>3</sub> is essentially inactive for silane redistribution reactions. Additionally, Al(C<sub>6</sub>F<sub>5</sub>)<sub>3</sub> catalyzes the hydrosilation of unactivated alkenes under mild conditions, with a 26-fold rate enhancement relative to B(C<sub>6</sub>F<sub>5</sub>)<sub>3</sub>. For both transformations, the Si–H⋯Al interaction promotes nucleophilic attack by either another equivalent of silane (for redistribution reactions) or alkene (for hydrosilation reactions). Lastly, Al(C<sub>6</sub>F<sub>5</sub>)<sub>3</sub> exhibited substantially diminished reactivity for ketone hydrosilation relative to B(C<sub>6</sub>F<sub>5</sub>)<sub>3</sub> (16% conversion of <sup>t</sup>BuC(O)Me and HSiPhMe<sub>2</sub> after 12 h with Al, versus >95% conversion after



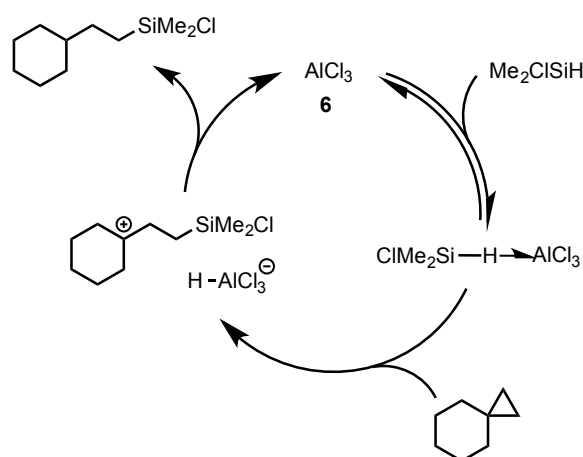
**Scheme 10.** Silane redistribution and alkene hydrosilation catalysed by Al(C<sub>6</sub>F<sub>5</sub>)<sub>3</sub>.

0.1 h with B). This lower activity was attributed to the high oxophilicity of Al(C<sub>6</sub>F<sub>5</sub>)<sub>3</sub>, which disfavors the ketone dissociation that is necessary to form the catalytically-active silane-alane adduct.

The different Lewis acidities of the aluminum compound **5** and its boron congener **1** may be exploited in some reactions. In particular, it was recently reported that **5** and **1** can act together to carry out the reduction of CO<sub>2</sub> to CH<sub>4</sub> using Et<sub>3</sub>SiH as a reductant (Scheme 11).<sup>[40]</sup> Loadings of 5 mol % of each catalyst provide a high yield of CH<sub>4</sub> (94 %) after 5 h at 80 °C in C<sub>6</sub>D<sub>5</sub>Br, while either catalyst alone provided at best a 16 % yield even after longer reaction times. The observed reactivity was attributed to the ability of each catalyst to mediate different portions of the multistep transformation of CO<sub>2</sub> into methane. It was determined that the more Lewis acidic aluminum catalyst **5** can easily activate CO<sub>2</sub> and the silane to undergo a monohydrosilation process at ambient temperatures. This process only occurs stoichiometrically because the resulting silyl formate product is too basic to dissociate from **5**. The less Lewis acidic boron catalyst **1** is incapable of activating CO<sub>2</sub> in this manner, but is capable of mediating the remaining hydrosilations steps to form methane from the initial silyl formate product.



**Scheme 11.** Differing reactivities of the Lewis acids Al(C<sub>6</sub>F<sub>5</sub>)<sub>3</sub> (**5**) and B(C<sub>6</sub>F<sub>5</sub>)<sub>3</sub> (**1**) provide a complete pathway for the reduction of CO<sub>2</sub> to CH<sub>4</sub> using Et<sub>3</sub>SiH.

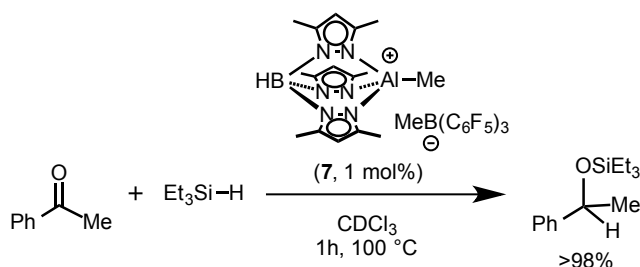


**Scheme 12.** Proposed mechanism of cyclopropyl hydrosilation catalysed by aluminum(III) chloride.



Aluminum(III) chloride (**6**) has been reported to catalyze the hydrosilation of cyclopropanes (Scheme 12).<sup>[41]</sup> Although mechanistic experiments are not reported, this transformation is proposed to proceed *via* silane coordination to  $\text{AlCl}_3$ , followed by electrophilic cyclopropyl ring opening and hydride transfer events.

Lastly, a well-defined cationic aluminum complex supported by a tridentate scorpionate ligand (**7**) has been reported to catalyze hydrosilations of ketones, aldehydes, and imines (Scheme 13).<sup>[42]</sup> Preliminary mechanistic studies indicate that acetophenone does not coordinate to the aluminum catalyst, whereas loss of  $\text{H-Si-CH}_2$  3-bond  $J$ -coupling is observed for triethylsilane in the presence of the catalyst **7** above 45 °C. Additionally, H/D exchange between  $\text{Et}_3\text{SiD}$  and  $\text{Ph}_2\text{SiH}_2$  is catalyzed by **7**. These observations are consistent with a hydrosilation mechanism analogous to that of  $\text{B}(\text{C}_6\text{F}_5)_3$ .



**Scheme 13.** Ketone hydrosilation catalyzed by a cationic aluminum complex.

### 2.3. Silicon catalysts

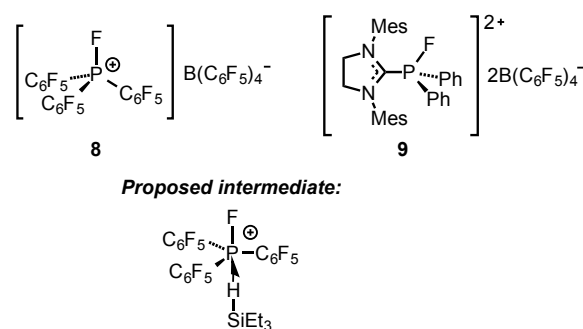
Both neutral and cationic silicon Lewis acids have been demonstrated to catalyze hydrosilations of aldehydes and ketones; however, mechanistic studies suggest that these catalysts activate the carbonyl-containing substrate rather than the silane reagent. For example, our research group has demonstrated that a neutral bis(perfluorocatecholato)silane compound catalyzes hydrosilation of electron-deficient aldehydes.<sup>[26c]</sup> Experiments using a chiral silane substrate,  $(R)\text{-Me}(\alpha\text{-Np})\text{PhSiH}$ , indicate that this reaction proceeds with predominant stereochemical retention at silicon, consistent with an aldehyde activation mechanism. There is evidence that cationic silylium species,  $\text{SiR}_3^+$ , also operate by analogous mechanisms.<sup>[21,43]</sup>

It is possible that other silicon-based catalysts may form electrophilic silane adducts that are catalytically competent. Promisingly, cationic silylium species can coordinate silanes to form nearly linear, symmetrical, hydride-bridged compounds of the form  $[\text{R}_3\text{Si-H-SiR}_3]^+$ . Three crystallographically characterized examples are  $[\text{Et}_3\text{Si-H-SiEt}_3][\text{CHB}_{11}\text{Cl}_{11}]$ ,  $[\text{Me}_3\text{Si-H-SiMe}_3][\text{CHB}_{11}\text{Cl}_{11}]$ , and  $[\text{Et}_3\text{Si-H-SiEt}_3][\text{B}(\text{C}_6\text{F}_5)_4]$ .<sup>[44]</sup> Oestreich has recently proposed that backside attack of a  $[\text{R}_3\text{Si-H-SiR}_3]^+$  species by an imine could be a viable pathway for silylium-catalyzed imine hydrosilation, provided that the silicon substrate is not sterically hindered.<sup>[45]</sup> Thorough mechanistic

studies are needed to assess whether  $\text{Si-H-Si}$  species are viable intermediates during catalysis.

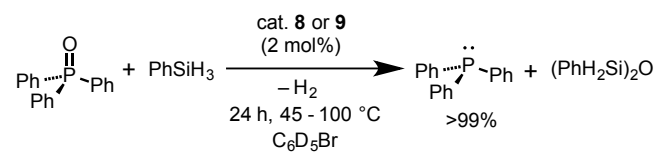
### 2.4. Phosphorus catalysts

Although P(III) compounds are generally Lewis bases, cationic P(III) and P(V) centers can exhibit potent Lewis acidity. Stephan has reported cationic and dicationic phosphonium compounds (**8** and **9**, Scheme 14) as efficient catalysts for the hydrosilation of alkenes, alkynes, ketones, imines, and nitriles.<sup>[46]</sup> The monocationic catalyst **8** requires perfluorinated ligands for strongly Lewis acidic properties, whereas the dicationic phosphonium salt **9** does not require ligand fluorination to attain comparable Lewis acidity. The  $^1\text{H}$  NMR  $\text{Si-H}$  signal of  $\text{Et}_3\text{SiH}$  is broadened, with loss of  $\text{H-Si-CH}_2$  3-bond  $J$ -coupling, upon treatment with  $[(\text{C}_6\text{F}_5)_3\text{PF}][\text{B}(\text{C}_6\text{F}_5)_4]$ , consistent with a  $\text{Si}\cdots\text{H}\cdots\text{P}$  interaction. DFT calculations suggest that the silane substrate interacts with the  $\sigma^*$  orbital opposite the  $\text{P-F}$  bond, and that this interaction results in a stabilization by  $\Delta\text{H} = -15.2$  kcal/mol. DFT studies of the ketone hydrosilation mechanism for  $[(\text{C}_6\text{F}_5)_3\text{PF}][\text{B}(\text{C}_6\text{F}_5)_4]$  have a slightly lower free energy barrier for the silane activation mechanism (19.0 kcal/mol) compared to a ketone activation pathway (21.5 kcal/mol).



**Scheme 14.** Cationic phosphonium hydrosilation catalysts.

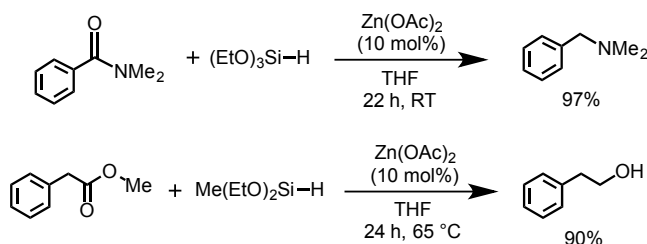
The reduction of phosphine oxides using silane reagents is also catalyzed by phosphonium compounds **8** and **9** (Scheme 15).<sup>[47]</sup> Catalysts **8** and **9** are more active phosphine deoxygenation catalysts than  $\text{B}(\text{C}_6\text{F}_5)_3$ , which is attributed to their greater Lewis acidity. The proposed mechanism is analogous to that suggested for hydrosilations catalyzed by  $\text{B}(\text{C}_6\text{F}_5)_3$ , with the phosphonium-silane interaction promoting nucleophilic attack at silicon by the phosphine oxide.



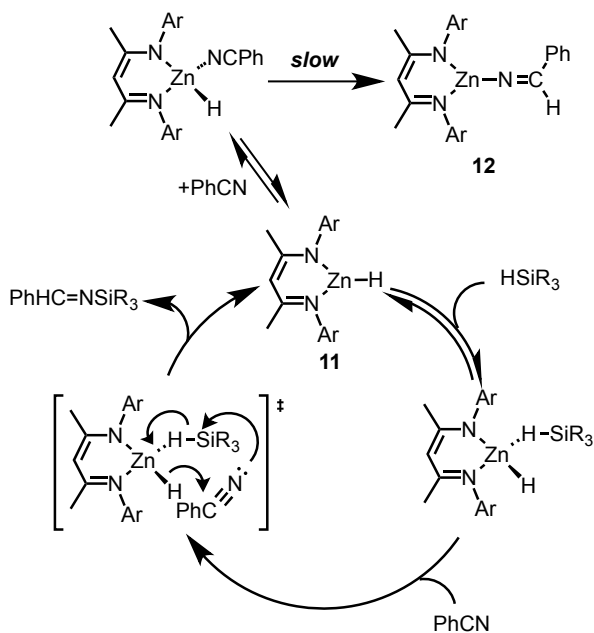
**Scheme 15.** Catalytic deoxygenation of phosphine oxides.

## 2.5. Zinc catalysts

Ionic hydrosilation mechanisms have been implicated in several recent examples of zinc-catalyzed transformations of challenging substrates. Zinc acetate (**10**) catalyzes the reduction of amides to amines<sup>[48a]</sup> and of esters to alcohols<sup>[48b]</sup> using silane reducing agents (Scheme 16). Preliminary mechanistic studies demonstrate that an adduct is formed between zinc acetate and triethoxysilane in THF-*d*<sub>8</sub>, as assessed by <sup>29</sup>Si NMR spectroscopy ( $\delta = 82.2$  ppm, versus 59.2 ppm for free (EtO)<sub>3</sub>SiH). Furthermore, no interaction between zinc acetate and *N,N*-dimethylbenzamide is observed by IR spectroscopy. Based on this evidence, zinc acetate is proposed to operate by an ionic hydrosilation mechanism.



**Scheme 16.** Reduction of amides and esters catalyzed by zinc acetate.



**Scheme 17.** Nitrile hydrosilation catalyzed by <sup>Ar</sup>NacNacZnH (Ar = 2,6-diisopropyl-phenyl).

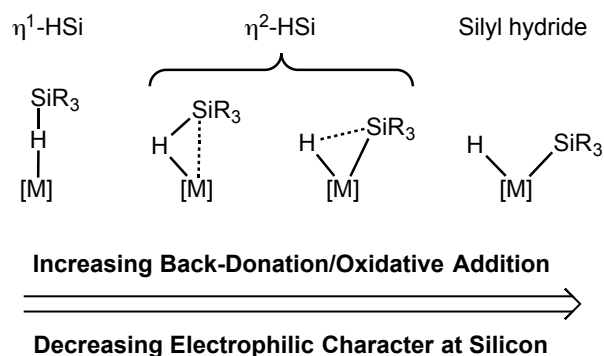
Nikonov and coworkers have reported nitrile hydrosilation to *N*-silyl imine products catalyzed by <sup>Ar</sup>NacNacZnH (**11**, Ar = 2,6-diisopropyl-phenyl), and thorough mechanistic experiments are consistent with an ionic hydrosilation mechanism (Scheme

17).<sup>[49]</sup> Treatment of <sup>Ar</sup>NacNacZnH with benzonitrile results in a vinylideneamido–zinc complex <sup>Ar</sup>NacNacZn–N=CHPh (**12**). However, this reaction is slow, and this zinc amide species fails to react with silanes to regenerate <sup>Ar</sup>NacNacZnH, which rules out a pathway involving insertion of the nitrile into the Zn–H bond. Instead, kinetics experiments are consistent with coordination of the silane to <sup>Ar</sup>NacNacZnH, followed by hydride transfer to the nitrile substrate and simultaneous N–Si bond formation *via* a six-membered transition state.

## 3. Hydrosilations by Electrophilic Transition Metal H–SiR<sub>3</sub> $\sigma$ -Complexes

### 3.1. General Considerations for the Study of Electrophilic Hydrosilation Mechanisms Involving Transition Metals

Many transition metal complexes feature highly electrophilic metal centers, and can conceivably activate Si–H bonds *via* the ionic hydrosilation mechanism demonstrated for main-group Lewis acids (Scheme 2A and Scheme 3). However, the comparatively complex reactivity of d-block metals makes the study of electrophilic Si–H activation more challenging for transition metals vs. main group Lewis acids. The most significant factor that complicates the study of mechanisms for d-block metal catalysts is back-donation from the transition metal center to the Si–H  $\sigma^*$ -orbital, which can compensate for the depletion of electron density from silicon upon coordination of the Si–H bond to the metal (Scheme 18).<sup>[50]</sup> Thus, it cannot generally be assumed that  $\eta^2$ -H–SiR<sub>3</sub> complexes of d-block metals feature a silicon center with substantial electrophilic character.<sup>[50c]</sup> However, cationic character of the metal complex is one obvious factor that correlates with electrophilic character at the silicon center of a coordinated silane. The positive charge on the metal center increases its electron-withdrawing power while also diminishing the strength of back-donation. As described in the following sections, cationic metal catalysts are usually (though not always) involved when electrophilic  $\sigma$ -H–SiR<sub>3</sub> ligands are implicated in transition metal catalyzed hydrosilation reactions.



**Scheme 18.** Comparison of interactions between transition metals and silanes with respect to structure, strength of back-donation, and electrophilicity at silicon.

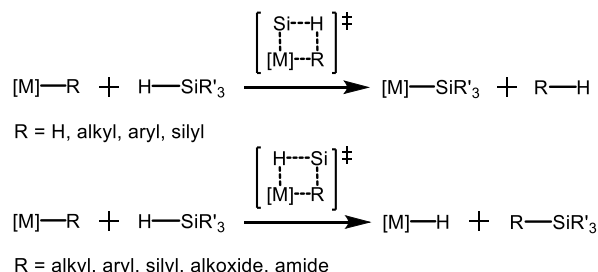
Analysis of bonding in Si—H  $\sigma$ -complexes reveals certain structural features that can be useful for indicating the extent of back-donation from the metal center. It has been shown that the M—Si distance is particularly sensitive to the extent of back-donation to the Si—H  $\sigma^*$ -orbital.<sup>[50a-c]</sup> This can be attributed to size and electronegativity differences between silicon and hydrogen that allow the electron-rich hydrogen atom to easily approach the metal center, while the larger and more electropositive silicon atom makes a greater contribution to the Si—H  $\sigma^*$ -orbital.<sup>[50e]</sup> Thus, it is expected that long M—Si distances (i.e. significantly longer than observed for silyl ligands of a given metal) will correlate with decreased back donation to silicon, and thus more electrophilic character at the silicon center (Scheme 18). Unfortunately, structural characterization data is only available for a small number of transition metal Si—H  $\sigma$ -complexes implicated in electrophilic mechanisms,<sup>[51]</sup> thus limiting experimental insight. One of the best characterized examples, [(POCOP)Ir(H)( $\eta^1$ -H—SiEt<sub>3</sub>)]<sup>+</sup>, features a linear Ir—H—Si angle that results in a very long Ir—Si distance (see Section 3.5),<sup>[51a]</sup> but there is no clear evidence that more common side-on bound  $\eta^2$ -H—SiR<sub>3</sub> ligands cannot also be electrophilic. Some complexes that structurally appear to be metal silyl hydride species might even act as sources of electrophilic silicon due to significant contributions from H—[M] $\rightarrow$ SiR<sub>3</sub><sup>+</sup> and [M]—H $\rightarrow$ SiR<sub>3</sub><sup>+</sup> resonance structures.<sup>[51b]</sup>

Oxidative addition of the Si—H bond is another complication to the study of electrophilic Si—H  $\sigma$ -complex mechanisms that results when the transition metal can provide very strong back-donation to the silane. As depicted in Scheme 1, oxidative addition of the Si—H bond is part of the Chalk-Harrod and modified Chalk-Harrod mechanisms for olefin hydrosilation, as well as the closely related Ojima mechanism for ketone hydrosilation (essentially the modified Chalk-Harrod cycle applied to carbonyl substrates).<sup>[17, 18]</sup> This provides a wider range of mechanistic possibilities for transition metal catalyzed hydrosilations than for main group Lewis acids. As a result, it is more difficult to clearly demonstrate when the electrophilic Si—H activation mechanism operates for transition metal catalysts. This can also be true even for transition metal complexes that do not engage in Si—H oxidative addition because there are other mechanisms available for Si—H activation at a transition metal complex (e.g.  $\sigma$ -bond metathesis,<sup>[52]</sup> or addition of Si—H bonds across metal-main group multiple bonds,<sup>[53]</sup> Scheme 19). Indeed, as described in Section 3.4, there are examples of rhenium-based hydrosilation catalysts for which it is very difficult to confidently distinguish between mechanisms that involve electrophilic Si—H activation, Si—H activation by  $\sigma$ -bond metathesis, or Si—H activation by a Re=O double bond.<sup>[54]</sup>

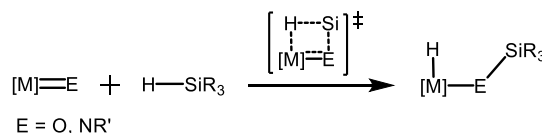
Considering the complexities of studying the mechanisms of transition metal catalyzed hydrosilations, it is unsurprising that the ionic hydrosilation mechanism was not demonstrated for transition metal catalysts until after it was identified for the main group Lewis acid B(C<sub>6</sub>F<sub>5</sub>)<sub>3</sub>. As described in the following sections, detailed studies conducted over the past decade provide convincing evidence for this hydrosilation mechanism involving several different transition metal catalysts, including complexes of tungsten, molybdenum, rhenium, ruthenium, and

iridium. Furthermore, this mechanism appears to be important for enabling some of these catalysts to facilitate hydrosilation reactions exhibiting unique selectivities or involving challenging substrates.

### A Si-H Activation by $\sigma$ -Bond Metathesis



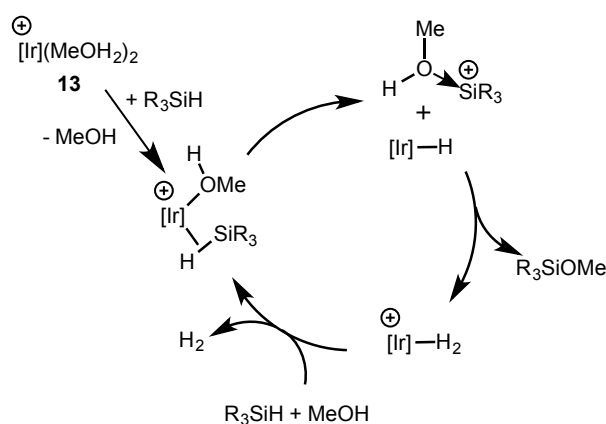
### B Si-H Activation by Metal Oxo or Imido



Scheme 19. Pathways for Si—H cleavage without oxidative addition.

## 3.2. History of the Study of Electrophilic Si—H $\sigma$ -Complexes: Catalytic Silane Hydrolysis and Alcoholysis

Before describing studies that reveal the involvement of electrophilic transition metal Si—H  $\sigma$ -complexes in hydrosilation reactions, it is worth highlighting the historical origins of these mechanisms in work on Si—H/O—H dehydrocoupling reactions (e.g. silane hydrolysis and alcoholysis). The first study of silane alcoholysis to implicate an electrophilic  $\eta^2$ -H—SiR<sub>3</sub> complex was reported by Crabtree in 1989 using the cationic iridium complex [(Ph<sub>3</sub>P)<sub>2</sub>(MeOH)<sub>2</sub>IrH<sub>2</sub>][SbF<sub>6</sub>] (**13**, Scheme 20) as a catalyst.<sup>[55]</sup>

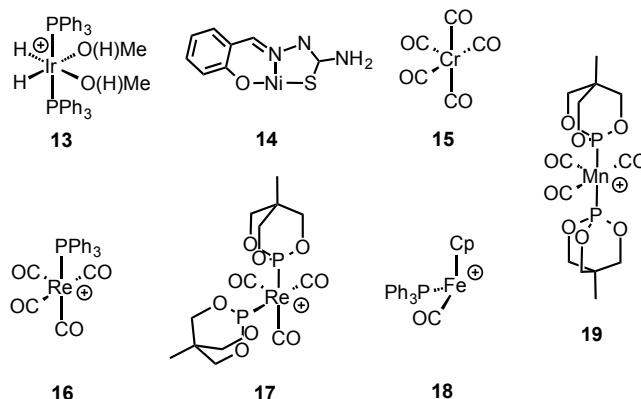


Scheme 20. Catalytic cycle for Ir<sup>+</sup>-catalyzed alcoholysis.

Previously known silane alcoholysis catalysts were believed to operate by mechanisms involving Si—H oxidative addition, but a number of observations suggested that **13** operates by a different mechanism than these other catalysts: 1) the cationic iridium complex exhibited considerably higher activity for the catalytic dehydrocoupling (TOF > 100,000 h<sup>-1</sup> for some substrates at ambient temperatures in CD<sub>2</sub>Cl<sub>2</sub>) than observed for previous catalysts (low or no activity without heating); 2) the iridium complex was inactive for olefin hydrosilation and weakly active for ketone hydrosilation reactions that were usually believed to involve Si—H oxidative addition steps; 3) prior studies of the iridium complex revealed that it does not engage in oxidative addition of reactive substrates such as H<sub>2</sub> or even CH<sub>3</sub>I.<sup>[56]</sup> Thus, a mechanism that does not involve Si—H oxidative addition was sought to account for the dehydrocoupling activity of the iridium catalyst.

It had previously been recognized that the cationic iridium center of [(Ph<sub>3</sub>P)<sub>2</sub>(THF)<sub>2</sub>IrH<sub>2</sub>][SbF<sub>6</sub>] could activate CH<sub>3</sub>I towards nucleophilic attack,<sup>[56b]</sup> and this suggested that this iridium center might similarly activate a silane upon formation of an η<sup>2</sup>-H—SiR<sub>3</sub> complex. Thus, the mechanism of silane alcoholysis was proposed to involve nucleophilic attack of the alcohol substrate on the silicon center of a coordinated silane (Scheme 20). Notably, the proposed mechanism involves intramolecular attack at silicon by an iridium-bound methanol ligand, whereas most subsequent studies of electrophilic Si—H activation involve intermolecular attack of the nucleophilic substrate at silicon. The proposed mechanism was supported by KIE investigations and other kinetics studies, but the proposed [(Ph<sub>3</sub>P)<sub>2</sub>Ir(H)<sub>2</sub>(MeOH)(η<sup>2</sup>-H—SiEt<sub>3</sub>)]<sup>+</sup> intermediate could not be isolated or observed. A bis-η<sup>2</sup>-H—SiEt<sub>3</sub> complex was tentatively observed by <sup>1</sup>H NMR spectroscopy at -80 °C in dry CD<sub>2</sub>Cl<sub>2</sub> in the absence of methanol, but this complex was unstable at room temperature. The fluorosilane Et<sub>3</sub>SiF was identified as a product of the decomposition, thus demonstrating the formation of an electrophilic silicon species capable of abstracting fluoride from the [SbF<sub>6</sub>]<sup>-</sup> anion.

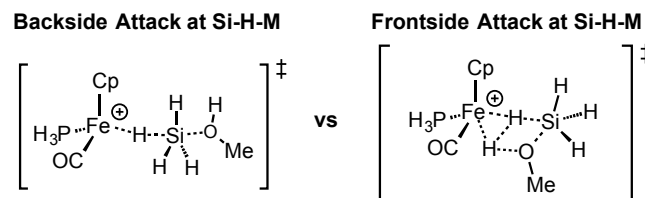
Since Crabtree's seminal study, similar mechanisms have been proposed for silane alcoholysis or hydrolysis involving a variety of different electrophilic catalysts that are shown in Scheme 21. Many of these catalysts feature a cationic metal center that enhances their ability to impart electrophilic character to the silicon center of a coordinated silane.<sup>[57]</sup> However, there are some examples in which this type of mechanism was implicated for neutral metal complexes such as **14**<sup>[58]</sup> and **15**.<sup>[59]</sup> For the neutral Ni(II) based catalyst **14**, it was noted that Si—H oxidative addition was unlikely since the ligand used was not expected to stabilize the unfavorable Ni(IV) oxidation state.<sup>[58]</sup> Other neutral electrophilic catalysts (e.g. Cr(CO)<sub>5</sub> (**15**)) involve relatively low oxidation states for their respective metal centers.<sup>[59]</sup> In these examples, electrophilic character of the metal center and resistance to oxidative addition can be attributed to the presence of several electron withdrawing carbonyl ligands.<sup>[60]</sup>



**Scheme 21.** Electrophilic metal fragments implicated in catalyzing silane alcoholysis reactions via electrophilic Si—H  $\sigma$ -complexes. With the exception of **13**, these illustrations depict the fragment that was proposed to directly activate the Si—H bond, rather than the pre-catalyst added to the reaction.

As with Crabtree's cationic iridium catalyst, the electrophilic η<sup>2</sup>-H—SiR<sub>3</sub> complexes generated from catalysts **14**–**19** were not isolated and fully characterized. The decomposition of the electrophilic η<sup>2</sup>-H—SiR<sub>3</sub> species was often attributed to reaction with adventitious water or to reaction with the counterion.<sup>[57a,d]</sup> Remarkably, the formation of R<sub>3</sub>SiF byproducts was observed in some examples using [B(C<sub>6</sub>F<sub>5</sub>)<sub>4</sub>]<sup>-</sup> as the counterion, which demonstrates that the electrophilic silicon center could cleave even a very strong C—F bond.<sup>[57d]</sup> Despite this high reactivity, the proposed η<sup>2</sup>-H—SiR<sub>3</sub> intermediates were often observed by NMR experiments conducted on samples generated *in situ* at low temperatures (commonly -78 °C in CD<sub>2</sub>Cl<sub>2</sub>),<sup>[57]</sup> and in some examples the Si—H  $\sigma$ -complex was stable at room temperature<sup>[57a]</sup> or could even be isolated.<sup>[57f]</sup> Improved NMR methods allowed for clearer identification of these silane  $\sigma$ -complexes (based on J<sub>SiH</sub> coupling constants)<sup>[50a,c]</sup> than had been possible with the initial study on the cationic iridium system.

The mechanisms proposed for these electrophilic catalysts involve intermolecular attack of the nucleophilic substrate at silicon, instead of intramolecular attack as described for the cationic iridium catalyst **13**. Aside from this difference, the catalytic cycles have usually been depicted as essentially the same as that shown in Scheme 20 regardless of the catalyst used. One exception to this catalytic cycle was implicated by a DFT study of alcoholysis reactions using the cationic iron catalyst [CpFe(PPh<sub>3</sub>)(CO)]<sup>+</sup> (**18**, Scheme 22).<sup>[57c]</sup> This computational investigation suggested that backside attack of

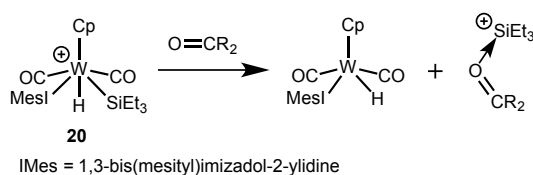


**Scheme 22.** Transition states determined by DFT calculations for electrophilic attack of methanol at the silicon center of the truncated model compound [Cp(H<sub>3</sub>P)(OC)Fe(η<sup>2</sup>-H—SiH<sub>3</sub>)]<sup>+</sup>.

the alcohol substrate on the coordinated Si—H bond was a viable mechanistic pathway, but a frontside attack pathway was also examined. This latter pathway provided concerted Si—H bond cleavage, Si—O bond formation, and Fe—( $\eta^2$ -H<sub>2</sub>) formation, thus bypassing oxonium and terminal hydride intermediates. The frontside attack pathway was determined to have a lower energy barrier by 3.4 kcal/mol, but the authors noted that this could be an unrealistic artifact of truncating the catalyst and silane structures (i.e. replacement of alkyl and aryl groups with H).

### 3.3. Early Transition Metals Involved in Electrophilic Si—H Activation: Tungsten, Molybdenum, and Zirconium.

Mechanisms analogous to those implicated in catalytic silane alcoholysis reactions were not proposed for transition metal catalyzed ketone hydrosilations until more than a decade after the first examples were reported for the former reaction. A few factors appear to have contributed to the lag time between the discovery of these mechanisms for alcoholysis reactions and the implication of similar mechanisms for ketone hydrosilations: other mechanisms were well established for transition metal catalyzed ketone hydrosilations (see Introduction and Section 3.1), it was assumed that ketones were insufficiently nucleophilic for the necessary attack at silicon, and the catalysts used for the alcoholysis reactions exhibited poor activity for ketone hydrosilation reactions. However, in 2003, a report on ketone hydrosilation reactions using molybdenum and tungsten catalysts proposed a catalytic cycle involving transfer of a silyl cation from the metal center to the ketone substrate (Scheme 23).<sup>[61]</sup> This mechanism was proposed in analogy to an ionic mechanism that was identified for ketone hydrogenations using related catalysts, but the hydrosilation mechanism was not investigated in detail aside from the synthesis and characterization of the tungsten silyl complex **20** depicted in Scheme 23.



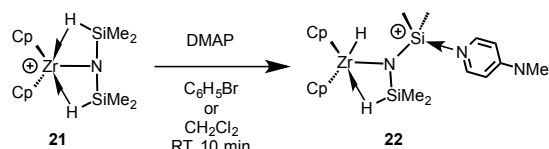
**Scheme 23.** Silyl cation transfer proposed by Bullock.

The mechanism proposed for the tungsten and molybdenum catalysts differs slightly from related mechanisms proposed for main group Lewis acids (Section 2). In particular, it was proposed that the ketone substrate attacks a silyl ligand on the metal center rather than an electrophilic  $\eta^2$ -H—SiR<sub>3</sub> ligand. However, it is conceivable that the isolated silyl hydride complex could exist in equilibrium with an electrophilic  $\eta^1$ - or  $\eta^2$ -H—SiR<sub>3</sub> complex, and that the latter species is actually responsible for activating the ketone substrate. Consistent with this possibility, a

computational study of imine hydrosilations catalyzed by MoO<sub>2</sub>Cl<sub>2</sub> implicated an  $\eta^1$ -H—SiR<sub>3</sub> complex as a key intermediate that transfers a silyl cation to the imine substrate.<sup>[62a]</sup> The authors of this study examined frontside and backside attack of the imine on the M—H—Si moiety, and found that the backside attack pathway was favored by ca. 8 kcal/mol. A recent computational analysis of this mechanism for carbonyl hydrosilations<sup>[62b]</sup> found that the ionic process involved much lower energy barriers than previously studied mechanisms that implicated Si—H activation by the metal-oxo groups of MoO<sub>2</sub>Cl<sub>2</sub>.<sup>[62c,d]</sup> Similar contrasting mechanistic proposals have been studied extensively for rhenium oxo, imido, and nitrido complexes, as discussed in the next section.

Regardless of the exact details, the group 6 metals molybdenum and tungsten appear to be the earliest metals for which hydrosilation catalysis is proposed to occur by a pathway that involves transfer of a silyl cation to the substrate. This is notable since earlier transition metals are more electropositive and favor harder ligands. Thus, it is somewhat surprising that these metals might be involved in the electrophilic activation of a Si—H bond (a soft ligand) or the generation of an electrophilic M—SiR<sub>3</sub> ligand. The positive charge or high oxidation state of the W and Mo catalysts likely contributes to their electrophilic character.

Even earlier metals might activate Si—H bonds towards heterolytic cleavage. For example, it was recently reported that a cationic zirconium complex **21** activates a  $\beta$ -agostic Si—H bond to undergo facile heterolytic cleavage upon attack of 4-(dimethylamino)pyridine at silicon (Scheme 24).<sup>[63]</sup> This process was not incorporated into a catalytic reaction, but this work clearly demonstrates that metals as early as group 4 are able to engage in this type of Si—H activation.

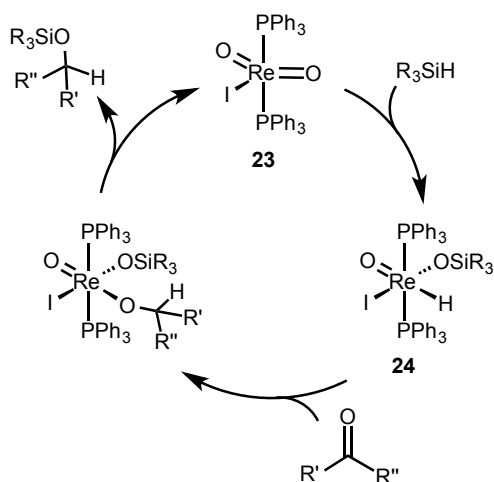


**Scheme 24.** Lewis base induced activation of a  $\beta$ -agostic Si—H bond.

It is interesting that the ionic hydrosilation mechanism may be possible for d<sup>0</sup> early metal catalysts since these catalysts are usually believed to operate by a variation of the Chalk-Harrod mechanism involving Si—C bond formation *via*  $\sigma$ -bond metathesis.<sup>[52]</sup> Note that electrophilic Si—H activation is also relevant to the  $\sigma$ -bond metathesis step since the transition state for this process involves attack by an X-type ligand at the silicon center of an Si—H bond that is interacting with an electrophilic metal center. However, the initial activation of the unsaturated substrate does not involve a silicon electrophile, and thus  $\sigma$ -bond metathesis mechanisms are not discussed further. The possibility that d<sup>0</sup> transition metal catalysts might instead operate by the ionic mechanism appears to warrant further examination.

### 3.4. Electrophilic Si—H Activation by Rhenium

Fascinating studies of hydrosilation mechanisms have been conducted using high-valent rhenium catalysts that feature one or more oxo, imido, or nitrido ligands.<sup>[54]</sup> A variety of mechanisms have been proposed to account for the activity of these catalysts, and these proposals include electrophilic  $\eta^2$ -H—SiR<sub>3</sub> activation by an ionic pathway.<sup>[54c,d]</sup> However, activation of an Si—H bond across a rhenium-ligand multiple bond has also been implicated in the catalytic cycle for these hydrosilations (Scheme 25).<sup>[54a,b]</sup> Several carefully designed mechanistic studies have been reported for these related rhenium catalysts, but a consensus has not yet been reached on the mechanisms of these reactions. This illustrates the difficulties involved in studying hydrosilation mechanisms for transition metal catalysts. Owing to the complexities and contradictory results of studies with rhenium-based catalysts, we consider it appropriate to review these mechanistic studies in detail.

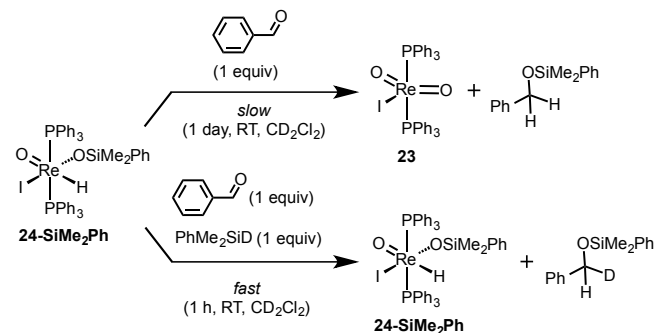


**Scheme 25.** Hydrosilation mechanism proposed for catalyst **23** that invokes Si—H activation across a Re=O double bond.

The first rhenium oxo complex used as a hydrosilation catalyst,  $(\text{Ph}_3\text{P})_2(\text{I})\text{Re}(\text{=O})_2$  (**23**), was reported by Toste and coworkers in 2003.<sup>[54a]</sup> Despite oxo complexes more typically being associated with oxidative transformations, the dioxo complex catalyzed the hydrosilation of aldehydes and ketones with  $\text{Me}_2\text{PhSiH}$  in good yields, though with modest activity (2 – 5 mol % loadings, heating to 60 – 75 °C in benzene). It was suggested that the catalytic cycle might involve activation of an Si—H bond across a Re=O double bond of **23** to afford a hydrido siloxide complex **24** (Scheme 25). Insertion of the carbonyl substrate into the Re—H bond of **24** would provide an alkoxide ligand, which could then abstract the silyl group from the siloxide ligand to form the product and regenerate the Re=O double bond. Subsequent studies from Toste *et al.* provided more detailed experimental support for this mechanism, including observation of Si—H addition across the Re=O double bond, isolation of the resulting rhenium hydride intermediate,

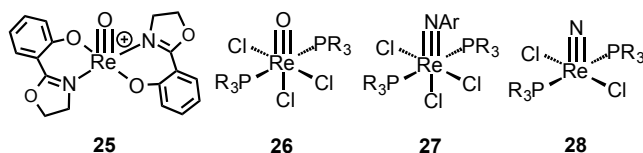
and reaction of this intermediate with benzaldehyde to form the hydrosilation product.<sup>[54b]</sup> Thus, key steps of the proposed catalytic cycle have been observed in stoichiometric processes. Computational studies have also supported the viability of this mechanism.<sup>[64]</sup>

Other researchers have subsequently presented convincing evidence that the mechanism proposed by Toste cannot always be the primary hydrosilation pathway in this system. In particular, Nikonov recently demonstrated that stoichiometric reaction of the observed catalyst resting state  $(\text{Ph}_3\text{P})_2(\text{O}=\text{I})\text{Re}(\text{H})(\text{OSiMe}_2\text{Ph})$  (**24**<sub>SiMe<sub>2</sub>Ph</sub>) with benzaldehyde and  $\text{DSiMe}_2\text{Ph}$  proceeds with formation of the *d<sub>1</sub>* hydrosilation product  $\text{PhMe}_2\text{Si—O—C}(\text{H})(\text{D})\text{Ph}$  and negligible incorporation of deuterium into the hydride position of the rhenium complex (Scheme 26).<sup>[65]</sup> It was also determined in this study that the reaction of the rhenium hydride species **24**<sub>SiMe<sub>2</sub>Ph</sub> with 1 equiv of benzaldehyde occurs at a considerably slower rate than reaction of the rhenium hydride species with 1 equiv of benzaldehyde and 1 equiv of  $\text{PhMe}_2\text{SiH}$  (Scheme 26). This latter finding is consistent with the rate law for the catalytic reaction ( $\text{rate} = k_{\text{obs}}[\text{PhMe}_2\text{SiH}][\text{benzaldehyde}][\text{Re}]$ ) that had previously been reported,<sup>[54b]</sup> but this rate law is actually inconsistent with the catalytic cycle in Scheme 25. The rate law for this catalytic cycle should not include the concentration of silane as a term since the reported resting state of the catalyst (**24**<sub>SiMe<sub>2</sub>Ph</sub>) occurs after addition of silane to the Re=O double bond when  $\text{PhMe}_2\text{SiH}$  is utilized as the substrate. Note that a different rate law and resting state were reported for another silane ( $\text{Ph}_2\text{MeSiH}$ ), and that this resting state and rate law are consistent with the catalytic cycle of Scheme 25. Thus, it is possible that different mechanisms operate for hydrosilation in this system, depending on relatively subtle changes in the substituents at silicon.



**Scheme 26.** Experiments demonstrating that the silyloxy group does not participate in the most efficient hydrosilation pathway in the Toste system.

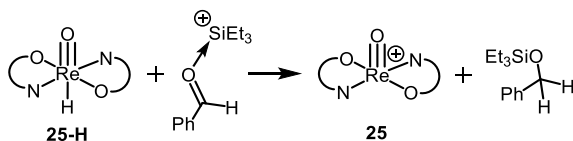
After Toste's initial report of hydrosilation catalysis using **23**, other rhenium oxo, imido, and nitrido complexes (Scheme 27) were investigated as ketone and aldehyde hydrosilation catalysts by Abu-Omar. The first such report featured the rhenium oxo complex **25** in which the metal center is supported by two 2-(2'-hydroxyphenyl)-oxazoline ligands.<sup>[54c]</sup> This complex was more active than **23**, providing moderate to high yields for the hydrosilation of ketones at ambient temperatures with only a



**Scheme 27.** Rhenium-based hydrosilation catalysts implicated in electrophilic Si—H activation mechanisms by the work of Abu-Omar.

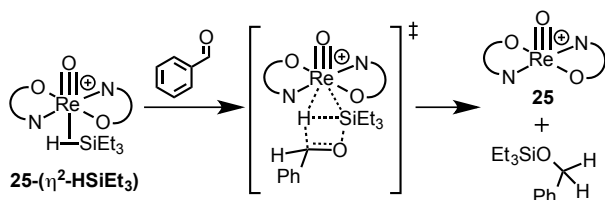
0.1 mol % loading of **25**. The Toste mechanistic proposal was considered in this system, but was ruled out since Si—H activation across the rhenium oxo group was not observed in stoichiometric reactions. Additionally, an  $^{18}\text{O}$  labeling study of silane hydrolysis mediated by this catalyst indicated that the oxo group did not participate in this related transformation.<sup>[66]</sup>

Support for an electrophilic  $\eta^2\text{-H-SiR}_3$  hydrosilation pathway was found by reaction of a hydride derivative of **25** (**25-H**) with an adduct of benzaldehyde and the  $\text{Et}_3\text{Si}^+$  cation (Scheme 28).<sup>[54c]</sup> This reaction produces the expected hydrosilation product, and thus models the key C—H bond forming step of the ionic hydrosilation pathway. Surprisingly though, the authors discounted the possibility of the typical ionic mechanism based on comparisons of hydride transfer from **25-H** or  $\text{Et}_3\text{SiH}$  to the cationic trityl species  $[\text{Ph}_3\text{C}][\text{B}(\text{C}_6\text{F}_5)_4]$ . The trityl cation reacted



**Scheme 28.** Hydride transfer from rhenium to an activated carbonyl group demonstrated by Abu-Omar.

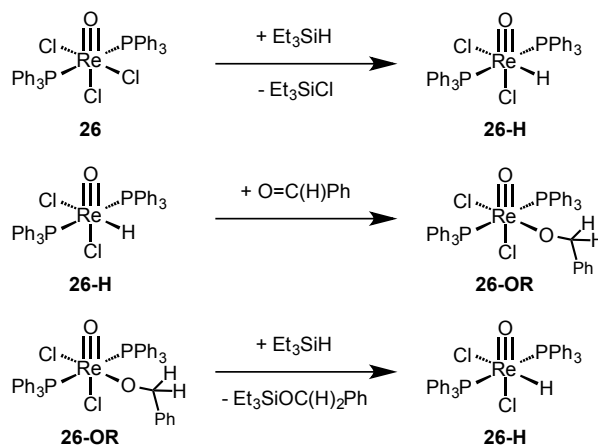
ca. 70 times faster with  $\text{Et}_3\text{SiH}$  than with the rhenium hydride species **25-H**. Thus, the authors conclude that **25-H** is insufficiently hydridic to compete with  $\text{Et}_3\text{SiH}$  for hydride transfer to a possible  $\text{Et}_3\text{Si}\leftarrow\text{O}=\text{C}(\text{H})\text{Ph}$  intermediate. Furthermore, the authors noted that **25** does not act as just an initiator for an  $\text{Et}_3\text{Si}^+$  mediated hydrosilation reaction, since the rhenium catalyst provided a different selectivity than  $\text{Et}_3\text{Si}^+$ -mediated hydrosilations. Thus, a variant of the electrophilic  $\eta^2\text{-H-SiEt}_3$  pathway was proposed, in which frontside attack of the carbonyl substrate at the Re—H—Si moiety of **25-( $\eta^2\text{-H-SiEt}_3$ )** allows Si—H and Re—H cleavage to occur simultaneously with Si—O and C—H bond formation (Scheme 29).



**Scheme 29.** Hydrosilation mechanism proposed for catalyst **25** involving simultaneous C—H bond formation and Si—H cleavage.

However, it may not be necessary to exclude the possibility of a more typical two-step, ionic hydrosilation mechanism for catalyst **25**. Due to steric effects, the kinetics of hydride transfer to  $\text{Ph}_3\text{C}^+$  do not always correlate with thermodynamic driving forces on the basis of hydride donating ability. Therefore, the rates of hydride transfer measured from  $\text{Et}_3\text{SiH}$  or **25-H** to  $\text{Ph}_3\text{C}^+$  do not necessarily reflect the rates that would be observed using other hydride acceptors, and hydride transfer to a less sterically hindered silylcarboxonium ion intermediate,  $[\text{Et}_3\text{Si}\leftarrow\text{O}=\text{CRR}]^+$ , may be significantly faster.<sup>[67]</sup> Furthermore, Abu-Omar demonstrated that  $\text{Et}_3\text{Si}^+$  abstracts hydride from **25-H** to form  $\text{Et}_3\text{SiH}$  and the cationic rhenium species **25**. Since **25-H** is a stronger hydride donor than  $\text{Et}_3\text{SiH}$ , there is no reason to rule out the standard electrophilic  $\eta^2\text{-H-SiR}_3$  hydrosilation pathway (i.e. the two-step ionic mechanism) that features backside attack of the carbonyl substrate at the silicon center of a putative adduct **25-( $\eta^2\text{-H-SiEt}_3$ )**.

In subsequent work, Abu-Omar investigated the hydrosilation mechanisms of several closely related rhenium catalysts (**26–28**, Scheme 27) that feature rhenium-ligand multiple bonds.<sup>[54d]</sup> These complexes catalyze the hydrosilation of benzaldehyde at ambient temperature in  $\text{CD}_2\text{Cl}_2$  with a 1 mol % catalyst loading, though the activity was found to be moderate. Derivatives of **27** were the most active (99 % yield after 0.5 – 1 day), followed by the oxo derivatives (99 % yields after 2 – 5 days), and then the poorly active nitrido complexes ( $\leq 29$  % yield after ca. 5 days). Activation of the silane at the oxo, imido, or nitrido groups was not observed in these systems, thus ruling out the involvement of a Toste-type catalytic cycle. Instead, stoichiometric reactions of **26** (Scheme 30) provide a complete mechanism for generation of a rhenium hydride complex and its hydrosilation activity for a carbonyl substrate. However, upon careful investigation of the kinetics of these individual reaction steps, Abu-Omar concluded that they could only account for ca. 20 % of the hydrosilation activity observed in this system. Additionally, the imido and nitrido complexes **27** and **28** were active hydrosilation catalysts, but did not exhibit all of the reactivity illustrated in Scheme 30 for the oxo derivative **26**. Thus, it was



**Scheme 30.** Stoichiometric reactions demonstrating a possible hydrosilation mechanism using catalyst **26**. All reactions were conducted in  $\text{CH}_2\text{Cl}_2$  or  $\text{CD}_2\text{Cl}_2$  at 25 °C.

proposed that the ionic mechanism involving an electrophilic  $\eta^2$ -H—SiEt<sub>3</sub> intermediate is the primary hydrosilation pathway using catalysts **26–28**. These results parallel those of the Toste system, in which insertion of a carbonyl group into a Re—H bond appears to be a viable step in the hydrosilation mechanism, but is eliminated as the primary reaction pathway (for at least some substrates) by careful analyses of reaction kinetics.

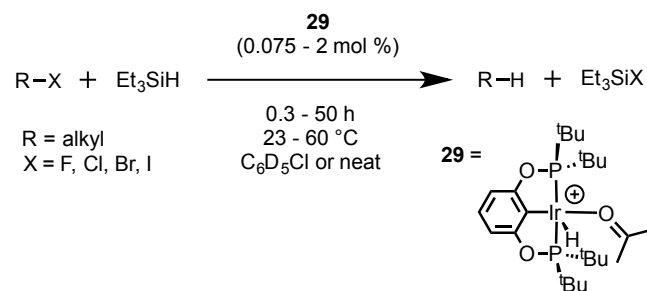
Computational studies (DFT) by Wei *et al.* investigated different possible mechanisms for some of the rhenium catalysts.<sup>[68]</sup> One study examined the electrophilic Si—H  $\sigma$ -complex pathway and the Toste mechanistic proposal for hydrosilation of imines and aldehydes using catalyst **23**.<sup>[68a]</sup> The authors concluded that the electrophilic Si—H activation pathway involving an  $\eta^1$ -H—SiR<sub>3</sub> complex is most favorable for the hydrosilation of imines, while the Toste proposal is slightly more favorable for benzaldehyde as the substrate. These results are consistent with experimental observations that indicate the possibility of different hydrosilation mechanisms depending on variations in the reaction substrates. A similar DFT study was used to examine carbonyl hydrosilation reactions mediated by **26**.<sup>[68b]</sup> This study found that hydrosilation involving attack of the carbonyl substrate at an electrophilic  $\eta^1$ -H—SiR<sub>3</sub> ligand was significantly more favorable than a pathway involving insertion of the carbonyl substrate into a Re—H bond. Thus, theoretical and experimental investigations provide reasonably strong support for the involvement of electrophilic Si—H  $\sigma$ -complexes in at least some hydrosilation reactions catalyzed by high-valent rhenium oxo-complexes. However, there is need for further investigation to clearly demonstrate when such intermediates are involved.

### 3.5. Electrophilic Si—H Activation by Iridium Complexes

Amongst transition metal catalysts, the most thoroughly studied and well supported examples of the ionic hydrosilation mechanism involve cationic iridium complexes.<sup>[13, 14]</sup> These catalysts are effective for hydrosilation and reduction reactions involving a range of substrates (aldehydes and ketones,<sup>[69]</sup> esters,<sup>[10]</sup> amides,<sup>[11]</sup> CO<sub>2</sub>,<sup>[12]</sup> ethers,<sup>[70]</sup> and alkyl halides<sup>[71]</sup>) that rival the breadth of those studied in B(C<sub>6</sub>F<sub>5</sub>)<sub>3</sub>-catalyzed hydrosilations. The earliest of these iridium studies was published a few years after the first reports implicating ionic hydrosilation with rhenium catalysis.<sup>[70a, 71a]</sup> Unlike the studies with rhenium, there is clear evidence that iridium hydrosilation catalysts operate by some variation of the ionic mechanism. Notably, the supporting evidence includes the isolation and structural characterization of an iridium  $\eta^1$ -H—SiR<sub>3</sub> complex.<sup>[51a]</sup> Subsequent mechanistic studies indicate that modifications of the standard ionic hydrosilation mechanism might be necessary for some iridium catalysts,<sup>[72]</sup> though the basic features of the mechanism are still well supported. This section describes the important contributions made to the study of ionic hydrosilation mechanisms using electrophilic iridium catalysts.

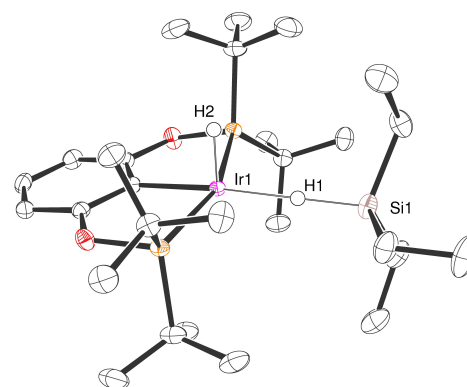
The most well-studied electrophilic Ir hydrosilation catalyst is [(POCOP)Ir(H)(acetone)]<sup>+</sup> (**29**, Scheme 31). These hydrosilation studies were initiated when Brookhart *et al.* reported the use of **29** for C—X (X = F, Cl, Br, I) reduction reactions that utilized

silanes as reducing agents (Scheme 31).<sup>[71a]</sup> For alkyl bromide and chloride substrates, these reactions proceeded quantitatively after ca. 0.3 – 20 h at 23 – 60 °C with a 0.5 mol % catalyst loading in C<sub>6</sub>D<sub>5</sub>Cl or using neat substrate as solvent. Fluoride and iodide substrates were less reactive (92 – 99 % conversion after 2 days at 60 °C) due to lower inherent reactivity (alkyl fluorides) or inhibition of catalysis by coordination of the substrate to iridium (alkyl iodides). For these reactions, the ionic hydrosilation mechanism was supported by kinetic measurements and *in situ* formation and observation of several key iridium complexes that were invoked as intermediates.



**Scheme 31.** Reduction of alkyl halides with silanes and a cationic iridium catalyst.

Shortly after the initial study with **29**, a key intermediate [(POCOP)Ir(H)( $\eta^1$ -H—SiEt<sub>3</sub>)]<sup>+</sup> (**30**) was isolated and structurally characterized (Scheme 32).<sup>[51a]</sup> This discovery represents the first time that a clearly electrophilic Si—H  $\sigma$ -complex was isolated and structurally characterized. It is notable that this synthetic accomplishment came shortly after initial reports invoking the ionic hydrosilation mechanism in this system. The analogous adducts of silanes bound to boranes and alanes would not be structurally characterized until several years later, which is 20 years after ionic hydrosilation was first invoked for B(C<sub>6</sub>F<sub>5</sub>)<sub>3</sub>! The groundbreaking discovery of **30** revealed that the electrophilic Si—H  $\sigma$ -complex has a linear Ir—H—Si moiety that precludes back-bonding from iridium to the Si—H bond. Thus,

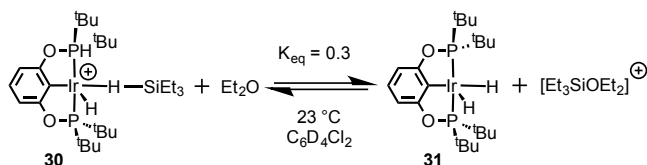


**Scheme 32.** Crystallographically determined structure of the key electrophilic intermediate [(POCOP)Ir(H)( $\eta^1$ -H—SiEt<sub>3</sub>)]<sup>+</sup> **30**.



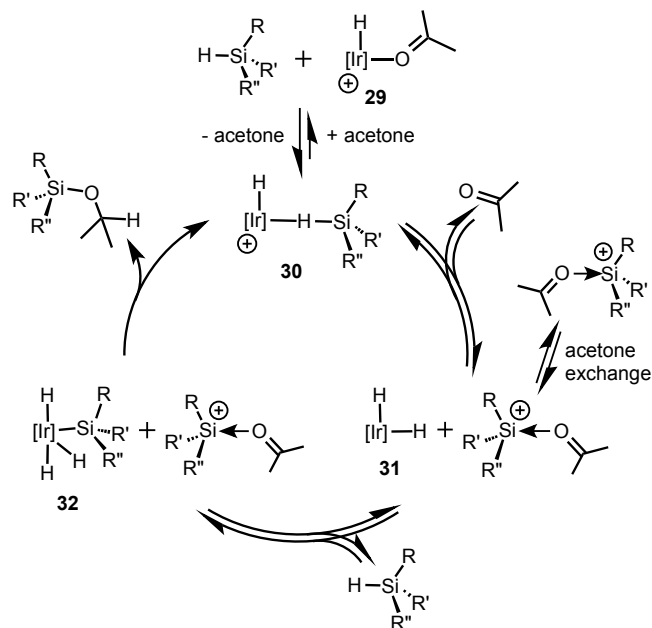
the iridium center acts solely as a strong Lewis acid, and similar linear B—H—Si and Al—H—Si angles are found in the silane adducts with boranes and alanes (see Sections 2.1 and 2.2). Further similarities between **30** and the main group Lewis acid adducts are found upon inspection of the interatomic distances resulting from the Ir—H—Si moiety: the Si—H1 distance (1.48(3) Å) is not elongated, while the Ir—H1 distance (1.94(3) Å) is much longer than the Ir—H2 distance (1.425(18) Å) of the terminal hydride.

The catalyst **29** was subsequently examined for use in ether cleavage reactions<sup>[70a]</sup> and hydrosilations of aldehydes and ketones.<sup>[69]</sup> Both of these classes of reactions were typically found to proceed to high conversion after < 3 h at 23 °C using 0.5 – 1 mol % loading of **29** in C<sub>6</sub>D<sub>5</sub>Cl or C<sub>6</sub>D<sub>4</sub>Cl<sub>2</sub>, though some less reactive substrates were also noted. These studies include detailed mechanistic investigations that provide strong support for the ionic hydrosilation mechanism in this system. For the ether cleavage reactions, it was shown that **30** and diethyl ether exist in equilibrium with a neutral iridium dihydride (**31**) and an ether stabilized silyl cation ([Et<sub>2</sub>OSiEt<sub>3</sub>]<sup>+</sup>, Scheme 33).<sup>[70a]</sup> The latter species was crystallized from the catalytic reaction mixture to provide unambiguous proof of the formation of this intermediate under catalytic conditions. Completion of the cycle involves transfer of a hydride from **31** to [Et<sub>2</sub>OSiEt<sub>3</sub>]<sup>+</sup>, and this hydride transfer was found to be ca. 30,000 times faster from **31** than from Et<sub>3</sub>SiH. Note, however, that Et<sub>3</sub>SiH was invoked as the key hydride donating species for less basic and more hindered ether substrates (e.g. EtOSiEt<sub>3</sub> and MeOPh).



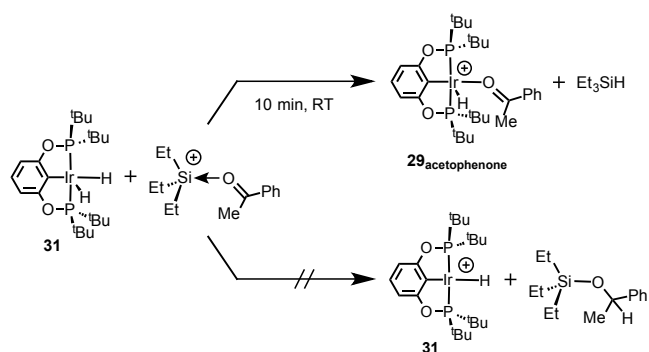
**Scheme 33.** Observation of heterolytic Si—H activation by iridium complex **30** and Et<sub>2</sub>O.

Mechanistic studies of ketone hydrosilations using **29** also point to the involvement of the ionic hydrosilation mechanism, though the initial report did not provide evidence as detailed as that obtained for ether substrates.<sup>[69]</sup> A follow-up study on the ketone hydrosilation mechanism using **29** was conducted by Oestreich *et al.*, and concluded that a complex variation of the ionic mechanism occurs in this system (Scheme 34).<sup>[72]</sup> One major finding of this study is that chiral silanes undergo full or partial racemization of the silicon center under the catalytic conditions reported by Brookhart (23 °C in C<sub>6</sub>H<sub>5</sub>Cl), rather than inversion of chirality as expected for the simplest version of the ionic hydrosilation mechanism. This result suggests that the intermediate [R<sub>3</sub>Si←O=CR'R'']<sup>+</sup> undergoes ketone exchange *via* an S<sub>N</sub>2 mechanism that results in multiple inversions of chirality at silicon prior to the hydride transfer step that forms the product.



**Scheme 34.** Modified ionic hydrosilation mechanism proposed by Oestreich based on experimental studies of catalysis using **30**.

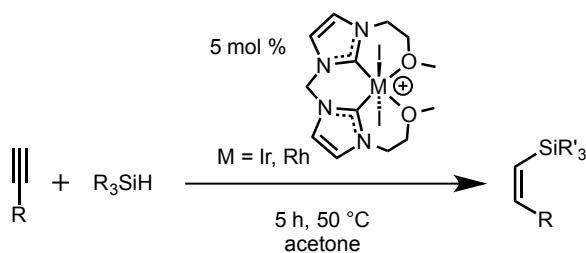
The authors of this study also argue that the hydride transfer does not involve the neutral iridium dihydride, **31**, as had initially been believed. This conclusion was based on the observation that [Et<sub>3</sub>Si←O=C(Me)Ph]<sup>+</sup> reacts rapidly with **31** to form Et<sub>3</sub>SiH and an iridium-acetophenone complex (**29**<sub>acetophenone</sub>) in a process that is the reverse of ketone attack at silicon (Scheme 35). Thus, the neutral dihydride complex **31** does not appear to rapidly transfer a hydride to the activated ketone. Instead, it was suggested that addition of R<sub>3</sub>SiH to **31** forms an Ir(V) silyl trihydride (**32**) with enhanced hydricity. This possibility is supported by DFT calculations confirming that the proposed intermediate, **32**, is more hydridic than **31**. However, it is worth noting that the hydride ligands of **32** would be much less sterically accessible than those of **31**. Additionally, Brookhart *et al.* reported that the catalyst resting state is the ketone complex



**Scheme 35.** Transfer of a hydride from complex **31** to the silicon center of [Et<sub>3</sub>Si←O=C(Me)Ph]<sup>+</sup> rather than to the carbonyl carbon.

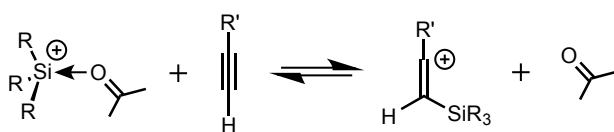
**29<sub>ketone</sub>** such that the proposed mechanism in Scheme 34 might result in a rate law that is second order in  $[R_3SiH]$ , whereas a first order dependence on the silane concentration had previously been determined. These two points were not addressed by Oestreich *et al.*, and thus additional work is needed to assess the involvement of **32** as an intermediate.

Another variation of the ionic hydrosilylation mechanism was proposed by Oro *et al.* to account for iridium and rhodium catalyzed hydrosilylations of alkynes that were only effective using acetone as solvent.<sup>[73]</sup> These transformations proceeded with gentle heating in acetone to provide the monohydrosilylation products in good yields and with high Z-selectivity (Scheme 36),



**Scheme 36.** Z-selective alkyne hydrosilylations mediated by hemilabile cationic iridium and rhodium complexes.

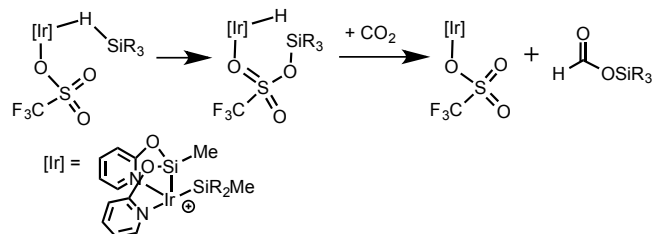
though the selectivity was lower when using the rhodium catalyst. In the proposed mechanism, acetone serves an important role as a shuttle for transferring  $R_3Si^+$  from an  $\eta^1\text{-H-SiEt}_3$  ligand to the alkyne substrate to form a new cationic intermediate  $[R_3Si\text{-(H)C=CR}]^+$  (Scheme 37). The latter species accepts a hydride from the neutral metal complex formed upon transfer of  $R_3Si^+$  to acetone. Support for this proposal came from the observation that the catalysts are resistant to Si—H oxidative addition and also do not react directly with alkynes. The details of the acetone-assisted alkyne hydrosilylation were probed by DFT calculations on the iridium system, and the results indicate that the proposed catalytic cycle can occur with accessible kinetic barriers.



**Scheme 37.** Solvent (acetone) mediated transfer of silyl cation to a hydrosilylation substrate (alkyne).

Oro *et al.* also reported an iridium catalyzed hydrosilylation of  $CO_2$  that was suggested to operate *via* an intermediary Lewis base that initially activates the Si—H bond (Scheme 38).<sup>[12b]</sup> The monohydrosilylation of  $CO_2$  was effective under mild conditions (25 °C, 3 – 8 bar  $CO_2$  in neat  $Me(Me_3SiO)_2SiH$ ) using a 1 mol % catalyst loading, though full conversion was only achieved after 6 days. A coordinated triflate anion was invoked as the base that assists iridium in the heterolytic cleavage of the Si—H bond. This process provides an iridium hydride/silyl triflate complex that simultaneously transfers the silyl cation and the hydride to

$CO_2$  to form the silyl formate product. DFT calculations indicated this pathway as having readily accessible transition states, while other possible mechanisms were predicted to have much higher energy barriers.

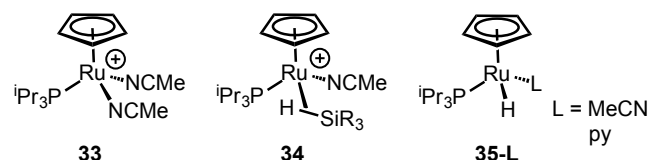


**Scheme 38.** Heterolytic Si—H cleavage assisted by an intramolecular Lewis base (triflate anion).

The above examples demonstrate how the use of a transition metal catalyst can alter the ionic mechanism while preserving its key features. The flexibility of this mechanism might be a key to the wide substrate scope and the selectivities exhibited by some iridium hydrosilylation catalysts. Variations of the ionic mechanism have been proposed for a number of other iridium catalyzed reactions, and examples include challenging and selective hydrosilylations of substrates such as esters,<sup>[10]</sup> amides,<sup>[11]</sup> and  $CO_2$ .<sup>[12]</sup> Additional studies are needed to provide the full details of the ionic mechanism in some of these reactions. However, considering the clear evidence of the ionic mechanism in related iridium catalyzed reactions, it is reasonable to expect that many of these other mechanistic proposals are accurate.

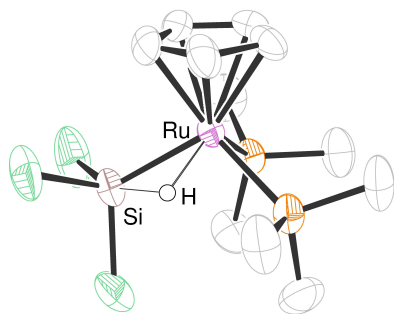
### 3.6. Electrophilic Si—H Activation by Ruthenium Complexes

Electrophilic  $\eta^2\text{-H-SiR}_3$  complexes of ruthenium have only recently been investigated as hydrosilylation catalysts,<sup>[74]</sup> and there are a limited number of reports in the literature. However, these catalysts have been shown to exhibit notable catalytic activity that includes the selective hydrosilylations of pyridines and nitriles.<sup>[75]</sup> Nikonov and coworkers have led most of these studies using the cationic ruthenium complex  $[Cp(\text{Pr}_3P)Ru(\text{NCMe})_2]^+$  (**33**) as a precatalyst (Scheme 39). Oestreich and colleagues have also contributed to this area, though their work involves generation of an electrophilic silicon center *via* Si—H activation across an Ru—S bond rather than by Si—H  $\sigma$ -complex formation.<sup>[76]</sup>



**Scheme 39.** Complexes involved in Nikonov's study of electrophilic hydrosilylation catalysts.

In a 2010 publication, Nikonov and coworkers described the use of **33** in hydrosilations of aldehydes and ketones, as well as for silane alcoholysis reactions.<sup>[74]</sup> These reactions typically proceeded in good yields at ambient temperatures in  $\text{CDCl}_3$  with a 3 – 5 mol % catalyst loading. It was determined that the acetonitrile ligands were labile under the reaction conditions, and thus could be exchanged for silanes to form cationic  $\eta^2\text{-H-SiR}_3$  complexes (**34**) that were spectroscopically observed. The  $\eta^2\text{-H-SiR}_3$  formulation was revealed by Si—H  $J$ -coupling values of ca. 50 Hz, which are much smaller than the ca. 100 Hz  $J_{\text{SiH}}$  values reported for  $\eta^1\text{-H-SiR}_3$  complexes with boranes, alanes, and iridium.<sup>[27, 28]</sup> The greater degree of Si—H activation in **34** is consistent with a structure that had previously been reported for a closely related ruthenium complex  $[\text{Cp}(\text{Me}_3\text{P})_2\text{Ru}(\eta^2\text{-H-SiCl}_3)]^+$  (Scheme 40).<sup>[77]</sup> This structure's short Ru—H ( $d_{\text{Ru-H}} = 1.60(5)$  Å) and Ru—Si ( $d_{\text{Ru-Si}} = 2.329(1)$  Å) distances and elongated Si—H bond ( $d_{\text{Si-H}} = 1.77(5)$  Å) point to significant activation of the Si—H bond. Despite the greater degree of back-donation apparent in **34** relative to many other electrophilic hydrosilation catalysts, DFT calculations showed that the ionic hydrosilation mechanism was favored in this system. Experimental evidence in support of these calculations is limited, consisting only of the observation that silane alcoholysis reactions are faster using more nucleophilic alcohol substrates.

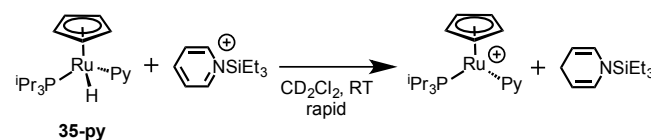


**Scheme 40.** Structure of a cationic  $\alpha$ -silane complex  $[\text{Cp}(\text{Me}_3\text{P})_2\text{Ru}(\eta^2\text{-H-SiCl}_3)]^+$  that is related to the proposed hydrosilation intermediate **34**.

Follow-up studies of the catalytic activity of **33** revealed its utility in challenging hydrosilation reactions such as the conversion of nitriles to N-silyl imines.<sup>[75a]</sup> For most substrates, these reactions provided quantitative yields after 0.3 – 48 h at ambient temperatures in  $\text{CDCl}_3$  with a 3 – 5 mol % loading of **33**. Remarkable selectivity for hydrosilation of the nitrile group was observed, such that aldehyde, ketone, nitro, pyridyl, and alkenyl functionalities in the substrates were unaffected during the reactions. Additionally, the use of one or two equivalents of silane provided perfect selectivity for the formation of an N-silyl imine (monohydrosilation product) or disilyl amine (double hydrosilation product, 24 – 66 h reaction times). A mechanistic study was not undertaken for these transformations, but it was proposed that **33** catalyzes nitrile hydrosilation by an ionic mechanism analogous to that reported for ketone hydrosilations using this catalyst. Consistent with this possibility, more

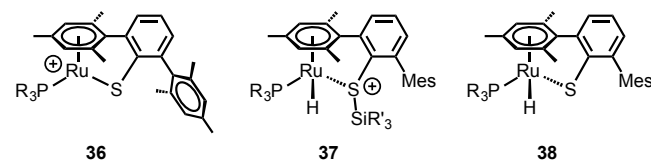
nucleophilic nitrile substrates were observed to reach quantitative conversion more rapidly than electron poor substrates.

Further work by Nikonov and coworkers demonstrated the utility of **33** in the challenging 1,4-hydrosilation of pyridines,<sup>[75b, 78]</sup> and subsequently applied a related catalyst for hydrosilations of phenanthroline, quinoline, acridine, and 1,3,5-triazine.<sup>[75c]</sup> It was observed that many pyridine substrates underwent regioselective 1,4-hydrosilation in excellent yields after 0.5 – 3 h at ambient temperature with a 5 mol % loading of **33** in  $\text{CH}_2\text{Cl}_2$ . However, substitution of the pyridines in the 2-, 4-, and/or 6-positions greatly diminishes the efficacy of 1,4-hydrosilations. This observation is consistent with the ionic hydrosilation mechanism, which might be expected to be less effective when steric hindrance is increased around the 1- and 4-positions of the pyridines. A neutral ruthenium hydride complex  $\text{Cp}(\text{Pr}_3\text{P})(\text{py})\text{RuH}$  (**35<sub>py</sub>**) was found to transfer  $\text{H}^-$  to  $[\text{Et}_3\text{Si}^+\text{py}]^+$  to form the expected 1,4-hydrosilation product (Scheme 41). Thus, a key step of the ionic hydrosilation mechanism could be observed as a stoichiometric process in this system. However, the formation of a C—C reductive coupling product from 4-acetylpyridine was observed, and this suggests that radical processes might also be possible in this system. Therefore, it is difficult to definitively conclude that these hydrosilations occur by an ionic mechanism.



**Scheme 41.** Hydride transfer observed from ruthenium to a silyl-pyridinium substrate.

Oestreich and coworkers have also proposed the involvement of electrophilic silicon species in ruthenium catalyzed hydrosilations and other transformations of silanes and organic substrates.<sup>[79]</sup> They invoke heterolytic activation of an Si—H bond across a Ru—S bond in the catalyst **36** (Scheme 42) to generate a metallasilylsulfonium group that acts as a reservoir of the electrophilic  $\text{R}_3\text{Si}^+$  cation. It is worth noting that this type of Si—H activation is reminiscent of Oro's mechanistic proposals (Schemes 36 and 37), invoking intermediary bases that serve as relays for the  $\text{R}_3\text{Si}^+$  cation. For catalyst **36**, this type of Si—H activation process has been studied in considerable detail that includes *in situ* observation of Si—H activation by NMR spectroscopy, deuterium labeling



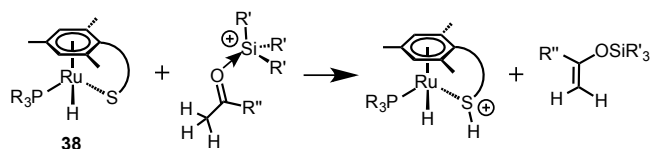
**Scheme 42.** Ruthenium complexes involved in Oestreich's study of bifunctional electrophilic hydrosilation catalysts.

experiments, examination of retention/inversion/racemization using chiral silanes, DFT calculations, and structural characterization of the key ruthenium hydride metallasilylsulfonium intermediate **37**.<sup>[76]</sup> Thus, the bifunctional Si—H activation in this system is well established.

Heterolytic Si—H activation by **36** has been invoked as a key step in a number of catalytic transformations with silane reagents, including hydrosilations of CO<sub>2</sub>,<sup>[79e]</sup> 1,4-hydrosilations of pyridine,<sup>[79d]</sup> dehydrogenative coupling of silanes with enolizable ketones and imines,<sup>[79f,g]</sup> C—F reductions,<sup>[79c]</sup> and C—H silylation reactions.<sup>[79a,b]</sup> These reactions were often found to proceed to high conversions at ambient temperatures or with moderate heating (50 – 80 °C) using 0.5 – 5 mol % loadings of **36**. Aromatic solvents (toluene and benzene) were most often utilized, though some reactions could be carried out in a neat mixture of reagents.

The hydrosilation and defluorination reactions are proposed to occur by a variation of the ionic mechanism in which the intermediate **37** transfers an R<sub>3</sub>Si<sup>+</sup> cation from sulfur to a nucleophilic substrate (e.g. CO<sub>2</sub>, pyridines, alkyl fluoride).<sup>[79c–e]</sup> The resulting [R<sub>3</sub>Si←substrate]<sup>+</sup> intermediate then accepts a hydride from the neutral Ru—H complex **38** to close the catalytic cycle in the same manner as other variants of the ionic hydrosilation mechanism. Despite mechanistic similarities to other ionic hydrosilation catalysts, **36** exhibits some distinct reactivity: unlike with **33**, 1,4-hydrosilations of pyridines with **36** proceed with much greater tolerance for substituents at the 2- and 4-positions;<sup>[79d]</sup> and CO<sub>2</sub> hydrosilation with **36** proceeds with high selectivity for the bis-silyl acetal product (heating to 80 °C) or silyl methyl ether product (heating to 150 °C) depending on the reaction temperature.<sup>[79e]</sup>

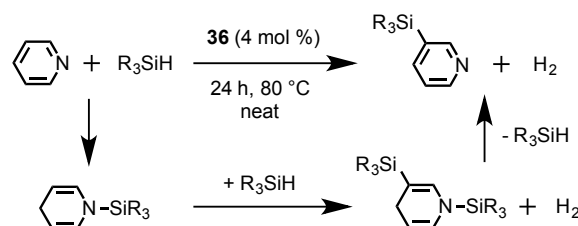
In addition to hydrosilations, catalyst **36** mediates the dehydrogenative silylation of enolizable ketones and imines to provide O-silylated enols and N-silylated enamines, respectively.<sup>[79f,g]</sup> A 0.5 – 1 mol % loading of **36** provided high yields for these reactions at ambient temperatures, and the formation of the enol and enamine products was greatly favored over the formation of hydrosilation products for most substrates examined. This selectivity shows an interesting preference for the neutral hydride intermediate **38** to engage in C—H deprotonation rather than hydride transfer with the [R<sub>3</sub>Si←substrate]<sup>+</sup> intermediate. One possible explanation for this preference is that the thiolate ligand in **38** serves as a base that deprotonates the acidic C—H bonds more rapidly than a hydride can be transferred from the Ru—H position to the substrate (Scheme 43).



**Scheme 43.** Possible explanation for selectivity towards dehydrogenative silylation processes using catalyst **36**.

The C—H deprotonating ability of **38** appears to be important for enabling **36** to catalyze C—H silylation reactions that are not mediated by other electrophilic hydrosilation catalysts. This was first demonstrated with the use of **36** as a catalyst for the C—H silylation of N-protected indoles, which proceeded to high yields at low temperatures (typically  $\leq 50$  °C) with a 1 mol % catalyst loading in neat substrate.<sup>[79a]</sup> These reactions were selective for substitution at the 3-position, which is consistent with a Friedel-Crafts type mechanism involving transfer of R<sub>3</sub>Si<sup>+</sup> to the aromatic  $\pi$ -system of the substrate, followed by C—H deprotonation by the sulfur thiolate ligand in the neutral intermediate **38**. It is worth pointing out that B(C<sub>6</sub>F<sub>5</sub>)<sub>3</sub> does not appear to catalyze this transformation, but instead engages indoles in hydrogenation using silanes as a hydrogen source.<sup>[80]</sup> This supports the possibility that the thiolate ligand in **36-38** might be important for the unique reactivity of **36** as a catalyst.

Remarkably, the C—H silylation methodology has very recently been extended to the selective functionalization of pyridines in the 3-position (Scheme 44).<sup>[79b]</sup> These reactions provided only moderate yields for most substrates after heating to 80 °C for 24 h in neat substrate using a 4 mol % loading of **36**. Thus, these transformations are relatively inefficient in comparison to most of the other silane transformations reported using **36**. However, it is worth pointing out that this regioselective pyridine hydrosilation is a particularly difficult transformation. The authors suggest that this challenging reaction was achieved by a sequence of: 1) 1,4-hydrosilation, 2) Friedel-Crafts silylation of the resulting enamine, and 3) retro-1,4-hydrosilation to provide the 3-functionalized pyridine. Retro-1,4-hydrosilation was also observed by Nikonov with **33** as a catalyst, but the C—H silylation was not reported with **33**.<sup>[75b]</sup> This further supports the conjecture that the thiolate ligand of **36** is important for providing this catalyst with high activity in reactions that involve C—H deprotonation, while also enabling a slightly modified ionic hydrosilation mechanism for carrying out simple hydrosilation reactions.



**Scheme 44.** C—H silylation catalyzed by **36** via a unique hydrosilation/C—H silylation/retro-hydrosilation pathway.

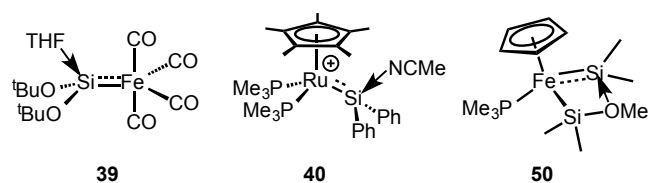
In conclusion, there is good evidence to indicate that the electrophilic ruthenium catalysts **33** and **36** carry out hydrosilation reactions by variants of the ionic hydrosilation mechanism. Additionally, the thiolate ligand in **36** appears to play multiple roles in catalysis, including acting as a base to promote Friedel-Crafts type C—H functionalization. Despite good progress in understanding these systems, there are

questions that remain. In particular, it is unclear why these catalysts are particularly effective for pyridine hydrosilation, while other electrophilic catalysts are much less active for this reaction. Additionally, the relatively large degree of Si—H activation in the  $\eta^2$ -H—SiR<sub>3</sub> complex **34** differs considerably from the silane adducts that have usually been observed for electrophilic catalysts, and it is not entirely clear how this influences hydrosilation reactions in this system. In addition to mechanistic investigations, there have been recent efforts at catalyst development in these systems that have focused on examining N-heterocyclic carbene supported analogues of **33** and **36**.<sup>[81]</sup>

## 4. Hydrosilations Involving Electrophilic Silylene Complexes

### 4.1. Overview of Silylene Complexes: History, Bonding, and Reactivity

Silane  $\sigma$ -complexes are not the only transition metal species that feature highly electrophilic silicon centers. Terminal silylene ligands usually exhibit Lewis acidity at silicon (Scheme 45), and this property features heavily in the reactivity of most silylene complexes.<sup>[15,16,82]</sup> A wide range of nucleophilic substrates (e.g. water,<sup>[83]</sup> alcohols,<sup>[84]</sup> ketones,<sup>[85]</sup> isocyanates,<sup>[86]</sup> olefins,<sup>[87]</sup> nitriles,<sup>[88]</sup> isocyanides<sup>[89]</sup>) undergo activation by the highly electrophilic silicon center of these complexes. However, unlike with electrophilic Si—H  $\sigma$ -complexes, most reports of the reactivity of silylene complexes involve stoichiometric reactions rather than catalysis. The following sections will focus mainly on the reports of catalytic hydrosilation reactivity in which silylene complexes are proposed as intermediates or used directly as catalysts. Some examples of the stoichiometric reactivity of silylene complexes will also be described in order to provide greater insight into the mechanisms of the catalytic reactions.

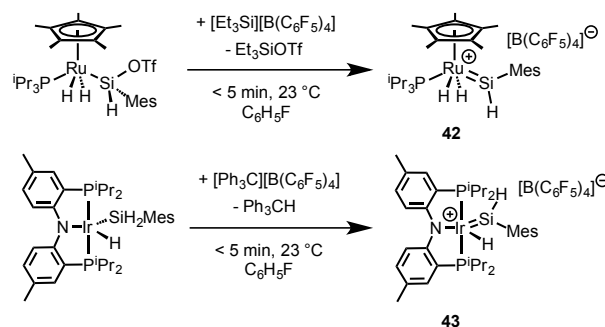


**Scheme 45.** Early examples of base-stabilized silylene complexes.

Before discussing specific examples of reactivity, it is important to provide background on the study of silylene complexes. The chemistry of silylene complexes has been developed since the late 1980's,<sup>[82]</sup> occurring in parallel with the study of electrophilic silane  $\sigma$ -complexes. However, there are considerable differences in the approaches that have been taken in studying silylene complexes and electrophilic  $\sigma$ -complexes. The latter have usually been studied in metal-ligand systems that were found to exhibit catalytic hydrosilation activity prior to observation of the involvement of an electrophilic Si—H  $\sigma$ -complex. Additionally, when the  $\sigma$ -complex could be directly

observed, it was formed relatively easily by mixing a silane with a simple metal complex precursor. In contrast, silylene complexes are very challenging to prepare,<sup>[15]</sup> and studies of these species were not initially focused on hydrosilation reactivity.<sup>[82]</sup> Instead, interest in silylene ligands stemmed from their possible involvement in other catalytic reactions (e.g. Rochow's Direct Process,<sup>[90]</sup> Si—Si bond formation<sup>[91]</sup>), as well as from fundamental interest in examining heavy analogues of carbene complexes. A variety of methods have been developed for preparing isolable silylene complexes,<sup>[15,16]</sup> and it has subsequently been discovered that many of these species participate in stoichiometric and catalytic hydrosilations.<sup>[85e,f,87a,c,d]</sup>

The focus on studying isolated and well-characterized silylene complexes may contribute to the tendency to observe their involvement in stoichiometric transformations rather than catalytic reactions. It is possible that silylene complexes that are better suited to catalytic turnover may be formed as transient intermediates that are difficult to observe. Insight into this possibility is provided by examining the synthetic methods that have been utilized to prepare silylene complexes. Some pathways, such as the capture of a free silylene by a metal complex,<sup>[92]</sup> are unlikely to be involved in catalytic hydrosilations since there are not viable routes by which free silylenes may form *in situ* from typical silanes (i.e. R<sub>n</sub>SiH<sub>4-n</sub>). A much more common route for the formation of silylene complexes involves abstraction of an anionic group (e.g. H<sup>-</sup>, Cl<sup>-</sup>, Br<sup>-</sup>, OTf<sup>-</sup>) from a metal silyl ligand.<sup>[82b,87c,93]</sup> This process has been used to form catalytically active silylene complexes (Scheme 46),<sup>[87c,93c]</sup> but in the catalytic cycles for these hydrosilations, the silylene ligand is regenerated from silanes by two sequential Si—H activations rather than repeated hydride abstractions. There do not appear to be any hydrosilation mechanisms in which anion abstraction from silicon is a part of the catalytic cycle, but there is some evidence that such pathways may be involved in silane redistribution reactions.<sup>[94]</sup>

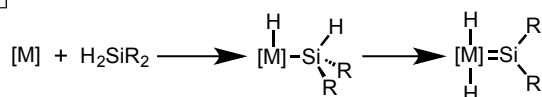


**Scheme 46.** Generation of catalytically active silylene complexes *via* anion abstraction from silyl complexes.

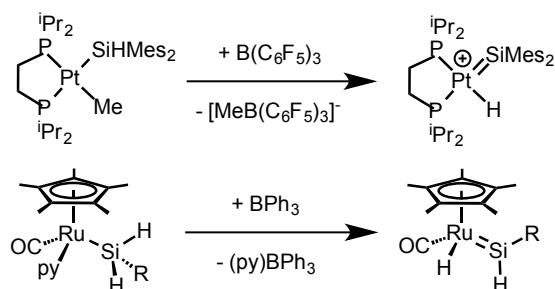
The sequential Si—H activation pathway (Scheme 47) is the most important route for the formation of silylene complexes as catalytic intermediates,<sup>[15]</sup> and thus, primary or secondary silanes are usually reactants in hydrosilation reactions involving silylene complexes. This process has typically been described as occurring by Si—H oxidative addition to form a silyl hydride

complex that then converts to a silylene complex *via* an  $\alpha$ -hydrogen migration step (Scheme 47A). The key  $\alpha$ -hydrogen migration step is well-established in the syntheses of isolable silylene complexes (Scheme 47B),<sup>[88b,95]</sup> and the entire double Si—H activation process has even been demonstrated synthetically (Scheme 47C).<sup>[96]</sup> These latter examples usually involve the elimination of a C—H bond in order to open a coordination site on the metal for  $\alpha$ -hydrogen migration, and this requirement could possibly limit the range of precatalysts from which silylene complexes can form. However, it was very recently demonstrated that H<sub>2</sub> elimination enables the formation of silylene complexes as transient species by reaction of a silane with a simple ruthenium complex (i.e. containing only phosphine and chloride ligands).<sup>[97]</sup> This discovery suggests that it is reasonable to propose that silylene intermediates form *in situ* under conditions commonly used for carrying out hydrosilations.

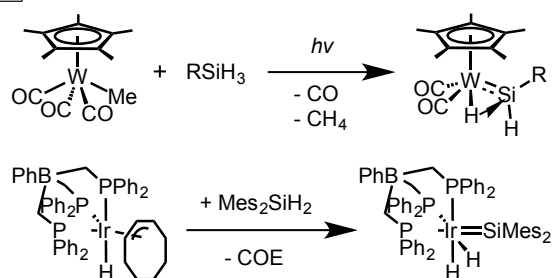
### A General Mechanism



### B Examples of 1,2-Hydrogen Migration



### C Examples of Double Si-H Activations



**Scheme 47.** Formation of silylene ligands by sequential double Si—H activations of a silane.

The bonding in transition metal silylene complexes is important in defining their role as electrophilic intermediates in hydrosilation reactions. The 3-coordinate silicon center is formally engaged in a M=Si double bond, but the  $\pi$ -bond is usually not very strong due to the poor ability of silicon 3p orbitals to engage in  $\pi$ -bonding.<sup>[15,98]</sup> Consequentially, it is easy

to disrupt the  $\pi$ -bond to form a significantly stronger dative  $\sigma$ -bond between silicon and a Lewis base. This is true even for neutral silylene complexes in which the filled d-orbital and silicon p-orbital are energetically well matched for forming a bond. The electrophilic character of the silylene ligand is particularly prominent for cationic complexes in which  $\pi$ -bonding is further weakened by lowering the energy of the filled metal d-orbitals. These systems feature considerable silylium cation character,<sup>[87b]</sup> and this characteristic appears to contribute to the reactivity of the catalytically relevant silylene complexes discussed below.<sup>[87a,c,99]</sup>

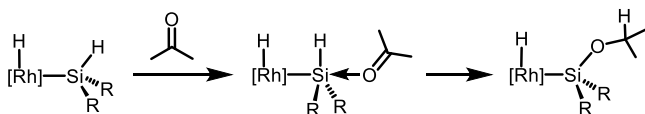
Notably, the absence of strong M→Si back-donation is a characteristic that electrophilic silylene complexes have in common with electrophilic silane  $\sigma$ -complexes. Thus, these observations reveal one important similarity between silylene mechanisms and electrophilic  $\sigma$ -complex mechanisms for hydrosilations. Additionally, the key  $\alpha$ -hydrogen migration step in silylene mechanisms is a type of heterolytic Si—H activation, and this detail provides another similarity between these two types of hydrosilation mechanisms. Furthermore, the  $\alpha$ -hydrogen migration forms a hydride ligand that can be transferred to the unsaturated substrate as part of the hydrosilation mechanism.<sup>[99]</sup> These latter examples exhibit a particularly strong similarity to the  $\sigma$ -complex mechanisms, though some other silylene mechanisms diverge considerably as discussed in Sections 4.3 and 4.4.<sup>[87a,c,d]</sup> Lastly, silylene hydrosilation mechanisms are strongly established for transition metals (rhodium,<sup>[99]</sup> iridium,<sup>[87c,d]</sup> ruthenium<sup>[87a]</sup>) that are the same or similar to those for which the normal ionic mechanism is the most prominent (see Sections 3.5 - 3.6).

## 4.2. Rhodium Silylene Complexes in Ketone Hydrosilations

A number of publications from the past several years implicate rhodium silylene complexes as intermediates in catalytic ketone hydrosilation reactions.<sup>[99]</sup> Though these studies are relatively recent, they have origins in much earlier work on the mechanism of rhodium catalyzed hydrosilations. In particular it has long been recognized that these reactions can occur with different rates and selectivities depending on the use of secondary or tertiary silane substrates.<sup>[100]</sup> These differences might conceivably result from steric effects if the classic Ojima mechanism operates with both classes of silanes, but it is also possible that the observed differences result from mechanistic changes that depend on the type of silane used.

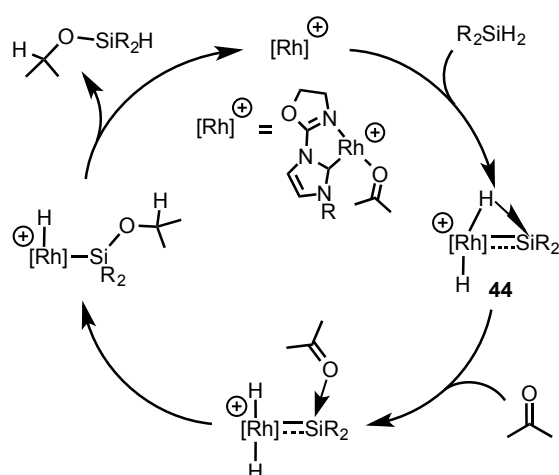
One possible alternative to the Ojima mechanism was proposed by Zheng and Chan in 1995 as part of a study on hydrosilation activity of (Ph<sub>3</sub>P)<sub>4</sub>RhH. The Zheng-Chan mechanistic proposal involves coordination of the ketone to the silicon center of a silyl ligand to generate a 5-coordinate silicon center.<sup>[24]</sup> When utilizing a secondary silane, the 5-coordinate silicon intermediate would possess an Si—H bond, and it was proposed that the carbonyl group could insert into this Si—H bond (Scheme 48). The availability of this mechanism was proposed to account for rate accelerations observed using secondary silanes. Additionally, this mechanism was used to

explain the selectivity observed for some transformations, such as a preference for 1,2-hydrosilation of the carbonyl group of  $\alpha,\beta$ -unsaturated ketones when using secondary silanes, while 1,4-hydrosilation was exclusively favored using tertiary silanes. However, silicon usually must have electronegative substituents (e.g. fluoride, chloride, alkoxide) in order to form low-energy 5-coordinate species,<sup>[101]</sup> and this makes the Zheng-Chan mechanistic proposal unlikely considering the mild conditions employed (ambient temperatures in  $\text{CH}_2\text{Cl}_2$  with  $\leq 0.5$  mol % catalyst loading). Note that there have been some very recent reports that provide evidence for metal complexes with a covalent M—Si bond involving a 5-coordinate silicon center,<sup>[102]</sup> but overall the Zheng-Chan mechanism has not been substantiated.



**Scheme 48.** Key steps of the hydrosilation mechanism proposed by Zheng and Chan.

Silylene complexes might also activate a ketone substrate by coordination of the substrate to a silicon center that is  $\sigma$ -bonded to rhodium. Unlike for the previously proposed silyl intermediates, coordination of the substrate to a silylene ligand is expected to be facile. Thus, the rate acceleration for secondary silanes might derive from their ability to undergo the sequential Si—H activations necessary to form the reactive silylene intermediates during catalysis. This mechanistic possibility was considered by Gade to account for the enantioselective ketone hydrosilation activity of a cationic rhodium catalyst featuring a chiral oxazoline-carbene chelating ligand (Scheme 49).<sup>[99a,b,103]</sup> This system provides good yields with a 1 mol % catalyst loading, even at  $-60$  °C in  $\text{CH}_2\text{Cl}_2$ . The efficiency of the reaction at low

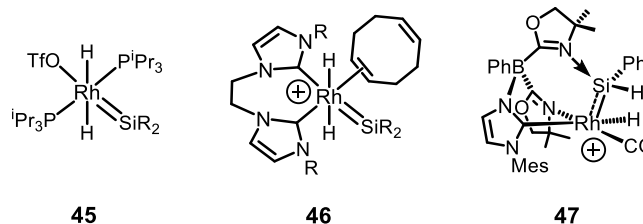


**Scheme 49.** Rhodium silylene hydrosilation mechanism proposed by Gade *et al.*

temperatures is important for achieving high enantioselectivities, and this led to interest in understanding the mechanism that provides such high activity. Some key experimental observations in this system are: 1) Much higher activity with secondary silanes (100 % conversion in  $\leq 1.5$  h at  $0$  °C) than with tertiary silanes ( $\leq 80$  % conversion in 7 h at  $0$  °C), 2) Different enantioselectivities of hydrosilations using secondary silanes (ca. 90 % ee at optimum temperature) versus tertiary silanes (ca. 20 % ee with slight temperature dependence), and 3) An inverse H/D KIE effect for hydrosilations using secondary silanes, but no KIE observed with tertiary silanes.<sup>[99a]</sup>

The silylene mechanism was investigated by DFT calculations, and was found to have lower energy barriers than the Ojima or Zheng-Chan hydrosilation mechanisms.<sup>[99a,b]</sup> The key silylene intermediate (**44**, Scheme 49) is formed by sequential Si—H activations at the cationic rhodium center, but notably, the second Si—H activation was determined to be incomplete in the silylene intermediate. The key Si—O bond forming step was found to involve coordination of the ketone oxygen to the silylene ligand, resulting in completion of the heterolytic cleavage of the second Si—H bond. Coordination of the ketone to silicon activates the carbonyl group to accept the hydride that was transferred to the rhodium center. Interestingly, if one ignores the Rh—Si  $\sigma$ -bond that remains unchanged during this part of the mechanism, then these two steps are very similar to those for Si—H cleavage, Si—O bond formation, and C—H bond formation processes of the ionic hydrosilation mechanism.

The experimental and computational investigations support the involvement of silylene intermediates in these hydrosilation reactions. However, rhodium silylene complexes like those proposed have never been isolated or directly observed, and thus, more definitive evidence supporting the proposed mechanism is elusive. Other researchers have contributed indirect evidence of silylene complex formation using related rhodium catalysts (Scheme 50). Reactions of silanes with bis-phosphine<sup>[104]</sup> and bis-NHC<sup>[99c]</sup> supported rhodium complexes have resulted in observation of dehydrogenative silane oligomerization and olefin hydrogenation processes that are consistent with the activation of both Si—H bonds of a secondary silane at a single rhodium center. Additionally, both studies used  $^t\text{BuMe}_2\text{SiOH}$  to trap the putative silylene intermediates in a silane alcoholysis process that was not observed with tertiary silanes. However, for most of the reactivity observed in these systems, there are other pathways that were not definitively ruled out, even if some of them seem less likely than the silylene pathway.

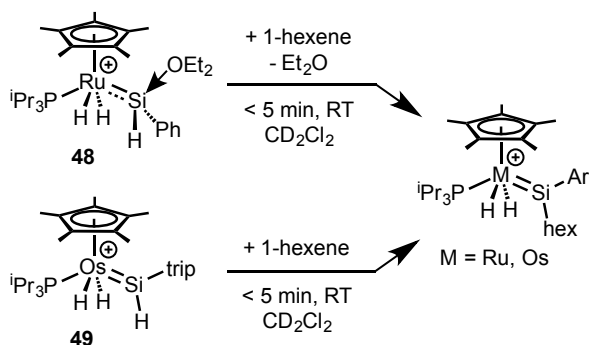


**Scheme 50.** Additional rhodium silylene complexes that have been proposed (**45–46**) or isolated (**47**).

An NHC-bis-oxazolonylborate rhodium silylene complex has recently been reported in which silicon is stabilized by intramolecular coordination of an oxazoline group to the silylene ligand.<sup>[105]</sup> This stabilized rhodium silylene complex was active as a catalyst for deoxygenation of a variety of carbonyl substrates, but it is unclear whether or not the base-stabilized silylene ligand participates in hydrosilations in the same way as an unstabilized silylene complex might. Nevertheless, it is notable that a terminal silylene complex of rhodium was isolated with similar supporting ligands to those used by Gade for catalytic hydrosilation studies. While there is still work to be done to confirm the existence of rhodium silylene intermediates, overall there is fairly good evidence that some catalytic hydrosilations involve rhodium silylene complexes or closely related species.

### 4.3. Group 8 Silylene Complexes in Olefin Hydrosilations

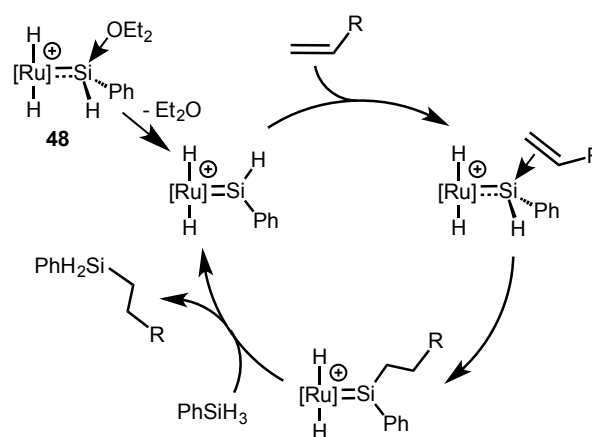
Our research group has studied catalytic olefin hydrosilation reactions involving cationic silylene complexes. As reported in 2003, the ether stabilized silylene complex  $[\text{Cp}^*(\text{iPr}_3\text{P})(\text{H})_2\text{Ru}=\text{Si}(\text{H})(\text{Ph})(\leftarrow\text{OEt}_2)]^+$  (**48**, Scheme 51) provided the first example of an isolated silylene complex that engages in catalytic hydrosilation reactivity.<sup>[87a]</sup> The involvement of a novel mechanistic pathway was evident from unique selectivity and substrate scope in this system (see below). Furthermore, the analogous osmium complex  $[\text{Cp}^*(\text{iPr}_3\text{P})(\text{H})_2\text{Os}=\text{Si}(\text{H})(\text{trip})]^+$  (**49**, trip = 2,4,6- $\text{iPr}_3\text{C}_6\text{H}_2$ , Scheme 51) was observed to undergo a stoichiometric hydrosilation process that models a key part of the mechanism in the ruthenium-catalyzed reactions.<sup>[87a]</sup> Thus, the involvement of a new hydrosilation mechanism was clearly established early on in these studies. Remarkably though, this system continues to offer surprises such as recent evidence that the proposed silylene intermediate  $[\text{Cp}^*(\text{iPr}_3\text{P})(\text{H})_2\text{Ru}=\text{Si}(\text{H})\text{R}]^+$  has considerable character as an  $\eta^3\text{-H}_2\text{Si}(\text{H})\text{R}$  complex  $[\text{Cp}^*(\text{iPr}_3\text{P})\text{Ru}(\eta^3\text{-H}_2\text{Si}(\text{H})\text{R})]^+$ .<sup>[29]</sup> This latter aspect of the work is discussed later in Section 5.2.



**Scheme 51.** Stoichiometric hydrosilation reactions using cationic group 8 silylene complexes.

It was observed that **48** and **49** engage in stoichiometric reactions with 1-hexene to provide new silylene complexes in

which the Si—H group has been converted to a Si—hexyl group. The ruthenium complex **48** can incorporate this process into catalytic hydrosilations, which provided 98 % conversions after 3 – 18 h at 60 °C using 0.5 – 5 mol % loadings of the silylene complex in  $\text{CD}_2\text{Cl}_2$ . These reactions exhibit a number of features that provide insight into the mechanism of the transformations: 1) only primary silanes (i.e.  $\text{RSiH}_3$ ) are effective as substrates, 2) the reactions provide exclusively anti-Markovnikov products, 3) high activity is observed even with the sterically hindered alkene 1-methylcyclohexane as a substrate, and 4) exclusive *syn*-addition of the Si—H bond to the alkene is observed. These observations led to the proposal of a new hydrosilation mechanism in which a key feature is the insertion of the alkene into the Si—H bond of a silylene intermediate (Scheme 52).<sup>[87a]</sup>



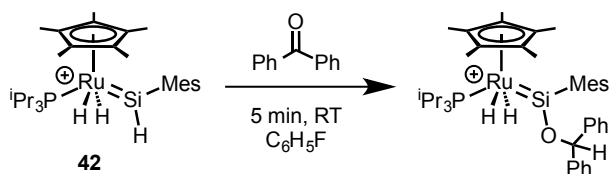
**Scheme 52.** Catalytic cycle for olefin hydrosilation mediated by a ruthenium silylene complex.

The weakly bound  $\text{Et}_2\text{O}$  in **48** is presumed to readily dissociate to provide the active catalyst that forms an intermediate adduct with the alkene substrate coordinated to silicon. The alkene then inserts into the terminal Si—H bond of the silylene ligand, in a process that is closely related to classic alkene hydroborations by  $\text{BH}_3$ . The secondary silane product is eliminated *via* a sequence of 1,2-hydrogen migration from Ru to Si, followed by Si—H reductive elimination. A double Si—H activation process (the reverse of the elimination steps) then regenerates the key silylene intermediate from the primary silane substrate. Notably, this mechanism explains every key observation in this system that is noted above, while other possible mechanisms (e.g. Chalk-Harrod type, ionic hydrosilation, or a hypothetical [2+2] alkene-Ru=Si cycloaddition) fail to explain the substrate scope and selectivities.

In the proposed olefin hydrosilation mechanism, the silylene complex is regenerated by the same type of double Si—H activation pathway as was proposed for rhodium silylene complexes during ketone hydrosilation reactions.<sup>[89a-c]</sup> However, the proposed olefin hydrosilation mechanism is unique in featuring the insertion of the alkene into an unactivated Si—H bond. This latter aspect of the mechanism is distinct from all of

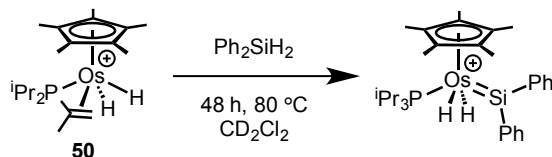


the other well-established electrophilic hydrosilation mechanisms. The ionic mechanism and the rhodium silylene mechanism involve insertion of the unsaturated substrate into an Si—H bond that is first activated by the catalyst. In this regard, the silylene mechanism for alkene hydrosilation is reminiscent of the Zheng-Chan mechanism for ketone hydrosilation, which proposed insertion of a ketone substrate into a terminal Si—H bond.<sup>[24]</sup> Subsequent studies have observed this type of reactivity in stoichiometric transformations of the silylene complex **42** and ketones such as benzophenone (Scheme 53).<sup>[85d]</sup> Note that this latter reactivity was confirmed to involve direct insertion into the Si—H bond of **42** since analogues of **42** that lack a free Si—H bond (i.e. [Ru]=SiRR' derivatives) only form simple adducts with ketones.



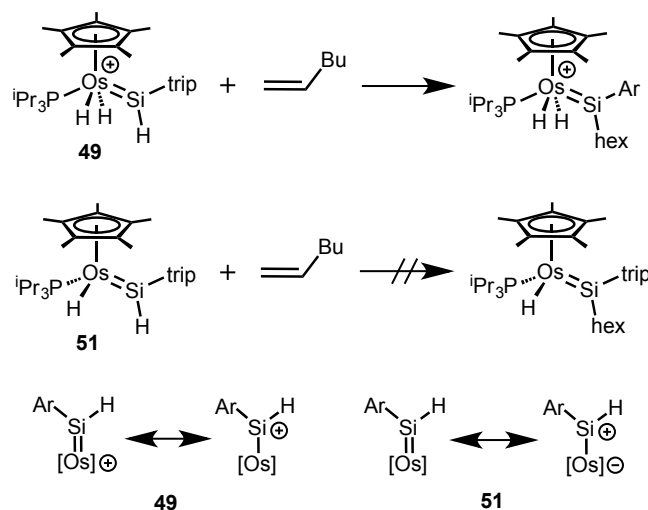
**Scheme 53.** Insertion of a ketone into the Si—H bond of a silylene ligand.

Many of the key steps of the silylene mechanism for olefin hydrosilation have been examined individually using closely related osmium derivatives. For example, a sequential Si—H activation process was observed to form a silylene complex starting from osmium complex **50** that serves as a synthon for the 14-electron fragment [Cp\*(iPr<sub>3</sub>P)Os]<sup>+</sup> (Scheme 54).<sup>[106]</sup>



**Scheme 54.** Demonstrating silylene formation by double Si—H activation using an osmium complex related to **42**.

The alkene insertion process was examined in greater detail by comparing the reactivity of **49** with a neutral silylene derivative Cp\*(iPr<sub>3</sub>P)(H)Os=Si(H)(trip) (**51**) that is formally related to **49** by a difference of one proton (Scheme 55).<sup>[87b]</sup> The neutral complex **51** does not exhibit reactivity with 1-hexene at 80 °C, while the cationic complex reacts rapidly at -78 °C. Calculations suggest that cationic character at Si in **49** is important for the high reactivity exhibited by this silylene complex, whereas in the neutral system this type of resonance structure requires unfavorable charge separation (Scheme 55).<sup>[87b]</sup> The silyl cation resonance structure of **49** results from an absence of  $\pi$ -back-donation from the metal, and this once again illustrates the importance of cationic character in a complex for rendering silicon electrophilic by reducing back-donation.



**Scheme 55.** Comparison of cationic and neutral osmium silylene complexes.

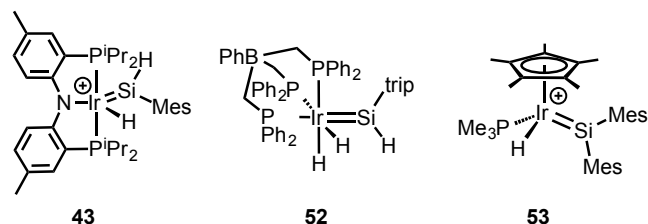
Notably, the adduct between the substrate and silicon in the active system can be described as an olefin coordinated to a silyl cation, and this bonding motif is reminiscent of intermediates in the ionic mechanism in which the substrate is bound to a silyl cation. Evidence for this type of intermediate with **49** was provided by determining  $k_H/k_D = 0.8(1)$  for the reaction with 1-hexene, which is consistent with a secondary KIE involving rehybridization of silicon from a trigonal planar to a tetrahedral geometry.

Computational studies provide support for the proposed role of silylene complexes in olefin hydrosilations.<sup>[107]</sup> Interestingly, however, these studies and a recent structural investigation reveal that the hydrides of the ruthenium silylene complex **42** interact strongly with the empty silicon 3p orbital.<sup>[29,107]</sup> This indicates that these silylene complexes have a significant degree of  $\eta^3\text{-H}_2\text{Si(H)R}$  character, and invites further comparison to other electrophilic Si—H  $\sigma$ -complexes. This aspect of the work on the silylene complex **42** is discussed further in Section 5.2.

#### 4.4. Olefin and Ketone Hydrosilations Using Iridium Silylene Complexes

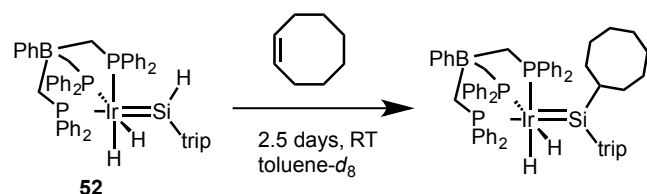
The olefin hydrosilation pathway elucidated for ruthenium and osmium silylene complexes is also possible for silylene complexes supported by other metals such as iridium (Scheme 56). This was demonstrated using the PNP-pincer supported cationic iridium silylene complexes **43**,<sup>[87c,d]</sup> which is an active catalyst for olefin hydrosilations with similar selectivities to those displayed by the ruthenium catalysts **42** and **48**. Further investigation provided additional support for mechanistic similarities between hydrosilations catalyzed by these different silylene complexes. Additionally, the iridium catalyst **43** was examined as a catalyst for carbonyl hydrosilation reactions, and a mechanism similar to the rhodium silylene mechanism may be possible using **43**.<sup>[85e]</sup> These studies support the possibility that a

variety of transition metals can support related reactivity involving silylene ligands.



**Scheme 56.** Iridium silylene complexes involved in olefin and/or ketone hydrosilation reactions.

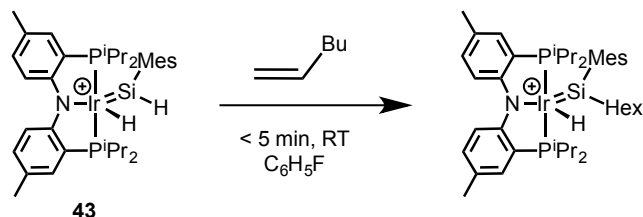
The earliest studies of iridium silylene complexes in hydrosilation reactions predate those of olefin hydrosilations catalyzed by ruthenium complex **42**. A study published in 2002 described the reactivity of the silylene complex  $[\text{BP}^{\text{Ph}}_3]\text{Ir}(\text{H})_2=\text{Si}(\text{H})\text{trip}$  (**52**, formed *in situ* and observed by NMR spectroscopy) with cyclooctene to provide a new silylene complex with a cyclooctyl group on silicon (Scheme 57).<sup>[108]</sup> Possible mechanisms for this transformation were considered, and these include pathways involving addition of the alkene across the Ir=Si bond or isomerization of the silylene complex to a silyl species, followed by Chalk-Harrod type hydrosilation steps. However, considering subsequent work on hydrosilations involving silylene complexes, the hydrosilation reaction observed for **52** likely involves direct insertion of the alkene into the silylene Si—H bond.



**Scheme 57.** Early example of a hydrosilation process observed between a silylene ligand and an olefin.

More detailed investigations of iridium silylene complexes in alkene hydrosilations were reported starting in 2008 using the PNP-supported silylene complex **43**.<sup>[87c]</sup> A 5 mol % loading of this complex was found to catalyze hydrosilations of 1-hexene and styrene at 60 °C in  $\text{C}_6\text{D}_5\text{Br}$ . This process was found to be effective using several primary silanes, but was ineffective with secondary silanes. The catalyst **43** was reported to engage in stoichiometric hydrosilations with 1-hexene and cyclooctene to form new silylene complexes with conversion of the Si—H bond to an alkyl group (Scheme 58). These results point toward a mechanism analogous to that operating for ruthenium silylenes. Additional support for this possibility was provided by DFT calculations, which indicated that the silicon center of **43** is electron deficient, as in **42** and **49**. Follow-up work on this system provided additional support for the proposed mechanism,

and focused on the product-forming, silane-exchange process rather than the Si—C and C—H bond-forming steps.<sup>[87d]</sup>

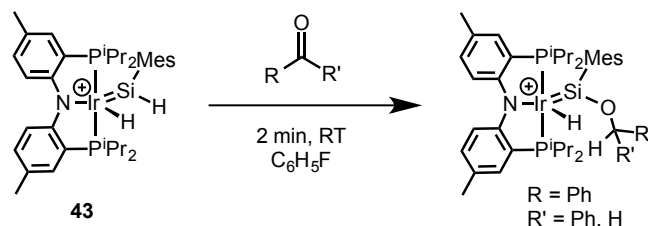


**Scheme 58.** Stoichiometric hydrosilation process observed between catalyst **43** and a terminal alkene.

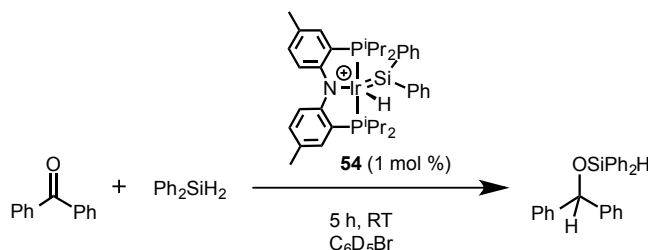
The silylene complex **43** and a closely related  $\text{SiPh}_2$  derivative **54** were examined as catalysts in hydrosilations of carbonyl containing substrates.<sup>[85e]</sup> Note that a different iridium silylene catalyst  $[\text{Cp}^*(\text{Me}_3\text{P})(\text{H})\text{Ir}=\text{SiAr}_2]^+$  (**53**) had previously been examined as a catalyst in ketone hydrosilations.<sup>[85f]</sup> This complex catalyzed the hydrosilation of a number of ketones with  $\text{Ph}_2\text{SiH}_2$ , but mechanistic investigations did not provide very clear insight into the catalytic cycle of these reactions. Thus, it is notable that the studies of **43** and **54** involve significant efforts to understand the mechanisms of hydrosilation reactivity.

Benzophenone and benzaldehyde were found to insert into the Si—H bond of **43** (Scheme 59), but this stoichiometric reactivity did not provide a route for catalytic hydrosilation of these substrates with the primary silane  $\text{MesSiH}_3$ . Complex **43** was, however, effective at catalyzing the hydrosilation of benzophenone with a secondary silane  $\text{Ph}_2\text{SiH}_2$ . Higher yields were obtained when  $\text{Ph}_2\text{SiH}_2$  was added to **43** prior to adding the ketone, and this suggested that a  $\text{Ph}_2\text{SiH}_2$ -derived silylene complex (i.e.  $[\text{Ir}]=\text{SiPh}_2$ , **54**, Scheme 60) might be the actual catalyst. Indeed, a 1 mol % loading of **54** (in isolated form) was effective at mediating the hydrosilation of benzophenone with  $\text{Ph}_2\text{SiH}_2$  after 5 h at ambient temperatures in  $\text{C}_6\text{D}_5\text{Br}$  (Scheme 60).

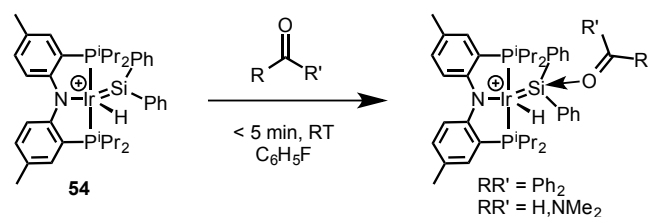
One mechanistic possibility for this transformation is analogous to the mechanism proposed for rhodium-catalyzed hydrosilations involving silylene complexes, and was supported by the observation of adduct formation between **54** and benzophenone or DMF to provide isolable base-stabilized silylene complexes (Scheme 61).<sup>[85e]</sup> However, the apparent stability of the benzophenone adduct of **54** (**54·O=CPh<sub>2</sub>**) is somewhat peculiar if it is an intermediate in a catalytic hydrosilation reaction that occurs readily at room temperature. It might be expected that **54·O=CPh<sub>2</sub>** would undergo facile hydride transfer from iridium to the ketone to provide a complex with an alkoxy-substituted silyl ligand. It is possible that this hydride transfer must be promoted by the coordination of an additional equivalent of  $\text{Ph}_2\text{SiH}_2$  to iridium, and thus does not occur under stoichiometric conditions. Unfortunately, further mechanistic investigation involving a deuterium labeling experiment failed to provide additional insight into the catalytic mechanism. Thus, it remains speculative as to whether the adduct **54·O=CPh<sub>2</sub>** is actually an intermediate, or just an off-cycle catalyst resting state.



**Scheme 59.** Stoichiometric hydrosilation reaction observed between the Si—H bond of **43** and the carbonyl group of a ketone or aldehyde.



**Scheme 60.** Ketone hydrosilation catalyzed by an iridium silylene complex derived from a secondary silane.



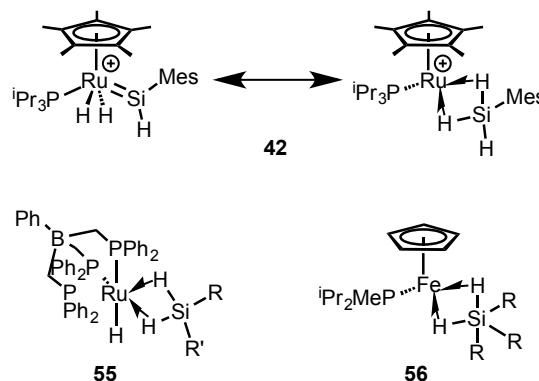
**Scheme 61.** Adduct formation observed between the ketone hydrosilation catalyst **54** and a ketone substrate.

## 5. Electrophilic Complexes with Multiple M—H—Si 3-Center 2-Electron Bonds

### 5.1. Types of M—(H)<sub>n</sub>—Si Species and Their Relationship to Electrophilic Silylene Complexes and $\sigma$ -Complexes

In addition to silylene complexes and  $\eta^1/\eta^2$ -H—SiR<sub>3</sub>  $\sigma$ -complexes, there are additional types of silicon-containing metal complexes with electrophilic silicon. For such complexes, the Lewis acidic behavior of the silicon center is derived from unusual bonding motifs involving multiple M—H—Si 3c 2e bonds and no direct M—Si  $\sigma$ -bond (Scheme 62).<sup>[25a,109]</sup> The chemistry of such species has been developed since the late 1990's,<sup>[110]</sup> making this area of study newer than that of silylene complexes and  $\sigma$ -complexes featuring a single M—H—Si 3c 2e bond. Bonding motifs with multiple M—H—Si interactions involving a single silicon center remain rare, but group 8 metals have been identified as reliably forming these types of complexes when supported by strongly donating, soft ligands such as Cp, Cp\*, and phosphines.<sup>[25a,109,110]</sup> The first examination of the reactivity of one of these species was reported less than ten years ago,<sup>[30a]</sup> and the only detailed hydrosilation studies have

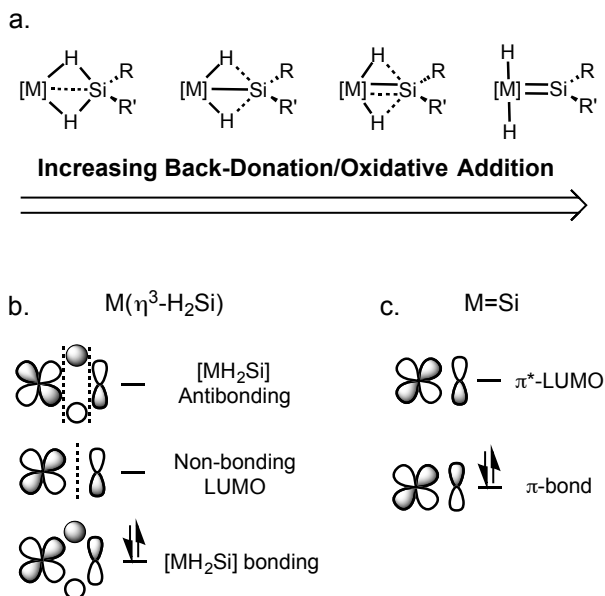
appeared in the past few years.<sup>[25,29]</sup> Despite the limited study of these complexes, they are notable for exhibiting similarities to silylene complexes and  $\eta^1/\eta^2$ -H—SiR<sub>3</sub> complexes. Studies of **42** and **55** were a significant factor in motivating us to compare and contrast these different types of electrophilic silicon species.



**Scheme 62.** Hydrosilation catalysts that feature multiple M—H—Si 3c 2e interactions with a single silicon center.

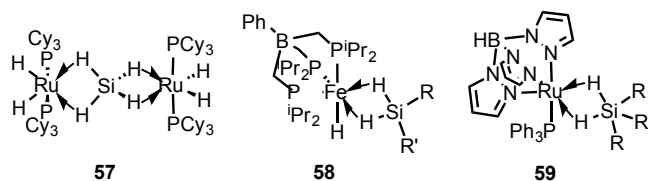
The ruthenium complexes **42** and **55** are the most important examples in the study of the reactivity of electrophilic species with multiple M—H—Si bonds. Complex **55** features an  $\eta^3$ -H<sub>2</sub>SiRR' ligand in which two Si—H bonds of the silane bind to two open coordination sites of the 14-electron [PhBP<sub>3</sub>]Ru—H moiety. Recent structural studies of complex **42** reveal that this species, previously described as a silylene complex, also has considerable  $\eta^3$ -H<sub>2</sub>Si(H)Mes character. The relation of  $\eta^3$ -H<sub>2</sub>SiRR' complexes to isomeric M(H)<sub>2</sub>=SiRR' species is an interesting aspect of the study of  $\eta^3$ -silane complexes, and can be understood as a continuum between the two structure types (Scheme 63).<sup>[25a,29]</sup> This continuum is comparable to that of structures between  $\eta^2$ -H—SiR<sub>3</sub> and H—M—SiR<sub>3</sub> complexes. As such, the distinction between  $\eta^3$ -H<sub>2</sub>SiRR' and M(H)<sub>2</sub>=SiRR' bonding motifs depends significantly on the role of back-donation in activating the Si—H bonds. Since greater M→Si back-donation leads to a more silylene-like electrophilic structure it is intuitive that  $\eta^3$ -H<sub>2</sub>SiRR' ligands, which receive less electron density from the metal, are also electrophilic. Thus, the Lewis acidity of the silicon center in  $\eta^3$ -H<sub>2</sub>SiRR' complexes can be understood in terms of Si—H→M donation without compensation by back-donation, much like the description of bonding in  $\eta^1$ -H—SiR<sub>3</sub> complexes.

An examination of the molecular orbitals involved in the M—(H)<sub>2</sub>—Si bonding motif reveals that the electrophilic character of silicon can be understood in greater detail by noting orbital similarities to silylene complexes (Scheme 63b,c). In particular, the LUMO's of both interactions consist of a  $\pi^*$ -symmetry combination of a ruthenium 4d orbital and a silicon 3p orbital.<sup>[25a]</sup> Note that the absence of hydrogen 1s orbitals in the LUMO of the  $\eta^3$ -H<sub>2</sub>Si complexes is a result of symmetry considerations, and makes this orbital non-bonding with respect to the Si—H and Ru—H interactions.



**Scheme 63.** a) Continuum between  $\eta^3$ -H<sub>2</sub>SiRR' and silylene structure types. b) Orbitals involved in M( $\eta^3$ -H<sub>2</sub>Si) bonding. c). Orbitals involved in the M=Si  $\pi$ -bond of silylene complexes

The first reports of  $\eta^3$ -H<sub>2</sub>Si bonding appeared in 2000 with the description of a diruthenium complex (**57**, Scheme 64) featuring SiH<sub>4</sub> bridging between two (Cy<sub>3</sub>P)<sub>2</sub>(H)<sub>2</sub>Ru fragments via a pair of  $\eta^3$ -H<sub>2</sub>Si interactions.<sup>[110e]</sup> This species was derived from a ruthenium-mediated redistribution of substituents on PhMeSiH<sub>2</sub>, but the reactivity of **57** has not been described. A mononuclear iron  $\eta^3$ -H<sub>2</sub>SiRR' complex [PhBP<sup>i</sup>Pr<sub>3</sub>]<sub>2</sub>Fe(H)( $\eta^3$ -H<sub>2</sub>SiRR') (**58**) was reported several years later,<sup>[30b]</sup> and is very similar to the ruthenium complex **55**. The reactivity of **58** has not been examined, though it was suggested that **58** might exist in equilibrium with an Fe<sup>IV</sup> tris-hydrido silylene complex. It would not be until more recent studies of **55** that the  $\eta^3$ -H<sub>2</sub>Si bonding motif would be recognized as providing a reactive, electrophilic silicon center without equilibration to a silylene structure.<sup>[25a]</sup>



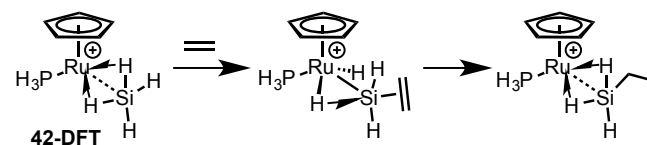
**Scheme 64.** Additional examples of complexes with multiple M—H—Si interactions.

Other bonding motifs with multiple M—H—Si 3c 2e bonds have been studied, and there are a small number of examples in which these species are implicated in hydrosilation reactions. These examples involve species that feature an R<sub>3</sub>Si—H→Ru interaction and also a Ru—H→Si interaction to render the silicon 5-coordinate.<sup>[30a,c]</sup> Though this bonding motif is relatively

uncommon, a number of examples have been discovered since the late 1990's.<sup>[110c,d]</sup> Note that the term SISHA (secondary interaction between silicon and hydrogen atoms) has been introduced to refer to the Ru—H→Si interaction.<sup>[109b]</sup> These complexes can alternatively be described as possessing an [ $\eta^3$ -H<sub>2</sub>SiR<sub>3</sub>] hydrosilicate ligand if both Si—H interactions are strong. This was the case for the iron complex Cp(<sup>i</sup>Pr<sub>2</sub>MeP)Fe( $\eta^3$ -H<sub>2</sub>SiR<sub>3</sub>) **56** that was described in 2008 as a ketone hydrosilation catalyst, in the first report of this type of species in catalysis.<sup>[30a]</sup>

## 5.2. $\eta^3$ -H<sub>2</sub>Si(H)R Character of the Olefin Hydrosilation Catalyst Cp\*(<sup>i</sup>Pr<sub>3</sub>P)Ru(H)<sub>2</sub>=Si(H)R

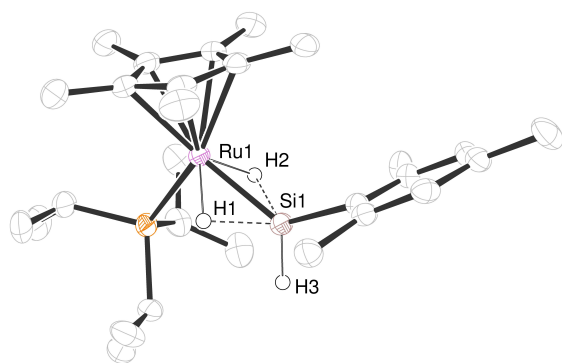
The first reports of silylene complexes in olefin hydrosilation catalysis utilized the Et<sub>2</sub>O stabilized silylene complex **48**, which was presumed to readily dissociate the coordinated Lewis base to provide a reactive silylene complex of the type **42**.<sup>[87a]</sup> Experimental hydrosilation studies with related osmium and iridium silylene complexes also suggest that silylene complexes can engage in olefin hydrosilation reactivity.<sup>[87b-d]</sup> Interestingly, however, there have been computational studies with the model complex **42-DFT** which features two significant Ru—H—Si interactions (Scheme 65), and thus can be described as the  $\eta^3$ -H<sub>2</sub>Si complex Cp(H<sub>3</sub>P)Ru( $\eta^3$ -H<sub>2</sub>SiH<sub>2</sub>).<sup>[107]</sup> The truncated ligands of **42-DFT** are significantly less electron-donating than those of the actual complex **42**, and it is possible that this discrepancy might account for the  $\eta^3$ -H<sub>2</sub>Si structure in **42-DFT** while the experimentally examined species **42** might still be better described as a silylene complex. This possibility could not initially be assessed experimentally since the silylene complex was available only in the stabilized form **48** and structural data was not available for this complex. Note also that the DFT calculations of the hydrosilation mechanism with **42-DFT** indicate that coordination of the olefin substrate results in significant lengthening of the Si—H distances (Scheme 65),<sup>[107]</sup> and this suggests that the structure of the base-stabilized complex **48** would not necessarily provide information about **42**.



**Scheme 65.** Hydrosilation mechanism examined by DFT calculations for the model complex **42-DFT**.<sup>[107]</sup>

New synthetic pathways to **42** (see Scheme 46) allow direct characterization of this species without coordinated solvent.<sup>[93c]</sup> Characterization of **42** by NMR spectroscopy revealed a downfield <sup>29</sup>Si resonance ( $\delta$  229) that is characteristic of a silylene ligand (typical <sup>29</sup>Si  $\delta$  > 200 ppm). However, the <sup>1</sup>H NMR spectrum revealed satellites for the Ru—H signal, and these demonstrate a large J<sub>SiH</sub> value (58 Hz). This data indicates the

presence of significant Ru—H—Si bonding, and is thus consistent with an  $\eta^3\text{-H}_2\text{Si(H)Mes}$  structure. The  $\eta^3\text{-H}_2\text{Si}$  and  $\text{M(H)}_2\text{=Si}$  structures appear to be close in energy, as evident from the observation that the  $\text{SiPh}_2$  derivative has a more downfield  $^{29}\text{Si}$  NMR chemical shift (339 ppm) and  $J_{\text{SiH}}$ -coupling is not detected for this silylene derivative. Further investigation of **42** included the determination of its solid state structure by single crystal X-ray diffraction (Scheme 66).<sup>[29]</sup> This revealed a structure with short Si—H<sub>hydride</sub> contacts ( $d_{\text{Si-H}} \approx 1.75 \text{ \AA}$ ) that indicate some elongation from unactivated silane Si—H bonds ( $d_{\text{Si-H}} \approx 1.48 \text{ \AA}$ ), but which still suggest fairly strong Si—H bonding. The NMR and structural characterization of **42** provide strong evidence that this species is best described by one of the intermediate resonance structures presented in Scheme 63a. Notably, this observation provides evidence for a double Si—H activation pathway in which the two Si—H bonds undergo symmetric, simultaneous elongation rather than two sequential single Si—H cleavage steps as presented in Scheme 47a.



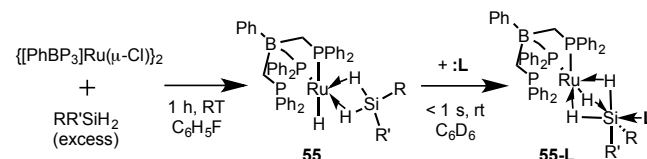
**Scheme 66.** Solid state structure determined for complex **42** that shows that the hydride ligands are tilted towards the silylene ligand.

### 5.3. Electrophilic Hydrosilation Reactivity of $[\text{PhBP}_3]\text{Ru(H)}(\eta^3\text{-H}_2\text{SiRR}')$ Complexes

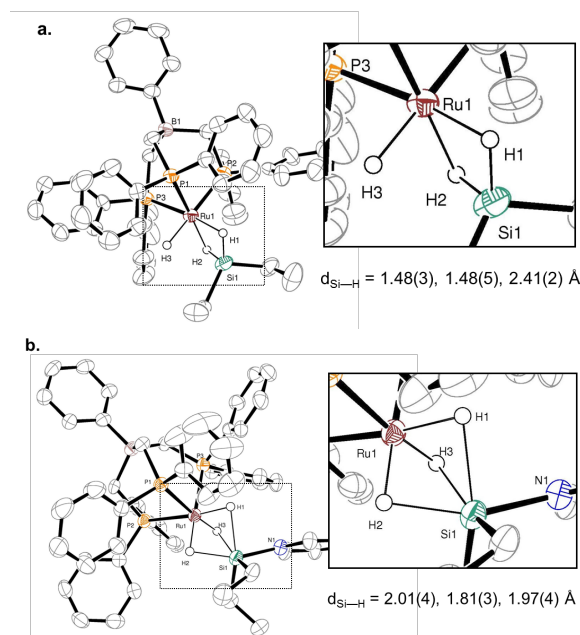
Shortly before the revelation that complex **42** has a structure that is a hybrid of silylene and  $\eta^3\text{-H}_2\text{Si}$  resonance contributors, we began studying the electrophilic character of a different ruthenium  $\eta^3\text{-H}_2\text{SiRR}'$  complex  $[\text{PhBP}_3]\text{Ru(H)}(\eta^3\text{-H}_2\text{SiRR}')$  (**55**).<sup>[25a]</sup> Though these studies are relatively recent, the  $[\text{PhBP}_3]$  ligand appears to provide good crystallinity for these complexes as well as useful NMR characteristics that have enabled progress in studying the electrophilic properties of **55** in stoichiometric and catalytic transformations.

Complex **55** is readily prepared by treatment of the dimeric ruthenium starting material  $\{[\text{PhBP}_3]\text{Ru}(\mu\text{-Cl})_2\}$  with a small excess of a secondary silane (Scheme 67). The straightforward synthesis of **55** is reminiscent of the simple reaction conditions often reported for the formation of electrophilic  $\eta^1\text{-}$  and  $\eta^2\text{-H-SiR}_3$  complexes. Structural and NMR spectroscopic characterization of derivatives of **55** revealed that these species are best described as  $\eta^3\text{-H}_2\text{SiRR}'$  complexes with essentially no contribution from silylene resonance structures. The solid-state

structures of derivatives of **55** (Scheme 68a) feature short Si—H distances ( $d_{\text{Si-H}} = 1.48 - 1.66 \text{ \AA}$ ) and long Ru—H distances



**Scheme 67.** Simple conditions for conversion of a ruthenium precatalyst into **55** and its base adducts **55-L**.

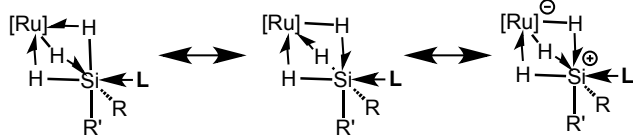


**Scheme 68.** Solid state structures of: a) The  $\text{SiEt}_2$  derivative **55**<sub>SiEt<sub>2</sub></sub> and b) The DMAP adduct **55**<sub>SiEt<sub>2</sub></sub>\*(DMAP).<sup>[111]</sup>

( $d_{\text{Ru-H}} = 1.73 - 1.85 \text{ \AA}$ ) that are comparable to the Si—H and Ir—H distance of the  $\text{Ir}(\eta^1\text{-H-Si})$  interaction in **30** ( $d_{\text{Si-H}} = 1.48(3) \text{ \AA}$ ,  $d_{\text{Ir-H}} = 1.94(3)$ ).<sup>[111]</sup> Interestingly, the geometry of the  $\text{Ru}(\eta^3\text{-H}_2\text{Si})$  interaction in **55** enforces very short Ru—Si distances that are comparable to those found in silylene complexes even though there is no direct Ru—Si bonding apparent in **55**. The  $^{29}\text{Si}$  chemical shifts ( $\delta 141 - 175 \text{ ppm}$ ) for **55** derivatives are downfield, but less so than those usually observed for terminal silylene ligands ( $^{29}\text{Si} > 200 \text{ ppm}$ ). Additionally, each Si—H interaction in **55** has a  $J_{\text{SiH}}$  value of ca. 100 Hz that is characteristic of an Si—H→M interaction with minimal back-donation from the metal. For comparison, note that the iridium  $\eta^1\text{-H-SiEt}_3$  complex **30** exhibits  $J_{\text{SiH}} = 79 \text{ Hz}$  for the bridging hydride ligand resonance.<sup>[51a]</sup>

Similar to silylene complexes, **55** forms stable adducts with a variety of Lewis bases (e.g. 4-dimethylaminopyridine (DMAP), THF, and  $\text{PMe}_3$ , Scheme 67), and this property distinguishes the reactivity of  $\eta^3\text{-H}_2\text{SiRR}'$   $\sigma$ -complexes from that of electrophilic  $\eta^1\text{-}$  and  $\eta^2\text{-H-Si}$  complexes. Interestingly, the base-adducts of **55** exhibit unique structural features (Scheme 68b) that differ from

the related adducts of silylene complexes with Lewis bases. As might be expected, the Si—H distances in **55**•base are elongated considerably from those of **55**, but these distances are not so elongated as to prevent Si—H bonding. Additionally, the terminal hydride in **55** engages in a bridging Ru—H—Si interaction in **55**•base, such that there are three Ru—H—Si interactions in these base adducts. The Si—H component of these interactions is relatively weak ( $d_{\text{Si—H}} = 1.8 - 2.1 \text{ \AA}$ ), but the sum of three of these interactions appears to be sufficient to preclude formation of a direct Ru—Si bond. Thus, coordination of a base to **55** does not result in complete Si—H activation to provide a base-stabilized silylene structure. Instead, the bonding in adducts **55**•base can be described by the resonance structures provided in Scheme 69. Note the inclusion of a charge-separated resonance structure in which silicon carries a formal positive charge. Thus, as with the other  $\sigma$ -complexes and silylene complexes, the electrophilic character of **55** can be understood in terms of the reactivity of a masked silyl cation. However, this description should be used cautiously in this system since the complicated bonding involving multiple Ru—H—Si interactions makes it particularly difficult to accurately attribute reactivity to a single resonance contributor.

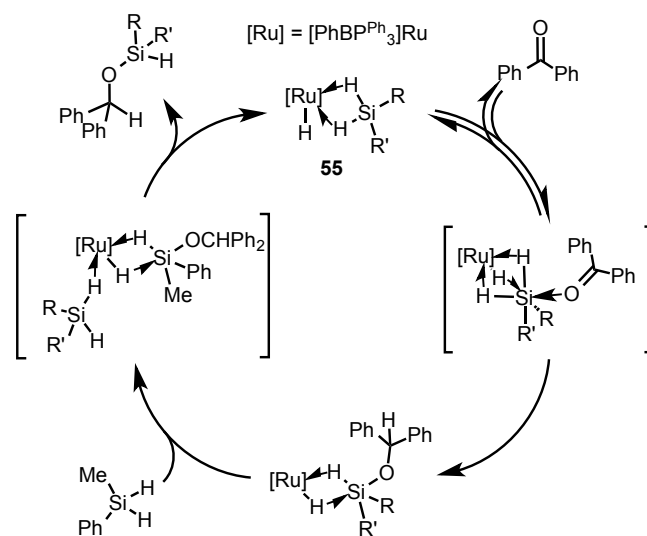


Scheme 69. Resonance structures of the base adducts of **55**.

Complex **55** was found to be a highly active catalyst in ketone hydrosilation reactions,<sup>[25b]</sup> providing quantitative hydrosilation of benzophenone with PhMeSiH<sub>2</sub> after 24 hours at 23 °C in C<sub>6</sub>D<sub>6</sub> using only a 0.01 mol % loading of **55**. Several other ketone substrates underwent hydrosilations in excellent yields, with catalyst loadings of 1 – 2.5 mol % most commonly being used. It seemed possible that the electrophilic  $\eta^3\text{-H}_2\text{SiRR}'$  ligand might be directly involved in this chemistry. Mechanistic studies revealed the availability of a Chalk-Harrod type hydrosilation pathway with a relatively small tertiary silane substrate EtMe<sub>2</sub>SiH, and a [PhBP<sub>3</sub>]Ru—OC(H)Ph<sub>2</sub> complex was observed as a resting state under these conditions (23 °C in CD<sub>2</sub>Cl<sub>2</sub>). However, tertiary silanes could not be used as substrates under conditions that provided high activity with secondary silane substrates (C<sub>6</sub>D<sub>6</sub> as solvent). Additionally, a different resting state was observed for reactions using secondary silanes. These observations suggest that hydrosilation occurs by a different mechanism for secondary silanes. This possibility is supported by the observation that secondary silanes react with [PhBP<sub>3</sub>]Ru—OC(H)Ph<sub>2</sub> in C<sub>6</sub>D<sub>6</sub> to give catalytically inactive ruthenium species as the major products. Thus, this alkoxide complex was ruled out as a possible intermediate in the hydrosilation reactions using secondary silanes.

A hydrosilation mechanism was proposed that involves formation of a **55**•ketone adduct, followed by transfer of a hydride from one of the Ru—H—Si positions to the carbonyl

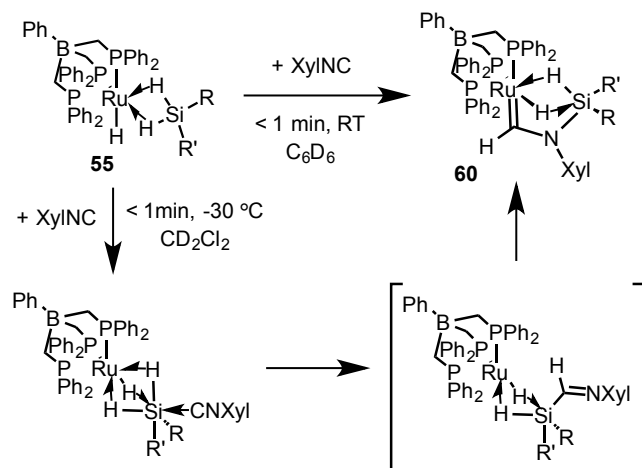
carbon (Scheme 70). The resulting  $\eta^2\text{-H—SiRR}'(\text{OC}(\text{H})\text{R}'^2)$  complex was identified as the resting state of the catalytic cycle by a variety of *in situ* NMR experiments, including some at low temperatures. At low temperatures, **55** was also observed as a resting state, and its Ru—H resonance exhibited perturbations consistent with equilibration between **55** a weakly bound ketone adduct. Rate law determinations and DFT calculations provided support for the mechanism depicted in Scheme 70. Note that many of the steps of this mechanism are similar to those of the Gade mechanism for ketone hydrosilation (Scheme 49) even though the intermediates involved in these two mechanisms differ considerably in structure. The mechanism for hydrosilation by **55** also has similarities to certain mechanisms proposed for hydrosilation reactions involving  $\eta^1\text{-}$  and  $\eta^2\text{-H—SiR}_3$  complexes. In particular, it has occasionally been proposed that substrates engage in frontside attack on the coordinated Si—H bond in these latter species to provide adducts and/or simultaneous Si—H and Ru—H cleavage. Though it is unclear if such processes actually occur for  $\eta^1/\eta^2$   $\sigma$ -complexes, these features are present in the mechanism that appears to operate using **55** as a catalyst.



Scheme 70. Possible mechanism of ketone hydrosilation utilizing the  $\eta^3\text{-H}_2\text{SiRR}'$  catalyst **55**.

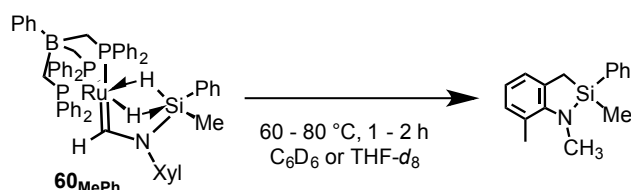
Complex **55** engages in an interesting stoichiometric hydrosilation reaction with the isocyanide substrate XylNC that proceeds quantitatively within 1 min at ambient temperatures (Scheme 71).<sup>[25c,d]</sup> This stoichiometric process provides insight into the ability of  $\eta^3\text{-H}_2\text{SiRR}'$  complexes to engage in hydrosilation reactivity. The transformation results in a 1,2-hydrosilation of the isocyanide, which also generates a carbene ligand bound to ruthenium. A possible mechanism for this transformation is depicted in Scheme 71 and involves coordination of the isocyanide to the silicon center of **55** to form **55**•XylNC. This latter species was identified *in situ* at low temperatures ( $\leq -30 \text{ °C}$  in CD<sub>2</sub>Cl<sub>2</sub>) by a variety of NMR experiments that clearly indicated its similarity to the isolable adduct **55**•DMAP. The role of **55**•XylNC as an intermediate in

the hydrosilation process was examined by DFT calculations. These calculations suggest that the silicon-bound isocyanide undergoes insertion into the Si—H portion of a Ru—H—Si interaction to form an iminoformyl silane intermediate that rearranges to the carbene complex product (**60**, Scheme 71). This mechanism was further supported by KIE studies. Note also that an alternate possible mechanism was eliminated by independently preparing a potential intermediate in which the isocyanide is bound to ruthenium, and observing that it does not form the carbene complex. Thus, the isocyanide hydrosilation mechanism appears to be well supported. Notably, the iminoformyl intermediate is formed by a 1,1-hydrosilation step that is similar to the 1,2-hydrosilation step indicated for ketone hydrosilations in this system.



**Scheme 71.** Stoichiometric hydrosilation of an isocyanide *via* electrophilic activation by an  $\eta^3\text{-H}_2\text{SiRR}'$  ligand.

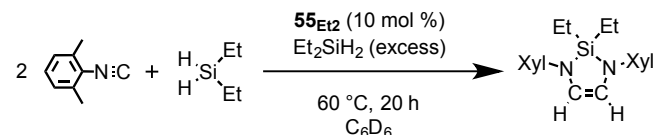
The carbene complex **60** was subsequently found to undergo further reactivity to form organosilicon products.<sup>[25d]</sup> The SiMePh derivative **60<sub>MePh</sub>** releases a silacycloindoline product upon heating ( $\geq 60 \text{ }^\circ\text{C}$ ,  $\text{C}_6\text{D}_6$  or  $\text{THF-}d_8$ , Scheme 72), and this product



**Scheme 72.** Elimination of an organosilicon product from the carbene complex **60<sub>MePh</sub>**.

is formally derived from hydrosilation, hydrogenation, and C—H functionalization of XylINC with  $\text{PhMeSiH}_2$ . The  $\eta^3\text{-H}_2\text{SiMePh}$  complex **55<sub>MePh</sub>** was regenerated in the presence of excess  $\text{PhMeSiH}_2$  in  $\text{THF-}d_8$ , and turnover of the formation of the organosilane product was achieved by stepwise addition of the

isocyanide. This pseudocatalytic process demonstrates that electrophilic  $\eta^3\text{-H}_2\text{SiRR}'$  complexes can participate in catalytic cycles for transformations that are more complex than simple hydrosilations. Interestingly, a different complex transformation catalyzed by **55<sub>Et2</sub>** was observed between  $\text{Et}_2\text{SiH}_2$  and two equivalents of XylINC, which results in the reductive coupling of the isocyanides to form a C=C bond (Scheme 73). This process also suffers from very



**Scheme 73.** Catalytic isocyanide reductive coupling involving hydrosilation of the isocyanide by an electrophilic catalyst.

limited efficiency, but catalytic turnover (TON = 2.7) was achieved in the presence of excess  $\text{Et}_2\text{SiH}_2$  in  $\text{THF-}d_8$ . Mechanistic investigations of both catalytic cycles suggested that the presence of multiple Ru—H—Si interactions in many of the intermediates was important for promoting the productive mechanistic pathways. Thus, the unusual bonding features of  $\eta^3\text{-H}_2\text{SiRR}'$  complexes and related structures appear to be important for enabling these unique transformations. The resulting mechanisms distinguish the electrophilic  $\eta^3\text{-H}_2\text{SiRR}'$  complexes from related electrophilic species such as silylene complexes and more common types of silane  $\sigma$ -complexes.

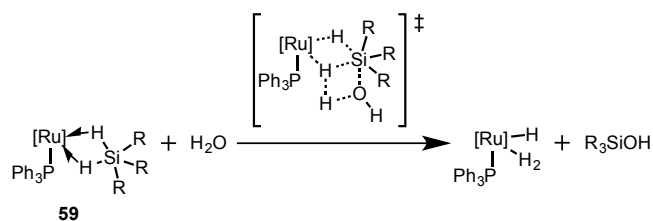
The studies of the  $\eta^3\text{-H}_2\text{SiRR}'$  complex **55** reveal that these complexes can mediate catalytic ketone hydrosilations and might also be useful for enabling new catalytic hydrosilation reactions. The participation of the electrophilic  $\eta^3\text{-H}_2\text{SiRR}'$  ligand in these processes appears to be well supported by experimental and computational studies. Additional studies are still needed in order to fully confirm these mechanistic proposals. In particular, **55** appears to exist in equilibrium with a silylene complex,<sup>[97]</sup> and this latter species may be involved in hydrosilation processes in this system. This seems somewhat unlikely, since the silylene species is relatively high in energy, but more experimental and computational studies might be useful to more fully rule out this mechanistic possibility. It is important to continue these studies since  $\eta^3\text{-H}_2\text{SiRR}'$ -mediated hydrosilations might be adapted to first-row transition metal catalysts or even main-group Lewis acid catalysts. These latter possibilities are discussed in more detail in Section 6 of this Review.

#### 5.4. Hydrosilation Reactions Involving Other Species with Multiple M—H—Si Bonds

Investigations of **42** and **55** provide the most detailed reports of hydrosilation reactions involving complexes with multiple M—H—Si 3c 2e bonds. Aside from  $\eta^3$ -silane complexes, there are other types of transition metal complexes that feature multiple M—H—Si bonds. Complexes **56** (Scheme 62) and **59** (Schemes

64 and 74) have been described as possessing hydridosilicate ligands [ $\eta^3\text{-H}_2\text{SiR}_3$ ] based on the presence of two nearly symmetric M—H—Si interactions.<sup>[30a,c]</sup> Note that the [PhBP<sub>3</sub>]Ru system also stabilizes hydridosilicate ligands,<sup>[112]</sup> but that these latter species have not been investigated as hydrosilation catalysts. In 2008, derivatives of **56** were examined as catalysts for the hydrosilation of benzaldehyde with PhSiH<sub>3</sub> or PhMeSiH<sub>2</sub> (50 °C, 3 – 12 h, 5 mol % catalyst loading), marking one of the earliest studies of such a species in catalysis.<sup>[30a]</sup> However, the mechanism of these reactions was not investigated and it is not clear what role, if any, the [ $\eta^3\text{-H}_2\text{SiR}_3$ ] ligand plays in catalysis. In this regard, it is relevant to note that a simple silane-free precursor complex [Cp(<sup>i</sup>Pr<sub>2</sub>MeP)Fe(NCMe)<sub>2</sub>]<sup>+</sup> was a more active catalyst for the hydrosilation of benzaldehyde than any of the hydridosilicate complexes examined.

Complex **59** has not been investigated in hydrosilation reactions, but this ruthenium complex has been examined as a catalyst for silane hydrolysis reactions.<sup>[30c]</sup> This catalyst exhibits relatively low activity in these reactions, requiring heating to 90 °C in order to obtain high yields within a reasonable time (2 – 24 h) with a 2 mol % loading of **59**. Despite the low activity, these studies are interesting for examining the role of the silicon species in the mechanism of the transformations. The authors proposed a mechanism that involves attack of water at the silicon center of the [ $\eta^3\text{-H}_2\text{SiR}_3$ ] ligand with concurrent deprotonation of the water by one of the hydride ligands to form an  $\eta^2\text{-H}_2$  ligand bound to ruthenium (Scheme 74). Note that this process involves frontside attack of the water molecule on a coordinated Si—H bond, and similar silane hydrolysis mechanisms have been proposed for reactions involving more common  $\eta^2\text{-H—SiR}_3$   $\sigma$ -complexes (see Scheme 22). Evidence for a frontside attack pathway using catalyst **59** was provided by the observation that the hydrolysis reactions proceed with retention of configuration when a chiral silane (R)-Me( $\alpha$ -Np)PhSiH is used as the substrate, and computational investigations also supported the proposed mechanism.



**Scheme 74.** Key step proposed in the silane hydrolysis reaction catalyzed by **59**.

The examples of catalytic Si—O bond formation involving complexes that can be described as [ $\eta^3\text{-H}_2\text{SiR}_3$ ] species have so far been very limited, and the two examples described above exhibit low activity. However, these studies are interesting in providing additional information about the roles that multiple M—H—Si bonded structures can play in hydrosilation reactions. The results appear to support the possibility that such structure types enable electrophilic reaction pathways that have occasionally been suggested for more typical Si—H  $\sigma$ -complexes, but which

are distinct from the well-established mechanisms for these complexes.

## 6. Summary and Outlook

It has been over 25 years since it was first suggested that Lewis acidic catalysts might transfer electrophilic character to a silane *via* the formation of Si—H  $\sigma$ -complexes. The earliest reported examples involve transition metal complexes, such as [(Ph<sub>3</sub>P)<sub>2</sub>(MeOH)<sub>2</sub>IrH<sub>2</sub>][SbF<sub>6</sub>] (**13**),<sup>[55]</sup> that were studied as catalysts for silane hydrolysis and alcoholysis reactions (see Section 3.2). However, these early studies provided only limited details of the electrophilic silicon intermediates involved in catalysis.<sup>[57-60]</sup> Subsequent improvements in synthetic techniques (e.g. use of fluorinated aryl borate or carborane anions) and analytical techniques (e.g. <sup>1</sup>H-<sup>29</sup>Si 2D NMR techniques and improved single-crystal XRD methods) have provided researchers with more powerful tools to study electrophilic silicon species that are formed from silanes and electrophilic catalysts. There has been vigorous progress in this field over the past 10 years, and there are now several types of electrophilic silicon species that have been characterized in detail: transition metal and main-group Lewis acids with  $\eta^1$ - or  $\eta^2\text{-H—SiR}_3$  ligands (Sections 2 and 3), transition metal silylene complexes (Section 4),  $\eta^3\text{-H}_2\text{SiR}_2$  complexes (Section 5.1-5.3), and other species with multiple M—H—Si interactions (Section 5.4). The recent advances in this field provide considerable insight into the similarities and differences among a wide range of electrophilic hydrosilation catalysts that have been studied over the past 20 years.

The most well studied electrophilic hydrosilation catalyst is B(C<sub>6</sub>F<sub>5</sub>)<sub>3</sub> (**1**), which in 1996 was reported to catalyze ketone hydrosilation reactions (see Section 2.1) by the ionic hydrosilation mechanism depicted in Scheme 3.<sup>[19]</sup> This mechanism has gained widespread acceptance and B(C<sub>6</sub>F<sub>5</sub>)<sub>3</sub> has become the most widely studied electrophilic hydrosilation catalyst, capable of catalyzing an incredibly wide range of transformations. Despite this history, it was only very recently that a key intermediate, a borane-silane adduct, was isolated and fully characterized.<sup>[27]</sup> A resurgence of interest in electrophilic transition metal hydrosilation catalysts has also led to in-depth study of catalysts such as [(POCOP)Ir(H)( $\eta^1\text{-H—SiEt}_3$ )]<sup>+</sup> (**30**).<sup>[71a]</sup> There is considerable evidence that **30** catalyzes a variety of silane transformations *via* the ionic mechanism, and the key  $\eta^1\text{-H—SiEt}_3$  intermediate was even isolated and structurally characterized<sup>[51a]</sup> prior to the reported isolation of a borane-silane adduct. Together, the studies of **1** and **30** provide the strongest evidence of hydrosilation catalysis that operates by the ionic mechanism.

A variety of other electrophilic main-group and transition-metal based catalysts might operate by some variant of the ionic mechanism. Notably, this wide range of catalysts includes examples as dissimilar as phosphorus-based Lewis acids<sup>[46]</sup> and mid-transition metal complexes.<sup>[61]</sup> It is valuable to explore the full range of electrophilic catalysts since these studies may result in the development of catalysts that avoid the use of expensive transition metals or relatively toxic fluorinated organic groups.



Additionally, some electrophilic catalysts have been reported to enable reactivity and/or selectivity that are not possible with other catalysts. For example, ruthenium  $\eta^2\text{-H-SiR}_3$  complexes catalyze challenging pyridine and nitrile hydrosilations in good yield and with high selectivity for a single product.<sup>[75,78]</sup> Even more interesting pyridine transformations were achieved with an electrophilic ruthenium complex possessing a cooperative basic site (a thiolate ligand). This latter complex catalyzes pyridine C—H silylations by a mechanism involving ionic hydrosilation/retrohydrosilation processes in addition to the C—H functionalization.<sup>[79b]</sup> Further investigation of the wide range of electrophilic hydrosilation catalysts may lead to the discovery of more examples of unusual and challenging transformations.

Other electrophilic catalysts operate by the formation of silylene ligands *via* the activation of two Si—H bonds of a primary or secondary silane. The 3-coordinate silicon center of the silylene ligand is electrophilic due to weak back-bonding from the electrophilic metal center, and thus, hydrosilation substrates can be activated upon binding to silicon.<sup>[15]</sup> The high reactivity of silylene complexes has been investigated for about as long as electrophilic Si—H  $\sigma$ -complexes have been studied, but notably, there are far fewer examples in which silylene complexes are associated with catalytic reactions. It is not entirely clear why these highly reactive species do not tend to engage in catalytic processes, but one possible explanation is that it is difficult to orchestrate the relatively sophisticated sequence of Si—H activations, reaction with the unsaturated substrate, and product releasing steps into a single catalytic cycle while avoiding potential deactivation pathways that result from the high reactivity of the silylene ligand. Nevertheless, there are examples of olefin hydrosilations involving silylene complexes that exhibit high catalytic activities and unique substrate selectivities.<sup>[87]</sup> Additionally, some hydrosilation reactions may occur *via* transient silylene complexes that form from simple precatalysts. Support for this possibility has been seen in investigations of rhodium-catalyzed ketone hydrosilations.<sup>[99]</sup> Considering the high reactivity of many silylene complexes, it is valuable to continue to explore these species as potential catalysts, with a particular emphasis on finding systems that are better able to release products to regenerate the silylene intermediates.

A new electrophilic Si—H activation pathway has recently been demonstrated to involve coordination of two geminal Si—H bonds to a transition metal center to provide an  $\eta^3\text{-H}_2\text{SiRR}'$  ligand. Interestingly, this activation pathway features similarities to the other  $\sigma$ -silane activation pathways and to the silylene activation pathway. The olefin hydrosilation catalyst **42** possesses bonding that can be described as intermediate between that of a silylene dihydride complex and an  $\eta^3\text{-H}_2\text{Si(H)Mes}$  complex,<sup>[29]</sup> while the ketone hydrosilation catalyst **55** has weakly activated Si—H bonds, consistent with primarily  $\eta^3\text{-H}_2\text{SiRR}'$   $\sigma$ -complex character.<sup>[25a,b]</sup> These observations illustrate the existence of a continuum between  $\eta^3\text{-H}_2\text{Si}$  and silylene dihydride structures. The two extremes of this continuum are formally related by an unusual type of Si—H oxidative addition in which both coordinated Si—H bonds of the  $\eta^3\text{-H}_2\text{SiRR}'$  ligand are activated and an M—Si bond is formed.

Simultaneous Si—H activation is also observed upon coordination of a substrate to the  $\eta^3\text{-H}_2\text{SiRR}'$  ligand, and in some cases this still does not fully cleave the Si—H bonds such that the resulting substrate $\rightarrow$ Si adduct maintains multiple M—H—Si interactions and a 5- or 6-coordinate silicon center.<sup>[25a]</sup> These latter types of structures are particularly recent discoveries that merit further investigation, since substrate activation *via* these unusual structures may prove useful for enabling novel reactivity or fine-tuning selectivities of catalytic hydrosilations.

Though there is considerable variety in the electrophilic silicon structures that are involved in hydrosilation reactions, these intermediates have several common features. In particular the absence of M $\rightarrow$ Si back-donation appears to be an important feature that leads to electrophilicity of  $\eta^1\text{-H-SiR}_3$  complexes,  $\eta^3\text{-H}_2\text{SiRR}'$  complex, and silylene complexes. There has been considerable recent progress towards understanding the full details of these silane activation pathways, and these advances may illuminate the path towards development of efficient catalysts utilizing abundant first row transition metals or p-block elements. For example, the  $\sigma$ -silane activation pathways involving a single Si—H bond appear to be possible for almost any type of sufficiently electrophilic metal or metalloid catalyst. In contrast, silylene mechanisms may be more difficult to adapt to first-row and main-group catalysts since these pathways often rely on the catalyst engaging in Si—H oxidative addition process. However, iron and nickel complexes can support the formation of silylene ligands,<sup>[113]</sup> and thus it may be possible to develop some first-row metal silylene complexes that serve as hydrosilation catalysts. Additionally,  $\eta^3\text{-H}_2\text{SiRR}'$  complexes appear to exhibit reactivity that is closely related to that of silylene complexes while avoiding the need for oxidative addition processes. It may thus be of value to investigate whether or not  $\eta^3\text{-H}_2\text{SiRR}'$  ligands can be supported by other transition metals or even main-group Lewis acids that have two adjacent binding sites.

## Acknowledgements

The authors would like to acknowledge the many coworkers over the years who have contributed to research described above. Aspects of our research in this area were funded by the Director, Office of Science, Office of Basic Energy Sciences of the US Department of Energy under contract no. DE-AC02-05CH11231, and by the U.S. National Science Foundation, most recently under Grant No. CHE-1566538.

**Keywords:** hydrosilation • main group • catalysis • silylene •  $\sigma$ -complex

- [1] a) D. Troegel and J. Stohrer, *Coord. Chem. Rev.* **2011**, *255*, 1440–1459; b) B. Marciniec, *Silicon Chem.* **2002**, *1*, 155–175; c) M. A. Brook, *Silicon in Organic, Organometallic, and Polymer Chemistry*, Wiley, New York, **2000**; d) I. Ojima, Z. Li, J. Zhu in *The Chemistry of Organic Silicon Compounds* (Eds.: Z. Rappoport, Y. Apeloig), Wiley, New York, **1998**, p. 1687; e) A. K. Roy, *Adv. Organomet. Chem.* **2007**, *55*, 1–59; f)

- Y. Nakajima, S. Shimada, *RSC Adv.* **2015**, *5*, 20603–20616; g) D. Addis, S. Das, K. Junge, M. Beller *Angew. Chem. Int. Ed.* **2011**, *50*, 6004–6011.
- [2] a) J. L. Speier, J. A. Webster, G. H. Barnes, *J. Am. Chem. Soc.* **1957**, *79*, 974–979; b) J. Stein, L. N. Lewis, Y. Gao, R. A. Scott, *J. Am. Chem. Soc.* **1999**, *121*, 3693–3703; c) I. E. Marko, S. Sterin, O. Buisine, G. Mignani, P. Branlard, B. Tinant, J.-P. Declercq, *Science* **2002**, *298*, 204–206; d) A. M. Tondreau, C. C. H. Atienza, K. J. Weller, S. A. Nye, K. M. Lewis, J. G. P. Delis, P. J. Chirik, *Science* **2012**, *335*, 567–570.
- [3] a) B. M. Trost, Z. T. Ball, *J. Am. Chem. Soc.* **2001**, *123*, 12726–12727; b) B. M. Trost, Z. T. Ball, *J. Am. Chem. Soc.* **2005**, *127*, 17644–17655; c) Y. Na, S. Chang, *Org. Lett.* **2000**, *2*, 1887–1889; d) I. Ojima, N. Clos, R. J. Donovan, P. Ingallina, *Organometallics* **1990**, *9*, 3127–3133; e) M. P. Doyle, K. G. High, C. L. Nesloney, T. W. Clayton, J. Lin, *Organometallics* **1991**, *10*, 1225–1226.
- [4] a) Y. Nishibayashi, I. Takei, S. Uemura, M. Hidai, *Organometallics* **1998**, *17*, 3420–3422; b) B. H. Lipshutz, K. Noson, W. Chrisman, A. Lower, *J. Am. Chem. Soc.* **2003**, *125*, 8779–8789; c) J. Yang, T. D. Tilley, *Angew. Chem. Int. Ed.* **2010**, *49*, 10186–10188; d) B. L. Tran, M. Pink, D. J. Mindiola, *Organometallics* **2009**, *28*, 2234–2243; e) N. S. Shaikh, K. Junge, M. Beller, *Org. Lett.* **2007**, *9*, 5429–5432.
- [5] a) S. C. Berk, K. A. Kreutzer, S. Buchwald, *J. Am. Chem. Soc.* **1991**, *113*, 5093–5095; b) Z. Mao, B. T. Gregg, A. R. Cutler, *J. Am. Chem. Soc.* **1995**, *117*, 10139–10140; c) M. Igarashi, R. Mizuno, T. Fuchikami, *Tetrahedron Lett.* **2001**, *42*, 2149–2151; d) J. Nakanishi, H. Tatamidani, Y. Fukumoto, N. Chatani, *Synlett* **2006**, 869–872.
- [6] a) S. Hanada, E. Tsutsumi, Y. Motoyama, H. Nagashima, *J. Am. Chem. Soc.* **2009**, *131*, 15032–15040; b) Y. Sunada, H. Kawakami, T. Imaoka, Y. Motoyama, H. Nagashima, *Angew. Chem. Int. Ed.* **2009**, *48*, 9511–9514; c) S. Das, D. Addis, S. Zhou, K. Junge, M. Beller, *J. Am. Chem. Soc.* **2010**, *132*, 1770–1771; d) T. Ohta, M. Kamiya, M. Nobutomo, K. Keisuke, I. Furukawa, *Bull. Chem. Soc. Jpn.* **2005**, *78*, 1856–1861; e) A. C. Fernandes, C. C. Romão, *J. Mol. Catal. A* **2006**, *253*, 96–98.
- [7] a) X. Verdaguier, U. E. W. Lange, M. T. Reding, S. L. Buchwald, *J. Am. Chem. Soc.* **1996**, *118*, 6784–6785; b) R. Becker, H. Brunner, S. Mahboobi, W. Wiegrebbe, *Angew. Chem. Int. Ed.* **1985**, *24*, 995–996; c) B. H. Lipshutz, H. Shimizu, *Angew. Chem. Int. Ed.* **2004**, *43*, 2228–2230.
- [8] a) R. J. P. Corriu, J. J. E. Moreau, M. Pataud-Sat, *J. Organomet. Chem.* **1982**, *228*, 301–308; b) T. Murai, T. Sakane, S. Kato, *J. Org. Chem.* **1990**, *55*, 449–453; c) A. M. Caporusso, N. Panziera, P. Pertici, E. Pitzalis, P. Salvadori, G. Vitulli, G. Martra, *J. Mol. Catal. A* **1999**, *137*, 275–285.
- [9] a) L. Hao, J. F. Harrod, A.-M. Lebusi, Y. Mu, R. Shu, E. Samuel, H.-G. Woo, *Angew. Chem. Int. Ed.* **1998**, *37*, 3126–3129; b) J. F. Harrod, R. Shu, H.-G. Woo, E. Samuel, *Can. J. Chem.* **2001**, *79*, 1075–1085.
- [10] C. Cheng, M. Brookhart, *Angew. Chem. Int. Ed.* **2012**, *51*, 9422–9424.
- [11] a) S. Park, M. Brookhart, *J. Am. Chem. Soc.* **2012**, *134*, 640–653; b) C. Cheng, M. Brookhart, *J. Am. Chem. Soc.* **2012**, *134*, 11304–11307.
- [12] a) S. Park, D. Bézier, M. Brookhart, *J. Am. Chem. Soc.* **2012**, *134*, 11404–11407; b) R. Lalrempuia, M. Iglesias, V. Polo, P. J. Sanz Miguel, F. J. Fernández-Alvarez, J. J. Pérez-Torrente, L. A. Oro, *Angew. Chem. Int. Ed.* **2012**, *51*, 12824–12827; c) A. Julián, V. Polo, E. A. Jaseer, F. J. Fernández-Alvarez, L. A. Oro, *Chem. Cat. Chem.* **2015**, *7*, 3895–3902.
- [13] T. Robert, M. Oestreich, *Angew. Chem. Int. Ed.* **2013**, *52*, 5216–5218.
- [14] M. Iglesias, F. J. Fernández-Alvarez, L. A. Oro, *Chem. Cat. Chem.* **2014**, *6*, 2486–2489.
- [15] R. Waterman, P. G. Hayes, T. D. Tilley, *Acc. Chem. Res.* **2007**, *40*, 712–719.
- [16] M. Okazaki, H. Tobita, H. Ogino, *Dalton Trans.* **2003**, 493–506.
- [17] a) A. F. Chalk, J. F. Harrod, *J. Am. Chem. Soc.* **1965**, *87*, 16–21; b) C. L. Randolph, M. S. Wrighton, *J. Am. Chem. Soc.* **1986**, *108*, 3366–3374; c) F. Seitz, M. S. Wrighton, *Angew. Chem., Int. Ed. Engl.* **1988**, *27*, 289–291; d) S. B. Duckett, R. N. Perutz, *Organometallics* **1992**, *11*, 90–98.
- [18] a) I. Ojima, M. Nihonyanagi, T. Kogure, M. Kumagai, S. Horiuchi, K. Nakatsugawa, *J. Organomet. Chem.* **1975**, *94*, 449–461; b) I. Ojima, T. Kogure, M. Kumagai, S. Horiuchi, T. Sato, *J. Organomet. Chem.* **1976**, *122*, 83–97.
- [19] D. J. Parks, W. E. Piers, *J. Am. Chem. Soc.* **1996**, *118*, 9440–9441.
- [20] M. Rubin, T. Schwiery, V. Gevorgyan, *J. Org. Chem.* **2002**, *67*, 1936–1940.
- [21] D. J. Parks, J. M. Blackwell, W. E. Piers, *J. Org. Chem.* **2000**, *65*, 3090–3098.
- [22] a) V. Gevorgyan, J.-X. Liu, M. Rubin, S. Benson, Y. Yamamoto, *Tetrahedron Lett.* **1999**, *40*, 8919–8922; b) V. Gevorgyan, M. Rubin, S. Benson, J.-X. Liu, Y. Yamamoto, *J. Org. Chem.* **2000**, *65*, 6179–6186; c) J. Chojnowski, S. Rubinsztajn, J. A. Cella, W. Fortuniak, M. Cypriak, J. Kurjata, K. Kaźmierski, *Organometallics* **2005**, *24*, 6077–6084.
- [23] C. B. Caputo, D. W. Stephan, *Organometallics* **2012**, *31*, 27–30.
- [24] G. Z. Zheng, T. H. Chan, *Organometallics* **1995**, *14*, 70–79.
- [25] a) M. C. Lipke, T. D. Tilley, *J. Am. Chem. Soc.* **2011**, *133*, 16374–16377; b) M. C. Lipke, T. D. Tilley, *J. Am. Chem. Soc.* **2014**, *136*, 16387–16398; c) M. C. Lipke, T. D. Tilley, *J. Am. Chem. Soc.* **2013**, *135*, 10298–10301; d) M. C. Lipke, A. L. Liberman-Martin, T. D. Tilley, *J. Am. Chem. Soc.* **2016**, *138*, 9704–9713.
- [26] a) M. P. Doyle, C. T. West, S. J. Donnelly, C. C. McOsker, *J. Organomet. Chem.* **1976**, *117*, 129–140; b) J. L. Fry, M. Orfanopoulos, M. G. Adlington, W. P. Dittman Jr., S. B. Silverman, *J. Org. Chem.* **1978**, *43*, 374–375; c) A. L. Liberman-Martin, R. G. Bergman, T. D. Tilley, *J. Am. Chem. Soc.* **2015**, *137*, 5328–5331; d) M. Hirai, J. Cho, F. P. Gabbai, *Chem. Eur. J.* **2016**, *22*, 6537–6541; e) M. P. Doyle, C. T. West, *J. Org. Chem.* **1975**, *40*, 3835–3838.
- [27] A. Y. Houghton, J. Hurmalainen, A. Mansikkamäki, W. E. Piers, H. M. Tuononen, *Nature Chem.* **2014**, *6*, 983–988.
- [28] J. Chen, E. Y.-X. Chen, *Angew. Chem., Int. Ed.* **2015**, *54*, 6842–6846.
- [29] M. E. Fasulo, M. C. Lipke, T. D. Tilley, *Chem. Sci.* **2013**, *4*, 3882–3887.
- [30] a) D. V. Gutsulyak, L. G. Kuzmina, J. A. K. Howard, S. F. Vyboishchikov, G. I. Nikonov, *J. Am. Chem. Soc.* **2008**, *130*, 3732–3733; b) C. M. Thomas, J. C. Peters, *Angew. Chem. Int. Ed.* **2006**, *45*, 776–780; c) T. Y. Lee, L. Dang, Z. Zhou, C. H. Yeung, Z. Lin, C. P. Lau, *Eur. J. Inorg. Chem.* **2010**, 5675–5684.
- [31] P. P. Power, *Nature* **2010**, *463*, 171–177.
- [32] M. Oestreich, J. Hermeke, J. Mohr, *Chem. Soc. Rev.* **2015**, *44*, 2202–2220.
- [33] S. Rendler, M. Oestreich, *Angew. Chem., Int. Ed.* **2008**, *47*, 5997–6000.
- [34] N. Gandhamsetty, S. Park, S. Chang, *J. Am. Chem. Soc.* **2015**, *137*, 15176–15184.
- [35] a) Q. Yin, H. F. T. Klare, M. Oestreich, *Angew. Chem., Int. Ed.* **2016**, *55*, 3204–3207; b) Y. Ma, B. Wang, L. Zhang, Z. Hou, *J. Am. Chem. Soc.* **2016**, *138*, 3663–3666.
- [36] J. Y. Corey, J. Braddock-Wilking, *Chem. Rev.* **1999**, *99*, 175–292.
- [37] A. Berkefeld, W. E. Piers, M. Parvez, L. Castro, L. Maron, O. Eisenstein, *J. Am. Chem. Soc.* **2012**, *134*, 10843–10851.
- [38] J. Chen, R. A. Lalancette, F. Jäkle, *Chem. Commun.* **2013**, *49*, 4893–4895.
- [39] S. E. Denmark, Y. Ueki, *Organometallics* **2013**, *32*, 6631–6634.
- [40] J. Chen, L. Falivene, L. Caporaso, L. Cavallo, E. Y.-X. Chen, *J. Am. Chem. Soc.* **2016**, *138*, 5321–5333.
- [41] S. Nagahara, T. Yamakawa, H. Yamamoto, *Tetrahedron Lett.* **2001**, *42*, 5057–5060.
- [42] J. Koller, R. G. Bergman, *Organometallics* **2012**, *31*, 2530–2533.
- [43] K. Mütter, M. Oestreich, *Chem. Commun.* **2011**, *47*, 334–336.
- [44] a) S. P. Hoffmann, T. Kato, F. S. Tham, C. A. Reed, *Chem. Commun.* **2006**, 767–769; b) S. J. Connelly, W. Kaminsky, D. M. Heinekey, *Organometallics* **2013**, *32*, 7478–7481.
- [45] K. Mütter, J. Mohr, M. Oestreich, *Organometallics* **2013**, *32*, 6643–6646.
- [46] a) M. Pérez, L. J. Hounjet, C. B. Caputo, R. Dobrovetsky, D. W. Stephan, *J. Am. Chem. Soc.* **2013**, *135*, 18308–18310; b) M. H. Holthausen, M. Mehta, D. W. Stephan, *Angew. Chem., Int. Ed.* **2014**, *53*, 6538–6541; c) M. Pérez, Z.-W. Qu, C. B. Caputo, V. Podgorny, L. J. Hounjet, A. Hansen, R. Dobrovetsky, S. Grimme, D. W. Stephan, *Chem. Eur. J.* **2015**, *21*, 6491–6500.
- [47] M. Mehta, I. G. de la Arada, M. Perez, D. Porwal, M. Oestreich, D. W. Stephan, *Organometallics* **2016**, *35*, 1030–1035.

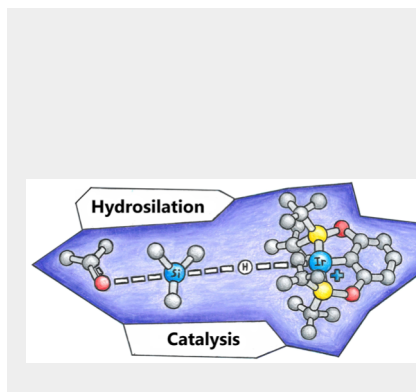
- [48] a) S. Das, D. Addis, S. Zhou, K. Junge, M. Beller, *J. Am. Chem. Soc.* **2010**, *132*, 1770–1771; b) S. Das, K. Möller, K. Junge, M. Beller, *Chem. Eur. J.* **2011**, *17*, 7414–7417.
- [49] C. Boone, I. Korobkov, G. I. Nikonov, *ACS Catal.* **2013**, *3*, 2336–2340.
- [50] a) U. Schubert, *Adv. Organomet. Chem.* **1990**, *30*, 151–187; b) U. Schubert, G. Scholz, J. Müller, K. Ackermann, B. Würle, R. F. D. Stansfield, *J. Organomet. Chem.* **1986**, *306*, 303–326; c) R. H. Crabtree, *Angew. Chem., Int. Ed. Engl.* **1993**, *32*, 789–805; d) Z. Lin, *Chem. Soc. Rev.* **2002**, *31*, 239–245; e) G. S. McGrady, P. Sirsch, N. P. Chatterton, A. Ostermann, C. Gatti, S. Altmannshofer, V. Herz, G. Eickerling, W. Scherer, *Inorg. Chem.* **2009**, *48*, 1588–1598.
- [51] a) J. Yang, P. S. White, C. K. Schauer, M. Brookhart, *Angew. Chem., Int. Ed.* **2008**, *47*, 4141–4143; b) Hamdaoui, M.; Ney, M.; Sarda, V.; Karmazin, L.; Bailly, C.; Sieffert, N.; Dohm, S.; Hansen, A.; Grimme, S.; Djukic, J.-P. *Organometallics* **2016**, *35*, 2207 – 2223.
- [52] a) R. Waterman, *Organometallics*, **2013**, *32*, 7249–7263; b) A. L. Reznichenko, K. C. Hultsch, *Struct. Bonding (Berlin)* **2010**, *137*, 1–48. c) G. A. Molander, M. Julius *J. Org. Chem.* **1992**, *57*, 6347 – 6351; d) P.-F. Fu, L. Brard, Y. Li, T. J. Marks *J. Am. Chem. Soc.* **1995**, *117*, 7157 – 7168.
- [53] a) Z. K. Sweeney, J. L. Polse, R. A. Andersen, R. G. Bergman, M. G. Kubinec, *J. Am. Chem. Soc.* **1997**, *119*, 4543–4544; b) T. I. Gountchev, T. D. Tilley, *J. Am. Chem. Soc.* **1997**, *119*, 12831–12841.
- [54] a) J. J. Kennedy-Smith, K. A. Nolin, H. P. Gunterman, F. D. Toste, *J. Am. Chem. Soc.* **2003**, *125*, 4056–4057; b) K. A. Nolin, J. R. Krumper, M. D. Pluth, R. G. Bergman, F. D. Toste, *J. Am. Chem. Soc.* **2007**, *129*, 14684–14696; c) E. A. Ison, E. R. Trivedi, R. A. Corbin, M. M. Abu-Omar, *J. Am. Chem. Soc.* **2005**, *127*, 15374–15375; d) G. Du, P. E. Fanwick, M. M. Abu-Omar, *J. Am. Chem. Soc.* **2007**, *129*, 5180–5187.
- [55] X.-L. Luo, R. H. Crabtree, *J. Am. Chem. Soc.* **1989**, *111*, 2527–2535.
- [56] a) R. H. Crabtree, M. Lavin, *J. Chem. Soc., Chem. Commun.* **1985**, 794–795; b) M. J. Burk, B. Segmuller, R. H. Crabtree, *Organometallics*, **1987**, *6*, 2241–2246.
- [57] a) E. Scharrer, S. Chang, M. Brookhart, *Organometallics* **1995**, *14*, 5686–5694; b) S. Chang, E. Scharrer, M. Brookhart, *J. Mol. Catal. A* **1998**, *130*, 107–119; c) M. Bühl, F. T. Mauschick, *Organometallics* **2003**, *22*, 1422–1431; d) J. Huhmann-Vincent, B. L. Scott, G. J. Kubas, *Inorg. Chim. Acta* **1999**, *294*, 240–254; e) X. Fang, J. Huhmann-Vincent, B. L. Scott, G. L. Kubas, *J. Organomet. Chem.* **2000**, *609*, 95–103; f) X. Fang, B. L. Scott, K. D. John, G. J. Kubas, *Organometallics* **2000**, *19*, 4141–4149.
- [58] D. E. Barber, Z. Lu, T. Richardson, R. H. Crabtree, *Inorg. Chem.* **1992**, *31*, 4709–4711.
- [59] S. L. Matthews, V. Pons, D. M. Heinekey, *Inorg. Chem.* **2006**, *45*, 6453–6459.
- [60] a) S. Zhang, G. R. Dobson, T. L. Brown, *J. Am. Chem. Soc.* **1991**, *113*, 6908–6916; b) S. L. Matthews, V. Pons, D. M. Heinekey, *J. Am. Chem. Soc.* **2005**, *127*, 850–851.
- [61] V. K. Dioumaev, R. M. Bullock, *Nature* **2003**, *424*, 530–532.
- [62] a) Y. Wang, P. Gu, W. Wang, H. Wei, *Catal. Sci. Technol.* **2014**, *4*, 43–46; b) Ning, X.; Wang, J.; Wei, H. *J. Phys. Chem. A* **2016**, *120*, 4167 – 4178; c) Drees, M.; Strassner, T. *Inorg. Chem.* **2007**, *46*, 10850 – 10859; d) Costa, P. J.; Romão, C. C.; Fernandes, A. C.; Royo, B.; Reis, P. M.; Calhorda, M. J. *Chem. Eur. J.* **2007**, *13*, 3934 – 3941.
- [63] K. Yan, J. J. Duchimaza Heredia, A. Ellern, M. S. Gordon, A. D. Sadow, *J. Am. Chem. Soc.* **2013**, *135*, 15225–15237.
- [64] L. W. Chung, H. G. Lee, Z. Lin, Y.-D. Wu, *J. Org. Chem.* **2006**, *71*, 6000–6009.
- [65] O. G. Shirobokov, L. G. Kuzmina, G. I. Nikonov, *J. Am. Chem. Soc.* **2011**, *133*, 6487–6489.
- [66] E. A. Ison, R. A. Corbin, M. M. Abu-Omar, *J. Am. Chem. Soc.* **2005**, *127*, 11938–11939.
- [67] T.-Y. Cheng, B. S. Brunshwig, R. M. Bullock, *J. Am. Chem. Soc.* **1998**, *120*, 13121–13137.
- [68] a) L. Huang, W. Wang, X. Wei, H. Wei, *J. Phys. Chem. A* **2015**, *119*, 3789–3799; b) L. Huang, Y. Zhang, H. Wei, *Eur. J. Inorg. Chem.* **2014**, 5714–5723.
- [69] S. Park, M. Brookhart, *Organometallics* **2010**, *29*, 6057–6064
- [70] a) J. Yang, P. S. White, M. Brookhart, *J. Am. Chem. Soc.* **2008**, *130*, 17509–17518; b) M. P. McLaughlin, L. L. Adduci, J. J. Becker, M. R. Gagné, *J. Am. Chem. Soc.* **2013**, *135*, 1225–1227.
- [71] a) J. Yang, M. Brookhart, *J. Am. Chem. Soc.* **2007**, *129*, 12656–12657; b) J. Yang, M. Brookhart, *Adv. Synth. Catal.* **2009**, *351*, 175–187.
- [72] T. T. Metsänen, P. Hrobárik, H. F. T. Klare, M. Kaupp, M. Oestreich, *J. Am. Chem. Soc.* **2014**, *136*, 6912–6915
- [73] M. Iglesias, P. J. Sanz Miguel, V. Polo, F. J. Fernández-Alvarez, J. J. Pérez-Torrente, L. A. Oro, *Chem. Eur. J.* **2013**, *19*, 17559–17566.
- [74] D. V. Gutsulyak, S. F. Vyboishchikov, G. I. Nikonov, *J. Am. Chem. Soc.* **2010**, *132*, 5950–5951.
- [75] a) D. V. Gutsulyak, G. I. Nikonov, *Angew. Chem. Int. Ed.* **2010**, *49*, 7553–7556; b) D. V. Gutsulyak, A. van der Est, G. I. Nikonov, *Angew. Chem. Int. Ed.* **2011**, *50*, 1384–1387; c) L. Sun-Hwa, D. V. Gutsulyak, G. I. Nikonov, *Organometallics* **2013**, *32*, 4457–4464.
- [76] T. Stahl, P. Hrobárik, C. D. F. Königs, Y. Ohki, K. Tatsumi, S. Kemper, M. Kaupp, H. F. T. Klare, M. Oestreich, *Chem. Sci.* **2015**, *6*, 4324–4334.
- [77] S. T. N. Freeman, F. R. Lemke, *Organometallics* **2002**, *21*, 2030–2032.
- [78] K. Osakada, *Angew. Chem. Int. Ed.* **2011**, *50*, 3845–3846.
- [79] a) H. F. T. Klare, M. Oestreich, J.-I. Ito, H. Nishiyama, Y. Ohki, K. Tatsumi, *J. Am. Chem. Soc.* **2011**, *133*, 3312–3315; b) S. Wübbolt, M. Oestreich, *Angew. Chem. Int. Ed.* **2015**, *54*, 15876–15879; c) T. Stahl, H. F. T. Klare, M. Oestreich, *J. Am. Chem. Soc.* **2013**, *135*, 1248–1251; d) D. F. Königs, H. F. T. Klare, M. Oestreich, *Angew. Chem. Int. Ed.* **2013**, *52*, 10076–10079; e) T. T. Metsänen, M. Oestreich, *Organometallics* **2015**, *34*, 543–546; f) D. F. Königs, H. F. T. Klare, Y. Ohki, K. Tatsumi, M. Oestreich, *Org. Lett.* **2012**, *14*, 2842–2845; g) J. Hermeke, H. F. T. Klare, M. Oestreich, *Chem. Eur. J.* **2014**, *20*, 9250–9254.
- [80] M. Tan, Y. Zhang, *Tet. Lett.* **2009**, *50*, 4912–4915.
- [81] a) V. H. Mai; I. Korobkov; G. I. Nikonov *Organometallics* **2016**, *35*, 936 –942; b) S. Bähr; A. Simonneau; E. Irran; M. Oestreich *Organometallics* **2016**, *35*, 925–928.
- [82] a) C. Zybill, G. Müller, *Angew. Chem., Int. Ed.* **1987**, *26*, 669–670; b) D. A. Straus, T. D. Tilley, *J. Am. Chem. Soc.* **1987**, *109*, 5872–5873; c) K. Ueno, H. Tobita, M. Shimoi, H. Ogino, *J. Am. Chem. Soc.* **1988**, *110*, 4092–4093.
- [83] a) D. A. Straus, C. Zhang, G. E. Quimbata, S. D. Grumbine, R. H. Heyn, T. D. Tilley, A. L. Rheingold, S. J. Geib, *J. Am. Chem. Soc.* **1990**, *112*, 2673–2681; b) H. Wada, H. Tobita, H. Ogino, *Organometallics*, **1997**, *16*, 2200–2203.
- [84] a) C. Zhang, S. D. Grumbine, T. D. Tilley, *Polyhedron* **1991**, *10*, 1173–1176; b) K. Ueno, H. Tobita, S. Seki, H. Ogino, *Chem. Lett.* **1993**, 1723–1726; c) R. J. P. Corriu, B. P. S. Chauhan, G. F. Lanneau, *Organometallics* **1995**, *14*, 1646–1656.
- [85] a) M. Ochiai, H. Hashimoto, H. Tobita, *Dalton Trans.* **2009**, 1812–1814; b) T. Watanabe, H. Hashimoto, H. Tobita, *J. Am. Chem. Soc.* **2007**, *129* 11338–11339; c) T. Watanabe, H. Hashimoto, H. Tobita, *Chem. Asian J.* **2012**, *7*, 1408–1416; d) M. E. Fasulo, T. D. Tilley, *Organometallics*, **2012**, *31*, 5049–5057; e) E. Calimano, T. D. Tilley, *Organometallics* **2010**, *29*, 1680–1692; f) S. R. Klei, T. D. Tilley, R. G. Bergman, *Organometallics* **2002**, *21*, 4648–4661.
- [86] a) M. Ochiai, H. Hashimoto, H. Tobita, *Organometallics* **2012**, *31*, 527–530; b) G. P. Mitchell, T. D. Tilley, *J. Am. Chem. Soc.* **1997**, *119*, 11236–11243.
- [87] a) P. B. Glaser, T. D. Tilley, *J. Am. Chem. Soc.* **2003**, *125*, 13640–13641; b) P. G. Hayes, C. Beddie, M. B. Hall, R. Waterman, T. D. Tilley *J. Am. Chem. Soc.* **2006**, *128*, 428–429; c) E. Calimano, T. D. Tilley, *J. Am. Chem. Soc.* **2008**, *130*, 9226–9227; d) E. Calimano, T. D. Tilley, *J. Am. Chem. Soc.* **2009**, *131*, 11161–11173.
- [88] a) T. Watanabe, H. Hashimoto, H. Tobita, *J. Am. Chem. Soc.* **2006**, *128*, 2176–2177; b) M. Oaciai, H. Hashimoto, H. Tobita, *Angew. Chem. Int. Ed.* **2007**, *46*, 8192–8194.
- [89] M. Hirotsu, T. Nunokawa, K. Ueno, *Organometallics* **2006**, *25*, 1554–1556.
- [90] W. Buechner, *J. Organomet. Chem. Lib.* **1980**, *9*, 409–431.
- [91] a) M. D. Curtis, P. S. Epstein, *Adv. Organomet. Chem.* **1981**, *19*, 213–255; b) I. Ojima, S.-I. Inaba, T. Kogure, Y. Nagai, *J. Organomet. Chem.* **1973**, *55*, C7–C8; c) M. Kumada, *J. Organomet. Chem.* **1975**, *100*, 127–138.

- [92] a) C. Watanabe, T. Iwamoto, C. Kabuto, M. Kira, *Angew. Chem. Int. Ed.* **2008**, *47*, 5386–5389; b) J. D. Feldman, G. P. Mitchell, J.-O. Nolte, T. D. Tilley, *J. Am. Chem. Soc.* **1998**, *120*, 11184–11185; c) S. H. A. Petri, S. D. Eikenberg, B. Neumann, H.-G. Stammler, P. Jutzi, *Organometallics* **1999**, *18*, 2615–2618.
- [93] a) S. K. Grumbine, T. D. Tilley, *J. Am. Chem. Soc.* **1994**, *116*, 5495–5496; b) P. W. Wanandi, P. B. Glaser, T. D. Tilley, *J. Am. Chem. Soc.* **2000**, *122*, 972–973; c) M. E. Fasulo, P. B. Glaser, T. D. Tilley, *Organometallics* **2011**, *30*, 5524–5531.
- [94] S. K. Grumbine, T. D. Tilley, *J. Am. Chem. Soc.* **1994**, *116*, 6951–6952.
- [95] G. P. Mitchell, T. D. Tilley, *Angew. Chem. Int. Ed.* **1998**, *37*, 2524–2526.
- [96] a) T. Watanabe, H. Hashimoto, H. Tobita, *Angew. Chem. Int. Ed.* **2004**, *43*, 218–221; b) J. C. Peters, J. D. Feldman, T. D. Tilley, *J. Am. Chem. Soc.* **1999**, *121*, 9871–9872.
- [97] M. C. Lipke, F. Neumeyer, T. D. Tilley, *J. Am. Chem. Soc.* **2014**, *136*, 6092–6102.
- [98] a) K. S. Pitzer, *J. Am. Chem. Soc.* **1948**, *70*, 2140 – 2145.; b) R. S. Mulliken, *J. Am. Chem. Soc.* **1955**, *77*, 884 – 887; c) R. West, *Polyhedron*, **2002**, *21*, 467 – 472.
- [99] a) N. Schneider, M. Finger, C. Haferkemper, S. Bellemin-Lapponnaz, P. Hofmann, L. H. Gade, *Angew. Chem. Int. Ed.* **2009**, *48*, 1609–1613; b) N. Schneider, M. Finger, C. Haferkemper, S. Bellemin-Lapponnaz, P. Hofmann, L. H. Gade, *Chem. Eur. J.* **2009**, *15*, 11515–11529; c) P. Gigler, B. Bechlars, W. A. Herrmann, F. E. Kühn, *J. Am. Chem. Soc.* **2010**, *133*, 1589–1596; d) K. Riener, M. P. Högerl, P. Gigler, F. E. Kühn, *ACS Catal.* **2012**, *2*, 613–621.
- [100] a) I. Ojima, M. Nihonyanagi, Y. Nagai, *Bull. Chem. Soc. Jpn.* **1972**, *45*, 3722; b) I. Ojima, T. Kogure, M. Nihonyanagi, Y. Nagai, *Bull. Chem. Soc. Jpn.* **1972**, *45*, 3506.
- [101] K.-Y. Akiba, *Chemistry of Hypervalent Compounds*; Wiley-VCH: Weinheim, 1999.
- [102] a) T. T. Metsänen, D. Gallego, T. Szilvási, M. Driess, M. Oestreich, *Chem. Sci.* **2015**, *6*, 7143–7149; b) J. Sun, C. Ou, C. Wang, M. Uchiyama, L. Deng, *Organometallics* **2015**, *34*, 1546–1551.
- [103] a) L. H. Gade, V. César, S. Bellemin-Lapponnaz, *Angew. Chem. Int. Ed.* **2004**, *43*, 1014–1017; b) V. César, S. Bellemin-Lapponnaz, H. Wadepohl, L. H. Gade, *Chem. Eur. J.* **2005**, *11*, 2862–2873.
- [104] R. Goikham, D. Milstein, *Chem. Eur. J.* **2005**, *11*, 2983–2988.
- [105] S. Xu, J. S. Boschen, A. Biswas, T. Kobayashi, M. Pruski, T. L. Windus, A. D. Sadow, *Dalton Trans.* **2015**, *44*, 15897–15904.
- [106] P. B. Glaser, T. D. Tilley, *Organometallics* **2004**, *23*, 5799–5812.
- [107] a) C. Beddie, M. B. Hall, *J. Am. Chem. Soc.* **2004**, *126*, 13564–13565; b) C. Beddie, M. B. Hall, *J. Phys. Chem. A* **2006**, *110*, 1416–1425.
- [108] J. D. Feldman, J. C. Peters, T. D. Tilley, *Organometallics* **2002**, *21*, 4065–4075.
- [109] a) G. I. Nikonov, *Angew. Chem., Int. Ed.* **2001**, *40*, 3353–3355; b) S. Lachaize, S. Sabo-Etienne, *Eur. J. Inorg. Chem.* **2006**, 2115–2127.
- [110] a) K. Hubler, U. Hubler, W. R. Roper, P. Schwerdtfeger, L. J. Wright, *Chem. Eur. J.* **1997**, *3*, 1608–1616; b) N. M. Yardy, F. R. Lemke, *Organometallics* **2001**, *20*, 5670–5674; c) F. Delpech, S. Sabo-Etienne, J.-C. Daran, B. Chaudret, K. Hussein, C. J. Marsden, J.-C. Barthelat, *J. Am. Chem. Soc.* **1999**, *121*, 6668–6682; d) S. Lachaize, S. Sabo-Etienne, B. Donnadiou, B. Chaudret, *Chem. Commun.* **2003**, 214–215; e) I. Atheaux, B. Dannadiou, V. Rodriguez, S. Sabo-Etienne, B. Chaudret, K. Hussein, J.-C. Barthelat, *J. Am. Chem. Soc.* **2000**, *122*, 5664–5665.
- [111] Structures of **55**<sub>SIMePh</sub> and of the DMAP adduct **55**<sub>SIPh2</sub>\*(DMAP) have previously been published (see ref 25a). To enable direct comparison of the Ru—H—Si interactions in these types of species, Scheme 68 provides images of the previously unpublished structures **55**<sub>SIEt2</sub> and its DMAP adduct **55**<sub>SIEt2</sub>\*(DMAP), which have been deposited in the Cambridge Structure Database. CCDC 1480967-1480968.
- [112] M. C. Lipke, T. D. Tilley, *Angew. Chem., Int. Ed.* **2012**, *51*, 11115–11121.
- [113] a) H. Tobita, A. Matsuda, H. Hashimoto, K. Ueno, H. Ogino *Angew. Chem. Int. Ed.* **2003**, *43*, 221 – 224; b) V. M. Iluc, G. L. Hillhouse *J. Am. Chem. Soc.* **2010**, *132*, 11890 – 11892.

## Entry for the Table of Contents

## REVIEW

Hydrosilations are important transformations in materials science and synthetic chemistry. Recent efforts in catalyst development include numerous investigations of catalysts, based on elements from Groups 4 – 15, that operate by electrophilic silane activation pathways. This review surveys these catalysts and describes several related mechanisms for electrophilic Si–H activation ( $\sigma$ -H–Si coordination,  $M(H)_2=SiRR'$  formation,  $\eta^3$ - $H_2SiRR'$  binding).



Mark C. Lipke, Allegra L. Liberman-Martin, T. Don Tilley\*

Page No. – Page No.

**Electrophilic Activation of Silicon–Hydrogen Bonds in Catalytic Hydrosilations**

Accepted Manuscript